The Getty Conservation Institute

research in conservation

Airborne Particles in Museums

William W. Nazaroff
Mary P. Ligocki
Lynn G. Salmon
Glen R. Cass
Theresa Fall
Michael C. Jones
Harvey I. H. Liu
Timothy Ma

Editor:	Dinah Berland
Copyeditor:	Lisa Kirk
Cover designer:	Joe Molloy
Designer and coordinator:	Irina Averkieff
Typographer:	FrameMaker / Adobe Palatino and Helvetica Condensed
Illustrator:	Ad•Infinitum
Printer:	Edwards Bros., Ann Arbor, Michigan

Printed in the United States of America.

Library of Congress Cataloging-in-Publication Data
Airborne particles in museums/
William W. Nazaroff… [et al.].
p. cm. -- (Research in conservation ;)
Includes bibliographical references and index.
ISBN 0–89236–187–5 :
1. Art--Conservation and restoration. 2. Air--Pollution.
I. Nazaroff, W. W. II. Series.
N8560.P76 1992
702′.8′8--dc20 92–35622
CIP

The Getty Conservation Institute

The Getty Conservation Institute, an operating program of the J. Paul Getty Trust, is committed to raising public awareness of the importance of preserving cultural heritage worldwide and to furthering scientific knowledge and professional practice in the field of conservation. The Institute conducts interdisciplinary programs in research, training, documentation, and conservation activities in several major areas including objects and collections, archaeological sites and monuments, and historic buildings and cities. This is accomplished through a combination of in-house projects and collaborative ventures with other organizations in the USA and abroad. Special activities such as field projects, international conferences, and publications strengthen the role of the Institute.

Research in Conservation

This reference series is born from the concern and efforts of the Getty Conservation Institute to publish and make available the findings of research conducted by the GCI and its individual and institutional research partners, as well as state-of-the-art reviews of conservation literature. Each volume covers a separate topic of current interest and concern to conservators.

Contents

The Authors

William W. Nazaroff William W. Nazaroff received his Ph.D. in environmental engineering science at the California Institute of Technology. He is currently Associate Professor of Civil Engineering, University of California at Berkeley. He is interested in the experimental and theoretical aspects of indoor air quality, including the behavior of small particles, photo-oxidants, and control of radon exposure indoors.

Mary Ligocki Mary P. Ligocki received her B.S. degrees in engineering and mathematics from the California Institute of Technology and her Ph.D. from the Oregon Graduate Institute of Science and Technology. She is presently a senior scientist at Systems Applications in San Rafael, California, and is engaged in air pollution research.

Lynn G. Salmon Lynn G. Salmon holds a B.S. degree in engineering from the Massachusetts Institute of Technology and an M.S. degree in engineering from the University of California, Los Angeles. She is presently a research engineer at the Environmental Engineering Science Department, California Institute of Technology, where she continues to work on problems of protection of cultural properties from damage due to environmental conditions.

Glen R. Cass Glen R. Cass received his Ph.D. in environmental engineering in 1978 from the California Institute of Technology, where he is presently Professor of Environmental Engineering and Mechanical Engineering. His current research interests center on control of air pollution problems, including the problem of protection of works of art from damage due to atmospheric particulate matter.

Theresa Fall Theresa Fall holds a B.S. degree in geology from the University of California, Los Angeles. She is presently a staff geologist at Woodward Clyde Consultants in Phoenix, Arizona.

Michael C. Jones Michael C. Jones received his B.S. degree in chemical engineering from the California Institute of Technology in 1990. He is presently a graduate student at the Massachusetts Institute of Technology.

Harvey I. H. Liu Harvey I. H. Liu received his B.S. degree in electrical engineering from the California Institute of Technology in 1989. He is presently a graduate student at Stanford University.

Timothy Ma Timothy Ma received his B.S. degree in electrical engineering from the California Institute of Technology in 1988. He is presently a design engineer at VLSI Technology Inc. in Encino, California.

Foreword

This study represents the latest in a series of research activities aimed at a better understanding of the origin and fate of air pollution within the built environment. Whether these buildings function as art museums, historical houses, archives, libraries, or other institutions housing cultural or natural collections, their contents may be subject to nearly the same risk levels for loss and deterioration from air pollution as if little or no environmental protection were present. Today we recognize this as fact, but this was not always the case. Once, many believed that as soon as objects were removed from the vagaries of everyday life and protected by institutions of learning and education, they would last in perpetuity. This complacent notion was shaken by Russell and Abney in 1888 and subsequently shattered. Throughout the 1960s, 70s, and 80s pictures emerged of life in a museum display or storage areas that were not the salubrious repose of nineteenth-century imagination. Buildings do provide objects with significant protection, but—apart from physical and chemical damage caused by humidity and temperature fluctuations and sheltering from general climate—damage caused by outdoor air pollution is only retarded, and is oftentimes replaced by new indoor pollutants equally as damaging.

Keeping pace with the new understanding about indoor pollutant interactions, control and monitoring methodologies have evolved to assist collection caretakers. Now it is possible, at least in theory if not practice, to provide better protection than that previously assumed to be adequate.

Most previous studies of air pollution in cultural institutions have focused on gases. Particles were ignored for many reasons: they seemed to be more easily removed by the building; gaseous air pollutants had been well studied by industry, and their effects on commercial products were heavily documented; and many particle types were considered chemically benign to almost all surfaces. Even carbon black, which is now known to pose enormous degradation risks to the optical and color qualities of paintings and tapestries, is almost totally inert. Recognizing this, and understanding that we needed to know much more about the physics of particle intrusion in museum buildings, in 1987 the Environmental Engineering Lab at the California Institute of Technology, under contract to the Getty Conservation Institute, began a detailed examination of five different museums in Southern California. These structures represent a diverse range of architectural and ventilation types. Through this study a powerful computer model was developed that could predict the soiling effects of changes made to the operation or maintenance of a building. This model can even be used to estimate the soiling rates of new buildings or major rehabilitations before any construction work is begun. We feel that this is an important contribution to both the conservation community and the broader field of air quality science.

Miguel Angel Corzo
Director
The Getty Conservation Institute

Introduction

The potential damage that may occur to museum collections from gaseous air pollutants is well documented. Until now, however, airborne particles have been largely ignored. Except for the work of Toishi and Kenjo (1968) on alkaline particles from new concrete construction, Baer and Banks (1985) found that surprisingly little was known about the chemical nature of indoor particulate matter. If they found little about the chemical nature of particles, they found still less about the transport or deposition of indoor particles.

The conservator's concern is twofold. First, research on damaged telecommunications equipment caused by hygroscopic nitrate particles suggests that metal objects in museum collections may be similarly sensitive. Nitrates were commonly found during the winter season at all the sites investigated in the present research, and were almost as high in concentration indoors as outdoors at the one historical house studied that used no filtration system. While this study took place in Southern California, the types of particles concerned are ubiquitous. Second, it is doubtful that once small particles settle on certain surfaces—such as feathers, fur, botanical specimens, large unframed tapestries and rugs, and unvarnished paintings—they can ever be removed. Larger particles may be partially blown off with an air current, but very small organic carbon and elemental (black) carbon particles cannot be dislodged in this way. A very soft brush may assist further, but once these small particles become imbedded in the surface texture, they become a permanent part of the structure. Just how permanent can be seen from the fact that no simple washing or bleaching technique is known to the field of paper conservation that will remove elemental carbon and that does not pose its own damage or risk of future effects on natural aging.

The conservation scientist's concerns begin where the conservator's end. Very small particles—including most of the carbon-based ones—are inefficiently filtered by heating, ventilating, and air-conditioning (HVAC) systems and are not generally removed by gravitation. Rather, their movement is almost totally dominated by the forces of the surrounding air. More precisely, their individual mass is so low that they act more like air molecules than like larger dirt particles that form dust and deposits. The significance of this is that loosely fitted vitrines, wall cases with sliding doors that are not snugly fitted, and Plexiglas panels mounted away from walls, provide less protection than one might otherwise believe. One researcher (J. Druzik) once found visible black carbon particle deposits inside a vitrine, securely screwed down to a wooden plinth.

In addition, some pigments and dyes are pH sensitive. The conservation literature contains evidence that these pigments are vulnerable to gases that are acid precursors, such as sulfur dioxide or nitrogen dioxide. Prolonged contact with sulfate, nitrate, and ammonium compounds has not been examined, yet incompatibilities between historic pigments are well known and this certainly adds to the general sense of insecurity.

The facilities manager's concerns thus become grave. The kinds of filtration used in the museums studied here provide minimum resistance to airflow. To improve the single-pass filtration efficiency of an HVAC system, more energy may be required to push the building's air volume though more restrictive filters. Energy is money—just how much money varies depending on the design and size of the building and its mechanical systems. Never as expensive as maintaining relative humidity, a classic energy guzzler, attendant costs could, nevertheless, easily run into the thousands, and tens of thousands, of dollars, even if available equipment could do the work. Often existing systems are inadequate, so the total costs may include capital improvements, which are seldom welcomed.

The museum director's concerns axiomatically become those of the facilities manager, conservation scientist, and conservator when the director takes the trustees on a visit of the storage rooms and hears these influential guests joke about the director's dirt problem.

This study contains many lessons. Not all of them are original, and not all of them follow purely from this research. Some of them are the direct result of the experience of the staffs of the five institutions involved in the study. The Norton Simon Museum is proportionally the cleanest environment of the five studied, not because of any single design effort, but because people made decisions along the way about how the building was to be constructed and run, and this resulted in a high-quality environment. Slightly more purposeful is the example of the Scott Gallery. During this study, the Scott Gallery was modified to control gaseous pollutants, encouraged to do so by earlier research by the same group from the California Institute of Technology that conducted this particle study. An energy conservation study was also in progress during the particle assessment. The administration of the Scott Gallery was therefore highly sensitized to all aspects of the building's performance. The results of reducing make-up air for thermal control from the original design limit of 25% to essentially zero are clearly reflected in the decrease in indoor fine-particle concentrations. At this point, air exchanges between the outdoor and indoor air were entirely due to infiltration, including door openings. Some decisions were intentional, others were synergistic.

This is not just an urban problem of developed countries. Every location characterized by large human populations that depend on low-end fuels for heating and cooking represent greater risks to cultural property than in more developed countries. This is also not just a problem of museums or other cultural institutions. Certain archaeological sites also suffer. A good example is the Yungang caves near Datong in the People's Republic of China. These caves are examples of internationally important sites completely exposed to outside air. The Yungang caves contain tens of thousands of carvings, many of which are polychromed. Windblown dust, human-generated smoke particles, and gaseous pollutants escaping from one of China's largest coal mining areas enter the caves with no physical restriction. As described by Cass in his proposal to study ways to mitigate this problem:

> Observation of the interior of the caves shows that many surfaces of the sculptures are buried in roughly a quarter-inch-deep blanket of grey particles that probably have been delivered by atmospheric deposition processes. Unless such severe particle deposition processes can be abated, any attempt to preserve or restore the sculptures in the caves may well be defeated by a continuing assault of abrasive and possibly chemically reactive airborne contaminants. Many other similar situations probably exist in other devotional caves, decorated underground tombs, and in salt mines containing important sculpture.

Taking the foregoing issues into account, it appeared to those involved at the Getty Conservation Institute that the study of soiling due to airborne particles in museums had to be undertaken. This study was a natural partner to the twenty other environmental research projects originally planned, and ultimately carried out as the thrust of an eight-year research program.

Background

Twenty-five years ago the International Institute for Conservation of Historic and Artistic Works (IIC) sponsored the 1967 London Conference on Museum Climatology, a conference which, for a whole generation of conservators and curators, represented the most comprehensive body of museum environmental knowledge then available. In 1978 came the first edition of *The Museum Environment* (Thomson), an even more exhaustive treatment. Indicative of the need, it was a runaway best seller in its field. It is not surprising then that in the United States in March 1979, the National Conservation Advisory Council submitted a *Report of the Study Committee on Scientific Support for Conservation of Cultural Properties* (1979) in which it identified "Deterioration Studies" as needing more basic research and the "Study of Environmental Effects and Counteractive Measures" as one of the four areas where developmental and applied research is especially needed.

> Research into the action and control of environmental sources of deterioration is crucial to the survival beyond the immediate future of many artifacts. Decaying stone and glass in monuments and buildings and fading watercolor pigments and textile dyes are but a few examples.
>
> Since only a portion of the nation's cultural property can be maintained under reasonably stable museum or library conditions, methods must be sought for protecting materials whose environments cannot be controlled. For instance, the wood, stone, and metal in historic houses are subjected to such destructive influences as exposure to atmospheric pollution, extremes of temperature and humidity, and the harmful agents employed by vandals.

Building further, Stolow's *Conservation and Exhibitions* (1987) includes two chapters on environmental monitoring and, in a third, specifically addresses environmental requirements in storage. Meanwhile, the second edition of *The Museum Environment* was issued in 1986 as interest in preventive conservation continued to grow. Between the two editions, the Canadian Conservation Institute (CCI) established its Environmental and Deterioration Research Division, which stated:

> Environmental factors to be controlled include:
>
> - outdoor-generated primary and secondary gaseous air pollution infiltrating the building
> - outdoor-generated man-made primary and secondary particles
> - indoor-generated gaseous air pollution
> - indoor-generated particles
> - temperature and relative humidity
> - macro- and microbiological activities
> - illumination (intensity and energy distribution)
> - mechanical stresses (vibration and handling)
> - vandals and nondeliberate forms of human intervention
>
> This control can be achieved on four different levels, all interrelated yet having their own unique boundary conditions.
>
> At the *building level*, the environment is largely dominated by the overall ventilation design, usually a compromise between aesthetic, economic, historical, geographical, and engineering conditions. Depending on the dominant parameters one wishes to emphasize, all buildings can be organized into any number of independent (rare) or interrelated (common) sets. Discussing just the mechanistic relationships between indoor and outdoor air quality, one possible set is arrayed in a distribution between two extremes: the typical historic house with convection flow facilitated by open windows, which may have rapid or slow air exchanges; and, at the other end, a large art museum, with elaborate multizoned climate control with or without chemical filtration. Regardless of where a given structure fits into this array, air still infiltrates and exfiltrates through numerous gaps in the building shell and is exchanged through bathrooms, kitchens, workshops, conservation lab spray booths, and fume hoods or theater exhaust systems. These routes ensure that all varieties of gases and particles liberally move between the outdoors and the indoor museum or library environment.
>
> Another set of buildings that Cammuffo (1983) has shown to be an important class among historic European structures, but is no less important in North America, takes into account the thermal and hygrometric parameters. Cammuffo's sets may be centered upon internal "dynamic climatology" such as his work in the early 1980s in the Sistine Chapel, or more recently, outdoor microclimate such as the study of Orvieto Cathedral (Cammuffo and Bernardi 1988).

A third set might be characterized by buildings in which the environment is controlled exclusively by HVAC systems, governed by remote sensors, and under manual or computer control. Ideally, these systems should be slightly pressurized, making the theoretical net flux outward. But this may not be the actual case if large gaps in the building envelope are created during public access to the building. In these instances, air infiltration often places a significant load on the resident HVAC system's ability to warm or cool and humidify or dehumidify. It was estimated that by 1987, the heat load associated with natural infiltration would cost about 15 billion dollars annually in the United States.

Volent and Baer (1985) point out one instance in which the HVAC system even contributed its own unique pollutant to indoor air. To prevent steam-pipe corrosion, diethyliamine ethanol (DEAE) was added routinely to the heating system of the Herbert F. Johnson Museum of Cornell University. In 1982, DEAE was detected visually on the surface of many artifacts and required cleanup of the entire building after numerous health complaints. Water in building environmental systems can encourage the growth of biological contaminants as well.

At the level of individual *rooms and galleries*, the HVAC system or overall ventilation strategy still dominates, but mixing occurs at boundaries between rooms where different air qualities may exist. This is especially noticeable in galleries immediately adjacent to entrances, exits, subterranean parking facilities, wood and paint shops, etc. Because of the combined effects of incandescent lighting, plumbing behind walls, variations in wall insulation, and air inlets, differential particle accumulation on surfaces occurs. Some walls and ceilings heat up, others cool down, and the temperature of the bulk air may be different still. Thermal gradients along the surface of cold walls drive particles in the air toward the surface, and the surface can soil rapidly. The mechanism will be described in greater detail. Suffice it to say now that this mechanism works at close distances to a surface, but the layer undergoing thermal precipitation is constantly being renewed by turbulent mixing and larger thermal convections from the room or gallery bulk-air volume. Nielsen (1940) showed that fractions of a degree Fahrenheit differences in wall or air temperature can cause perceptible soiling. At this level, visitor traffic serves to keep heavier particles stirred up, creates new types such as carpet dust, and emits its own bioeffluents (water vapor, methanol, ethanol, acetone, butyric acid, acetic acid, etc.).

Storage and display areas are influenced both by the building air-delivery system and by mixing ratios between rooms; but at this level, air exchanges between adjacent architectural spaces may become slow enough to permit some indoor-generated pollutants to increase above background concentrations. The fact that small containers have dramatically different surface-to-volume ratios as compared to those of very large rooms may result in two effects: to enhance the role that container surfaces play in depleting some reactive gas and aerosol concentrations regardless of their origins, and to allow the containers to serve as reservoirs or sources for other types of pollutants.

Buildings in which an energy conservation maintenance policy is being pursued may have their 24-hour ventilation rates intentionally reduced, or more dramatically, cut drastically during nonvisiting hours, which would exacerbate the already slower exchanges in storage. If an indoor source of a reactive pollutant species exists, its concentration might increase enough to visibly interact with artifacts. On the other hand, if no important sources of indoor pollutants exist within a given structure, reduced ventilation rates may be used to advantage for slowing particulate soiling and other damage by outdoor gaseous pollutants.

Sealed individual objects may be shielded from outdoor conditions and buffered against cyclical indoor conditions, yet by doing so the object is left to "stew in its own juices," so to speak. Experimental results are scanty but the generally held opinion of most experts within the paper conservation field, and the universal fear as well, is that autocatalytic degradation may be accelerated with encapsulation if certain protective measures are not taken. If these measures have been systematically investigated, they do not appear in the literature other than in one isolated reference by Shahani (1986).

Somewhat less dependent but still influenced by these basic four levels are problems associated with microorganisms, insects and pests, and photochemical deterioration.

Understanding This Report

This research report, although scaled down from the final complete research report (also available from the Getty Conservation Institute [GCI]), still contains a great deal of information not normally encountered by the conservator. This section attempts to alert the reader to important points and useful features in the main body of the text chapter by chapter. When necessary, examples from conservation practice are used for illustration purposes and to allow the reader to draw connections, where appropriate, to related GCI research. Technical terms are also defined here to clarify certain engineering or chemical descriptions that may be unfamiliar. Please refer to the tables and figures cited in the text.

This introduction is not designed to perform the same function as the two-part structure of Thomson's *The Museum Environment* (1978)—the first half for conservators and the second half for conservation scientists. Conservation scientists can simply refer to the final report of this survey, which includes all the mathematical underpinnings for the work. Rather, consider it more like participating in running a race in which this introduction offers all participants the opportunity of a short warm-up exercise. For those who wish to sprint off, feel free to do so and jump right into Chapter 1.

Chapter 1: Soiling Due to Airborne Particles

Chapter 1 provides the objectives and the approach of the study. Here three key concepts are encountered that will become very important later in this report: (1) movement of fine particles by Brownian diffusion, (2) particle deposition velocity, and (3) the characteristic time for soiling.

That particles settle on horizontal surfaces is well known to everyone, and gravity is universally assumed to be responsible although other processes do participate. Why particles settle on vertical surfaces or ceilings, however, is less obvious. The reason is complex because there are several ways any particle can come into contact with any surface. The smaller a particle, the more it acts like a large molecule rather than a particle. As a result, it becomes less influenced by gravity and more influenced by gas molecules smaller than itself. This means that the gas molecules that make up the atmosphere have an effect on small particles simply from the physical effects of their collision. Normally, in a static environment there will be a statistically similar number of collisions on all sides of the particle, causing it to jump around erratically but essentially remain in place. A cloud of particles will expand slowly under this diffusive motion, and if a small particle strikes a surface it will generally stick. If some condition exists that causes more energetic gas/particle collisions on one side of the particle than another, particles will drift in a particular direction. One such important condition, called thermophoresis, is encountered if a thermal gradient exists. This commonly occurs when a surface is cooler than the ambient air. Gas molecules near the cool surface move less energetically than those farther away. Collisions on the cooler surface side of the particle will be less energetic than the other side. Therefore, particles will drift in the cooler direction. This can be seen in black streaks on walls where differential movement occurs because of cooler water pipes or structural supports located behind a wall's surface.

The second important concept is the "particle deposition velocity." This is defined not as a true velocity in the sense of particles moving toward a wall, but rather as the ratio of particle flux to a surface divided by the particle number concentration in the ambient air adjacent to that surface. This definition can be applied as a function of particle size in order to track different types and sizes of particles that have different deposition rates as they collect on surfaces. These different rates are affected by gravitational settling and air movement close to surfaces. They are also affected by thermophoresis. The same-sized particles will behave differently in a quickly ventilated airflow with turbulence than in one where large volumes of air are introduced with minimal movement and turbulence.

The third and most important concept discussed in this report is the characteristic time before visible soiling. This will be the single most important concept developed within the scope of this study from the conservator's point of view. It will be the measuring stick used to predict the aesthetic degradation of surfaces—for example large textiles and exposed objects—and the means by which to estimate the levels of improvement possible in altering a building. It also offers a method by which soiling can be monitored in a building by a conservator.

Chapter 2: Characteristics of Airborne Particles Inside Southern California Museums

Chapter 2 describes in some detail how airborne particles were measured in five museums in Southern California. This is provided to demonstrate methods that can be used elsewhere. More detailed information may be found in the final report.

The five structures studied here represent a useful range for comparison. The J. Paul Getty Museum, the Norton Simon Museum, and the Scott Gallery are all HVAC-equipped buildings with particle filtration. Their geographic locations range from a cleaner oceanside location to the heart of the Los Angeles air pollution corridor in Pasadena and San Marino. The facilities studied also have very different particle filtration characteristics. Two other museums are investigated, the Sepulveda House and the Southwest Museum. The former has no HVAC or particle filtration, and the Southwest Museum is a hybrid structure combining HVAC and non-mechanically controlled regions.

During the period in which data were being collected, it was decided to amass information on a wide range of chemically unique particles even though the central thrust of the work was to assess and design control methods for preventing soiling by black elemental carbon particles and by soil dust. This was because if, in the future, a link becomes established between damage and some unique chemical classes of particles about which we now know very little, the data will already have been collected to hypothesize about the risks to museum collections. These data now exist for sulfates, nitrates, ammonium, sodium chloride, soil dust, and elemental and organic carbon.

Chapter 2 clearly defines the soiling risks to museum objects from elemental carbon. Even though the elimination of elemental carbon was highest in the Norton Simon Museum and in the Scott Gallery, the authors found that elemental carbon represented the second largest component of the indoor fine aerosol in the winter samples at those two sites. For buildings with particle filtration systems, this level can be 20 to 50% of the outdoor levels; for nonfiltered buildings, the level is 50 to 100%. A disturbing finding was that in two of the museums studied, particulate organic matter concentrations indoors were higher than the outdoor concentrations, suggesting that indoor sources augment the outdoor ones.

Chapter 3: Mathematical Modeling of Indoor Airborne Particle Dynamics

To elevate the experimental data to a level at which it can serve as a management and engineering tool, mathematical modeling is required. The model developed here is one of the important contributions of this study, yet it may remain the most obtuse and difficult for many to understand. But this need not be the case. To gain a general appreciation of mathematical modeling, one need only consider familiar examples.

A home budget and tax returns are simple models that describe your financial environment. As a true mathematical model, you can change any factor and predict the altered

outcome. For instance, when planning for a new car, the model equations demand that other expenses be suppressed and savings increased over time. In planning retirement income, the model covers a greater time span during which the prime interest rate will surely change many times. It also makes use of simple or compounded interest rates for numerous investment options, which, for security, should be diversified. Models such as these have been validated thousands of times, so they can be reliably trusted even if you are using them for the first time. However, unique models, those built for specific engineering or scientific purposes, have no track record and therefore must be initially vindicated to show that they have been designed to take the important aspects of a complex problem into account. Such vindication is called model validation and usually proceeds by ascertaining if the model predicts, with reasonably good agreement, the same conclusions produced by laboriously collected experimental observations. Your financial model will be validated by year-end bank accounts; the present particle model developed in this case was validated against experimental studies of environmental tobacco smoke.

The authors' model is complex because it must be designed to be adapted to represent many radically different buildings accurately. Its job is, in part, to help assess the risk to museum collections from particle soiling when the objects to be protected must be assumed to be irreplaceable. The conservation scientist will, therefore, wish to have both accuracy and the ability to view different building designs through the computations of the same model. One consequence of the high level detail is that this model is unlikely to be employed frequently, unlike models for energy calculations in buildings which have greater availability. Therefore, later in the report, the authors have applied the model to a variety of important cases such that the conclusions drawn can be assimilated without actually running the model yourself.

Chapter 4: Concentration and Fate of Airborne Particles in Museums

With the model validated, the next step is to compare actual measured and predicted concentrations as a point of departure for more sophisticated predictions, including those of importance for conservators and curators. In order to do this, several parameters needed to be measured, including filter efficiency, temperature differentials between air and walls, and air velocities, particularly near the surface of walls.

One important observation made in this study concerns the enhanced efficiency of particle filters as they became loaded. The low-efficiency fibrous-mat filter used at the Norton Simon Museum is only marginally useful when new, but dramatically efficient as it becomes loaded. Figure 4.2 (p. 79) shows this very well. For particles larger than 1 μm, the loaded filter (F_{A3}) ranges from 75 to 90% effective. A new filter would be about 5% efficient regardless of the particle sizes measured. The loaded filter is also much more effective in removing particles 0.1 to 0.3 μm in diameter. This may be counterintuitive for many conservators. These kinds of filters

do not wear out or become exhausted like gaseous filters. They actually behave in the opposite manner, getting better the dirtier they become. This can be seen in another way in Table 4.3 (p. 71). The Norton Simon Museum was modeled assuming different cases: Case A in which the make-up air filter was new and the recirculated filter loaded, and Case C in which both filters were loaded. Coarse elemental carbon and soil dust for Case B were only 5% as high as in Case A. For fine particles, the differences are far less, but the simulations still show improvements around 20%. The reduction of particles in the Norton Simon Museum is also due to the fact that recirculated air is continuously passing through F_{A3} which serves to polish the indoor air quality when make-up air is severely restricted or cut to zero.

Figure 4.3 (pp. 80–82) illustrates the next important set of measurements required by the present model: temperature of the bulk air supply versus the wall temperature and surface air velocities. Two reasons are immediately obvious as to why these are important measurements: First, they permit calculation of thermophoresis as a deposition process that causes particle motion perpendicular to walls; this mechanism produces tiny but persistent net velocities. Second, and more important, air velocities parallel to walls that are huge by comparison (5 to 30 cm per second) lead to particle deposition by convective diffusion.

The study of the Scott Gallery on April 24–25, 1988 (Fig. 4.3) represents a fine example of building physics. Roughly at noon on that day, the air conditioning was interrupted and the air temperature began to rise quickly (negative values below the zero line mean the air is warmer than the walls; positive values above this line represent warmer walls relative to the air). Suddenly, at 3:45 p.m., the air conditioning resumed, quickly cooling the air, seen in the graph by the strip recorder jumping up. During the time the air conditioning was off, the gallery and perhaps the entire building went into a semistratification mode as seen by the drop in surface-boundary air velocity. Air stratification in buildings may have important practical implications for preventive conservation, since objects react differently depending on their location within thermal and/or humidity gradients. In this situation, two different types of measurements not normally found in museums detected the onset of a possibly hazardous stratification almost immediately. Stratification does not always indicate a problem. If an object or surface is thermally or hygroscopically insensitive, stratification permits useful control of deposition.

Figure 4.4 (pp. 83–85) compares measured and modeled, outdoor and indoor particle concentrations and shows why the model justifies confidence in it. It also shows why bigger dust problems typically exist in our houses than in museums.

Figure 4.6 (pp. 88–90) summarizes the fate of deposited particles. The conservator need only recognize that for museums with particle filtration, elemental carbon and other small particles (smaller than 1μm) are the major particles that deposit on ceilings and walls. Elemental carbon poses the more significant risk to visible soiling, but the other fine particles represent most of the aerosols produced from air pollution, including an assortment of potentially

chemically reactive ones. It is not within the scope of this study to identify chemical risks from particle deposition, but the literature contains more than a few references to indicate that the dangers are clearly worth future investigation.

The authors of this report make one important point on the limitations of their calculations for museum collections. Calculations were done for vertical surfaces that are smooth. For varnished paintings this is true, but for some textiles, ethnographic materials, and natural collections it is not true. Therefore, as indicated previously, rough, porous, and fragile surfaces require special protective consideration.

The comments above introduced the notion of the characteristic time for soiling. This was described as the time it would take for a white surface to become noticeably soiled as determined by an observer. For a smooth white surface, this condition has been determined to represent a coverage of about 0.2% of the surface by black dots too small to be visually resolved. Since white surfaces would be the first to show change, they are logical to use as our standard. Table 4.5 (p. 76) applies this characteristic time of noticeable soiling to the three museums that have been extensively studied in this report. Taking only Case A, the results are impressive. For ceilings, the time to observe soiling varies from centuries to decades to years between the buildings studied; for walls, from decades to less than a year; for floors, from years to weeks. These data have far-reaching ramifications. The fact that vast improvements in indoor-particle air quality are being shown for buildings equipped with HVAC systems is almost irrelevant for institutions desiring to build new facilities in developing countries or elsewhere where HVAC systems are unlikely to be built because of maintenance and operating costs. However, there may exist passive or less capital-intensive environmental control systems for existing structures, that only filter air through low-tech materials (rather than cool it) that could achieve these types of results. Unlike the stereotypical HVAC installation, such filtration equipment is robust and operates at a fraction of the energy usage typically mandated for temperature and especially humidity control. These and many more techniques may be applied to achieve the same type of results at the Sepulveda House as observed at the Norton Simon Museum and the Scott Gallery, as this report will show.

Chapter 5: Measurements of the Rates of Soiling Inside Museums Due to Deposition of Airborne Particles

Chapter 5 continues with the particle collection phase of the survey begun in Chapter 2 and relates the deposition rates of elemental carbon and the optical measurements of the darkening of white paper and canvas surfaces. Chapter 4 presents, in Table 4.5 (p. 76), the calculated times for perceptible soiling to occur based on the mathematical model. These are in good agreement with the experimentally determined value presented in Table 5.3 (p. 96).

Deposition of soiling particles was measured on three substrates: white artists' canvas, Whatman 42 filter paper, and quartz cloth. The measurement of soiling was carried out on a Diano Match-scan II reflectance spectrophotometer. Visual observation of the quartz cloths was also recorded for the horizontal surfaces. It is somewhat discouraging to note that during the sampling period of three months to a year the canvas and the paper samples changed at every site. At two sites where unfiltered outdoor air penetrated the galleries, vertical soiling was visible after one year. Worse yet, inside display cases at the Southwest Museum where sliding glass doors had gaps as large as 4 mm, the change found for a horizontal collection surface in one year was approximately equal to 44 weeks in the open gallery. For all intents and purposes, the protection from particle deposition provided by these cases was small (the cases are, however, useful for reducing ozone concentration within the cases).

Tables 5.2 and 5.3 (pp. 95, 96), calculated from the measurement plan of the survey, tell the full story. What emerges is that the filtered environments of the first three museums have the lowest dark particle buildups (flux), while the unfiltered museums had two to thirteen times the mass of elemental carbon deposited on vertical surfaces. Table 5.3 (p. 96) extrapolates from these data and represents the authors' best estimates of the times required for perceptible soiling to occur on indoor vertical and horizontal surfaces.

The soiling time on vertical surfaces for filtered museums ranges from 18 years down to 4.8 years, with the J. Paul Getty Museum the fastest soiling of the three. This is due to a combination of two principal factors: The main floor (Antiquities) is served only by ventilation of filtered air between the hours of 8 a.m. and 6 p.m. While open to the public, that same floor has open doors allowing outdoor air to enter the building. For the two unfiltered museums the soiling time collapses further down to 2 and 0.3 years.

Chapter 6: Protecting Museum Collections from Soiling Due to Deposition of Airborne Particles

Chapter 6 focuses all that has been learned to provide advice on how perceptible soiling times in the relatively open structure of the Sepulveda House can be lengthened to meet or exceed the performance of even the Norton Simon Museum.

The Sepulveda House is a two-story historical museum located at El Pueblo de Los Angeles Historic Park in downtown Los Angeles. The building structure is typical of tens of thousands of similar structures throughout the world. There is no mechanical ventilation, and air is provided by large gaps in the building shell—skylight vents and open doors and windows. The house exchanges its air with the outdoors approximately every 15 minutes. Both model calculations and observations of the white quartz deposition surfaces agree that perceptible soiling of walls takes one year or less. By applying what has been learned, the soiling rates in this building can be reduced by more than one hundredfold. The following exercise carried out at the

Sepulveda House can be accomplished at virtually any building for which a particle-reduction strategy is being considered or for which particle reduction may be included in a more general management plan.

Seven steps are presented that build on each other in improving the management of soiling. In its original state, the Sepulveda House had a characteristic soiling time of 0.9 and 1.5 years for walls and ceiling respectively. By adding a conventional mechanical system with filtration only good enough to protect the ventilation system itself—i.e., efficiencies of 15 to 35% per pass through the filters depending on the size of the particles—and sealing the major gaps in the shell, a reduction in the soiling rate of both types of surfaces of slightly better than 40% can be achieved. This type of operation would have been popular prior to the 1970s, before energy conservation was such an important issue. But since the 1970s, reducing high levels of outdoor airflow through the building has been a priority. This outdoor air is called make-up air. By providing just the right amount of outdoor air required for a design occupancy of 20 persons per 1,000 square feet (ASHRAE 1985), plus reducing all make-up air at night and when the building is closed, improvements of 50 to 60% are possible.

The next level of improvement has been discussed by the conservation field itself through debate on the draft ANSI standard (1985) for the storage of library and archival documents. Using these suggested filtration requirements as the basis for substituting higher efficiency filters in the mechanical system, the reduction in soiling time jumps by tenfold, or to 30 to 45 years for walls and ceilings. Even without further modifications soiling rates are achieved that are twice as slow as the sophisticated HVAC-equipped Norton Simon Museum with its nevertheless lower efficiency filters.

Often older buildings have extant ducting for central furnace-style heating. However, when they do not, or when economics plays a vital role, the authors do consider ductless consoles as a potential solution. The reader is cautioned about going down this road, because in a study by Offermann et al. in 1985, half the units tested had effective cleaning rates so small they would be useful for little more than closets. These units may have worked adequately in large display cases, but the conservation field does not need preventive steps that do too little too late.

Thirty to forty-five years is a very long time before visible soiling may occur. Arguably, most museum directors would hesitate to go further, knowing full well that their institutions would now rank among the highest in performance. Since this period of time is longer than the average career length of a museum director, this may also play a part in a spiritless response. Notwithstanding, for those with the will to persevere—and, in particular, for those engaged in new building construction—soiling risks can be reduced from decades to centuries.

The improvements the authors suggest have been shown to work within the boundaries of common design. To go beyond these initial levels of improvement requires an

understanding of how soiling rates are influenced by the surface-boundary layer of a wall or ceiling, airflow in and adjacent to those layers, and any temperature variations present. In general, three air flow regimes types exist that have dynamic roles to play on surface soiling: homogeneous turbulence, natural convection, and laminar airflow. Turbulent airflow is popular and conventional because it ensures rapid air mixing for thermal and humidity control, but it also promotes particle deposition. Air is usually discharged by small vents near the top of walls at relatively high velocity. Natural convection can be turbulent or nonturbulent depending on other climatic variables and/or building geometry. But laminar airflow, or displacement, ventilation models provide the least particle deposition because they have the smallest disruptive effect on surface-boundary layers. The Norton Simon Museum is an excellent example of an environment in which a large volume of air is introduced through perforated acoustical ceiling tiles and returned via gallery halls. Rather than small registers injecting air at high velocity, millions of tiny holes provide a system closer to an overhead diffuser than to a conventional ventilation system. By designing the building to operate in this manner, almost 22,000 cubic meters of air are recirculated every ten minutes. The experimentally derived particle-deposition velocities that result are the lowest of the five museums in this study.

Results such as these excite the imagination. If all factors that contribute to the destruction of cultural and natural objects were divided into basic classes, one might postulate that there are only two possible classes: that which is *intrinsic* to the object and that which is *extrinsic.*

Intrinsic deterioration includes both inherent vice contributed by the artist or artisan in which faulty or incompatible materials or construction methods are used, and chemical composition unique to the object. Acidic hydrolysis of paper, loss of plasticizers from cellulose nitrate, incompatible pigments, and buffered storage products in contact with some photographic processes are all intrinsic problems. Even further, because oxygen cannot be excluded from museums in general, in spite of improvements in display-case technology, oxidation from atmospheric oxygen is effectively a materials-intrinsic process.

Extrinsic deterioration is by far the larger and more ominous class. It is here that one may bundle the effects of light, humidity, temperature, gaseous and particle air pollution, natural and manufactured disasters, and all possible synergistic interconnections of these influences. It is precisely this class that the conservation and museum communities have identified as the most important class when they prioritize preventive conservation over treatment.

Ironically, it is this class that the scientific community knows most about. Conservation scientists have measured the effects of light on everything from silk to dyes; of humidity and temperature on paintings, paper, and textiles; of air pollution on pigments, dyes, metals,

paper, textiles, and synthetic polymers; and of natural disaster and wars on whole cultural patrimonies. We know so much, yet frequently do so little. From all the available literature, it is theoretically possible to build a museum in which the life spans of objects are determined solely by their intrinsic decomposition. In this ideal setting, one could establish an environment in which the most fragile of such collections would outlive any present or past civilization and—barring external destruction—could last, not centuries but many millennia. Whether such a museum is ever built, one may be encouraged by the knowledge that it remains within our province to approximate that goal.

James R. Druzik
Conservation Scientist
The Getty Conservation Institute

1 Soiling Due to Airborne Particles

The soiling of works of art due to deposition of airborne particulate matter poses a hazard to museum collections. Over long periods of time, dark deposits build up on the surfaces of paintings, sculptures, and stone buildings necessitating cleaning procedures that are expensive and that may pose some risk to the works themselves. Some objects such as old, fragile textiles and tapestries may be almost impossible to clean once they have become soiled.

In addition to soiling by airborne particles, the conservation literature suggests that deposited airborne material can attack collections chemically. Alkaline particles released indoors such as dust from concrete in new buildings are reported to have caused problems in Japan (Toishi and Kenjo 1967, 1968, 1975). Also, one expects metal corrosion to be accelerated by deposition of the acidic particles present in photochemical smog. A recent review of the literature on how to protect museum collections from air pollutants, however, notes that surprisingly little is known about the chemical nature of indoor particulate matter (Baer and Banks 1985).

The rate of deposition of particles onto surfaces is governed by the atmospheric particle concentration and by the size distribution of those particles. Large particles sediment out of the atmosphere under the influence of gravity. Fine particles are driven to surfaces by Brownian diffusion, assisted at times by other processes such as thermophoresis. Once the particles have deposited, their optical appearance and chemical interaction with works of art depend on the details of the chemical composition and morphology of the particles. The effectiveness of air-cleaning devices also depends on particle size, with fine particles (smaller than 1 μm in diameter) being much more difficult to remove than larger coarse particles (Friedlander 1977). The technology for protecting works of art from airborne particles must rest on a firm understanding of the chemical composition and size of the particles present.

Experience with outdoor air-pollutant measurements shows that airborne coarse particles cluster into distinctly different size ranges with different chemical properties. Coarse particles (with diameters of about 2 μm and larger) consist largely of soil dust, road dust, and sea salt. Fine particles smaller than 2 μm in diameter consist of vehicle exhaust material, soot, ammonium sulfate, ammonium nitrate, and sometimes sulfuric acid. Under polluted conditions, the outdoor air fed to building ventilation systems contains roughly comparable amounts, by mass, of coarse- and fine-particle material. Fine airborne particulate matter contains soot and acidic materials and is characteristically black, while coarse material contains soil-dust components and thus appears brown when collected on a white surface (such as paper). If soiling is to be prevented, control of both fine and coarse particles must be considered.

Air-filtration devices characteristically remove coarse particles quite efficiently, but often leave the fine soot-containing fraction uncollected. Yocom et al. (1971) examined indoor and outdoor soiling index ratios in air-conditioned versus non-air-conditioned buildings. They found that the soiling index ratios did not appear significantly different, indicating that

soiling particles were not effectively removed by the filters in the air-conditioning systems studied. If such a situation prevails in a museum, then the possibility of damage to the collection over long periods should be seriously considered.

Objectives and Approach

The purpose of the research effort reported here is to establish some of the physical and chemical pathways by which airborne particulate matter acts to damage works of art. Emphasis will be placed on understanding how to break the chain of events leading to the soiling of art objects by particulate matter. We seek to answer the following questions:

1. What are the ranges of chemical composition, concentration, and size distribution of the airborne particulate matter found in the indoor atmosphere of museums?
2. What physical mechanisms govern the transfer of particles from room air to the surface of works of art? How rapid are these deposition processes?
3. How do the deposited particles alter the appearance of a surface?
4. Can particulate matter deposition processes within buildings be modeled on the computer in a way that will aid in the design of a new museum?
5. What approaches can be devised that will protect works of art from damage by airborne particulate matter?

A program of measurements and computer-based data analyses addresses these questions. In Chapter 2 of this research summary, indoor and outdoor measurements of airborne particle composition and particle deposition rates at five Southern California museums are reported. This work provides baseline data on existing conditions in a variety of museums and helps to explain significant differences between the museums, based on the general nature of their construction and ventilation system design. Chapter 3 describes a mathematical model that predicts the concentration, chemical composition, and size distribution of indoor airborne particles as well as particle deposition rates to indoor surfaces. The purpose of this model is to provide a tool that can be used to evaluate particle deposition control methods prior to the construction of a new museum and to provide a method for examining the degree of improvement that could be obtained by modifying an existing facility. This model is tested against a detailed program of airborne particle concentration and particle deposition measurements made at Southern California museums, as reported in Chapter 4. In Chapter 5, the measured and computed particle fluxes to indoor surfaces in museums are compared to the changes in the optical appearance of white surfaces placed in Southern California museums in order to test the connection between particle deposition and observable soiling.

Protection of works of art from soiling due to the deposition of airborne particles is discussed in Chapter 6. The completed indoor-outdoor particulate air quality and deposition model is employed to study the effect of alternative control measures that could be employed to retard soiling by airborne particles. These methods include:

1. Increasing the efficiency of airborne particle filtration by mechanical ventilation systems
2. Reducing the rate of induction of outdoor particles into a building
3. Placing objects within display cases or glass frames
4. Managing the outdoor area surrounding the building to achieve lowered outdoor particulate matter concentrations
5. Eliminating indoor particle sources
6. Reducing the particle deposition velocity (e.g., the particle flux per unit of atmospheric particle concentration) onto surfaces of concern

The simultaneous use of several of these control measures may be advisable in order to lengthen the time before soiling due to deposited particles would become noticeable.

The present report serves as a summary of the major findings of this research effort and is prepared as a condensed version of the final project report (Nazaroff et al. 1990).

2 Characteristics of Airborne Particles Inside Southern California Museums

In the absence of particle-filtration systems, concentrations of suspended particles indoors can be as high as or higher than those outdoors (Biscontin et al. 1980, Dockery and Spengler 1981). Filters for particle removal have been incorporated into most museum heating, ventilation, and air-conditioning (HVAC) systems for many years. But surprisingly little attention has been paid to the effect that these particle-removal systems have on the concentration, chemical composition, and size distribution of airborne particles within museums. Studies that have been conducted on particle composition and removal within museums generally have been designed to resolve specific problems encountered in a particular building; for example, the generation and deposition of cement dust inside a freshly poured concrete structure (Toishi and Kenjo 1967, 1975).

An experimental program was initiated to determine the extent to which museum ventilation systems modify the concentration and composition of airborne particulate matter entering from outdoors. Information was sought to identify particulate chemical species for which there may be indoor sources. Additional facets of the present study include measurements of the accumulation rates and deposition velocities of particles to vertical and horizontal surfaces inside museums, and modeling studies of indoor particle concentrations and deposition on surfaces. Taken as a whole, this information provides a series of methods for assessing the effectiveness of building ventilation systems in protecting artifacts from damage due to the intrusion of outdoor particulate air pollution. The present chapter defines baseline conditions for particulate air quality inside and outside the museum sites studied, presents evidence for indoor sources of particles, and examines the particle-deposition rates to surfaces within the museums studied.

Experimental Methods: Sample Collection

Five California sites were chosen for indoor and outdoor airborne particle sampling: (1) the J. Paul Getty Museum in Malibu, (2) the Norton Simon Museum in Pasadena, (3) the Virginia Steele Scott Gallery located at the Huntington Library in San Marino, (4) the Southwest Museum in Los Angeles, and (5) the Sepulveda House located in El Pueblo de Los Angeles State Historic Park in downtown Los Angeles. The first three sites are modern museum structures equipped with sophisticated HVAC systems that include filters for particle removal. The Southwest Museum is a turn-of-the-century poured-concrete structure that has central heating and zonal air conditioning in the hall in which sampling was conducted, but no supplementary particle-filtration system. The Sepulveda House is a partially restored nineteenth-century brick building

that has no mechanical ventilation system whatsoever. Building characteristics, ventilation system parameters, and particle-filtration devices at each museum are described in Table 2.1.

Site	Use[a]	Ventilation system[b]	Outdoor air exchange rate (h^{-1})[c]	Indoor air recirculation rate (h^{-1})[d]
Sepulveda House	1	I	1.6–3.6	0
Southwest Museum (California Room)	2	II	0.3[e]	nd[f]
Norton Simon Museum	3	III	0.4–0.7	5.4
Scott Gallery	3	III	0.3–1.0[g]	8.2
Getty Museum (Gallery 121)	3	III	1.2–1.3[f]	7.1

a. Uses: (1) historical museum, (2) archaeological museum, (3) art museum.
b. Ventilation system types: (I) no mechanical ventilation system, (II) partial forced ventilation system, no additional particle filtration, (III) modern heating, ventilation, and air-conditioning (HVAC) system with particle filtration.
c. Air changes per hour due to outdoor make-up air plus infiltration. Range of measurements obtained from perfluorocarbon tracer tests from the summer and winter sampling periods, and sulfur hexafluoride tracer tests for a 24-hour period in spring of 1988.
d. Air changes per hour provided by recirculation of indoor air.
e. Summer and winter seasons.
f. nd = not determined.
g. Summer and spring seasons.

Table 2.1. Building characteristics of the study sites.

Ambient 24-hour samples of both fine ($d_p < 2.1$ μm) and total airborne particulate matter were collected indoors and outdoors at each site. A schematic of the samplers used is presented in Figure 2.1 (p. 37). Air drawn through the fine-particle sampler first passed through a cyclone separator (John and Reischl 1980) for removal of coarse particles ($d_p > 2.1$ μm). The airflow was then divided between several parallel 47-mm diameter filter assemblies, each containing a filter substrate compatible with a particular chemical analysis procedure. The chemical analysis procedures used allowed measurements to be taken of an almost complete material balance on the chemical composition of the particles present including organic carbon, elemental carbon (black soot), ionic materials, and trace metals. These chemical analysis procedures are described in detail in the final project report (Nazaroff et al. 1990). In the total particle sampler, the same filter substrates were employed in open-face filter holders. A Teflon-coated metal sheet was positioned above the open-face filter holders in order to prevent the sedimentation of large particles onto the filters. Critical flow orifices (Millipore; Bedford, Mass.) were used in both the fine- and total-particle samplers to control the flow rate individually through each filter assembly.

Each indoor total-aerosol sampler contained a polycarbonate membrane filter (Nuclepore, 1.0 or 0.4 μm pore size) that had been precoated with vapor-deposited carbon for examination with an automated scanning electron microscope (SEM). The flow rate through the Nuclepore filters was set at 1 LPM to minimize overloading of particles on the filter surface.

Each site was equipped with indoor-vertical and upward-facing horizontal deposition plates. The deposition plates used for single-particle analysis by automated SEM techniques consisted of freshly cleaved mica sheets (Ted Pella, Inc., Redding, Calif.) that had been precoated with a layer of vapor-deposited carbon in order to provide a conductive surface for the electron beam. The plates had dimensions of 5.1 cm x 7.6 cm and approximate thicknesses of 0.03 cm. Some of the mica plates were attached to the walls with thermal joint compound (Thermalcote; Thermalloy, Inc., Dallas) to ensure good thermal contact with the wall. Other mica plates were attached to small, stretched artists' canvases that were then hung on the walls. Other deposition plates were deployed to collect material for analysis by bulk chemical and optical methods. These plates employed a variety of collection substrates mounted in thin (3 mm) aluminum frames. The frames were machined with beveled edges to minimize disruption of the boundary layer airflow along the wall. Deposition surfaces included Teflon-membrane filter material (20.3 cm x 25.4 cm, 1 μm pore size, Zefluor; Gelman, Ann Arbor, Mich.) for collection of material to be analyzed for ionic species, quartz fiber filter material for elemental and organic carbon determination, and paper and canvas for optical analysis. (Results from the carbon and optical analyses will be presented in Chapter 5.) Also included were polycarbonate membrane deposition surfaces (Nuclepore filter material without holes; Nuclepore, Pleasanton, Calif.) that were precoated with vapor-deposited carbon and used as alternative substrates for the automated SEM analysis. The aluminum deposition-plate frames were also affixed to the walls with thermal joint compound and secured with small nails at the edges.

The ambient and deposition sampling was conducted during a summer period (July 2 through August 31, 1987) and a winter period (November 23, 1987, through January 30, 1988). During each of these periods, ambient samples were collected every sixth day. The deposition plates were placed at each site approximately one week prior to each seasonal sampling period, and remained in place throughout the sampling period. An additional set of vertical deposition plates was deployed at the beginning of the summer period and left in place for a full year. The vertical plates were attached to walls at heights of 3 to 4 m to avoid public interference. The upward-facing horizontal plates were located on top of display cases at the Southwest Museum and Scott Gallery, on a high ledge at the Getty Museum, on an alcove off a stairway landing at the Sepulveda House, and on a small table behind a partition at the Norton Simon Museum. At each site, except at the Sepulveda House, the deposition plates and ambient samplers were located in galleries where artworks or artifacts were displayed. At the Sepulveda House, the aerosol samplers and a full set of deposition plates were located in the central corri-

dor of the building. Most of the artifacts on display at the Sepulveda House during 1987–88 were located in a small room that was isolated from the rest of the building by a glass partition. An additional subset of deposition plates was placed in this room, but long-term ambient sampling was not possible there.

Results and Discussion

Indoor and Outdoor Particle Mass Concentrations

The time series of indoor and outdoor fine- and coarse-particle concentrations, with the summer and winter periods for each, are shown in Figures 2.2 and 2.3 (pp. 38–39, 40–41) respectively. The highest outdoor concentrations for both fine and coarse particles were observed at the Sepulveda House site (mean concentrations for fine and coarse particles were 30 and 86 $\mu g\ m^{-3}$ in the summer, 62 and 70 $\mu g\ m^{-3}$ in the winter; highest fine concentration was 154 $\mu g\ m^{-3}$ on December 11, 1987, and highest coarse concentration was 132 $\mu g\ m^{-3}$ on January 22, 1988). The lowest outdoor concentrations were found at the Getty Museum, which is located generally upwind of the city of Los Angeles, near the coast (mean concentrations for fine and coarse particles were, 15 and 34 $\mu g\ m^{-3}$ in the summer; 21 and 27 $\mu g\ m^{-3}$ in the winter; highest fine concentration was 49 $\mu g\ m^{-3}$ on December 11, 1987; and highest coarse concentration was 52 $\mu g\ m^{-3}$ on August 19, 1987).

Figure 2.2 (pp. 38–39) shows that indoor fine-particle concentrations at the Sepulveda House were nearly identical to those outdoors. This is not surprising in view of the fact that the building has no air-filtration system and that, during the hours when the building is open to the public (10 a.m. to 3 p.m. daily, except Sunday), two large doors on the lower floor and several windows on the upper floor are kept open, leading to large outdoor air-exchange rates. In addition, large gaps around the exterior doors, combined with ceiling vents, lead to relatively large outdoor air-exchange rates even when the building is closed. However, as shown in Figure 2.3 (pp. 40–41), coarse-particle concentrations indoors at the Sepulveda House are substantially lower than those outdoors even under these rapid ventilation conditions. This reduction in coarse-particle concentration represents particle depletion by gravitational settling of airborne particles onto indoor surfaces, combined with their possible removal during the passage of air through narrow cracks in the building shell.

The Southwest Museum has no central air-conditioning system and relies on a system of high-powered fans to circulate air through the main section of the building. The California Room, in which the ambient samplers were located, has a local air-conditioning system that draws air from an interior hallway connected to the main, unconditioned space in the building. Consequently, the outdoor air-exchange rate for this room is lower than that for the main

portion of the building. There is less correlation between the indoor and outdoor concentrations at the Southwest Museum than was observed at the Sepulveda House. While indoor fine-particle concentrations at the Southwest Museum were considerably lower than outdoor concentrations on some days, they were occasionally higher than outdoor concentrations.

In contrast to the situations at the Sepulveda House and Southwest Museum, indoor particle concentrations at the three facilities employing sophisticated HVAC systems with particle filtration are substantially below those measured outdoors. The lowest indoor particle concentrations were found at the Norton Simon Museum. At this site, the outdoor air entering the ventilation system passes through a fibrous mat filter and an activated carbon filter, and is then blended with return air that has also passed through a fibrous mat filter. The supply-air blower at the Norton Simon Museum is shut off to improve thermal control, resulting in a low outdoor air-exchange rate and a high internal air-recirculation rate (Table 2.1). The high recirculation rate results in repeated passes of the indoor air through the particle filters before the air exits the building. The benefits of such a high ratio of recirculated air to outdoor air are demonstrated by the observed average fine-particle concentration reduction of 82% achieved at the Norton Simon Museum, in spite of the fact that the single-pass filtration efficiency of the filters used at the Norton Simon Museum ranges from only 5% for 0.3 μm diameter particles to 95% for 2 μm diameter particles, with a weighted average single-pass filtration efficiency for the fine fraction of about 35% (see Chapter 4). As shown in Figure 2.3 (pp. 40–41), the concentrations of coarse particles inside the Norton Simon Museum were extremely low.

Between the summer and winter study periods, an activated carbon system was added to the particle filtration system already in place at the Scott Gallery. At that time, the outdoor air-intake dampers to the mechanical ventilation system were closed, again in order to improve thermal control. Thus, during the winter study, the building was operated with a higher ratio of recirculated air to outdoor air. That change in operations is clearly reflected in the decrease in indoor fine-particle concentrations during the winter period.

At the Getty Museum, the indoor particle concentrations are low in an absolute sense, but the percentage reduction of the indoor concentrations relative to those outdoors is not as impressive as that achieved at the Norton Simon Museum. The Getty Museum employs bag filters for particle removal. However, the ventilation system that serves the main (Antiquities) floor only operates between the hours of 8 a.m. and 6 p.m. In addition, when the museum is open to the public, gallery doors on that floor are generally left open, allowing some unfiltered outdoor air to enter directly into the galleries despite attempts to pressurize the building so the airflow is directed outward.

Summer and winter seasonal average indoor-outdoor concentration ratios for fine and coarse mass at all sites are presented in Figure 2.4 (p. 42). The average indoor-outdoor ratios for particle mass ranged from 0.06 for coarse mass at both the Norton Simon Museum and

the Scott Gallery in the summertime, to 0.96 for fine mass at the Sepulveda House in the summer. In general, the indoor-outdoor ratios were larger for fine than for coarse particles, reflecting the decreased filtration efficiency for fine particles relative to coarse particles. With the exception of the Scott Gallery, no systematic differences were observed in the indoor-outdoor ratios between the summer and winter sampling periods. At the Scott Gallery, the elimination of outdoor make-up air supplied to the building's HVAC system, combined with an increase in the number of passes of recirculated air through the particle filters, resulted in a dramatic decrease in the mean indoor-outdoor ratios for fine mass from 0.63 in the summer to 0.19 in the winter. However, a corresponding change in the indoor-outdoor ratios for coarse particles was not observed. The indoor-outdoor coarse mass ratio at the Scott Gallery moved in the opposite direction, from 0.06 in the summer to 0.16 in the winter. This probably can be attributed to the fact that eliminating the outdoor make-up air to the mechanical ventilation system forces the exhaust from the building to be balanced by an increase in the amount of air that leaks unfiltered into the building or enters through the doors, rather than entering through the ventilation system.

Aerosol Chemical Composition

Material balances taken on the chemical composition of the outdoor and indoor aerosol samples in the fine mode are shown in Figure 2.5 (p. 43). In the fine mode, from 90 to 95% of the mass concentration measured at each site in the summer study was accounted for on the basis of the measured chemical species, while 83 to 92% was accounted for in the winter study. The fine-mass balances on the outdoor aerosol indicate a chemical composition similar to that found previously in the Los Angeles basin (Gray et al. 1986). The outdoor fine-particulate levels and composition at the Sepulveda House, the Southwest Museum, the Norton Simon Museum, and the Scott Gallery show similarities that reflect the fact that all are located within a 15 km x 5 km area in the central Los Angeles basin. Organic matter dominates the outdoor fine-particle mass at these sites comprising about 40% in both summer and winter. Sulfate is the second largest component of the fine mass in the summer (20%), while nitrate accounts for 20% of the fine mass in the winter. The outdoor fine-particle composition at the coastal Getty Museum site differs somewhat from that found at the sites in the central Los Angeles basin. Sulfates comprise about 30% of the fine-particle mass at this site in the summer, with organic matter comprising only 20%. In the winter, a chemical composition similar to that found at the other four sites is observed at the Getty Museum, although it is lower in absolute concentration.

At every site, the fine-particle mode indoors is dominated by organic material, comprising about 40% of the fine mass at the Sepulveda House, and up to 80% or more at the Getty and Norton Simon museums. Indoor concentrations of elemental carbon are of particular concern from a soiling perspective. The indoor concentrations of elemental carbon were uniformly higher in the winter than in the summer. The indoor seasonal averages for fine elemental

carbon ranged from 0.14 μg m^{-3} at the Getty Museum in the summertime to 7.4 μg m^{-3} at Sepulveda House in the wintertime. At the Norton Simon Museum and the Scott Gallery, the average indoor elemental carbon concentrations during the winter period were 0.7 μg m^{-3}. This concentration is not large compared to the concentrations observed at the Sepulveda House; but nonetheless, elemental carbon represented the second largest component of the indoor fine aerosol in the winter samples at those two sites.

Material balances on the chemical composition of the outdoor and indoor aerosol samples in the coarse mode are shown in Figure 2.6 (p. 44). Soil dust is the major component of the coarse-particle fraction. At the Getty Museum, the coarse-particle mode outdoors contains nearly equal amounts of soil-dust and sea-salt (Na + Cl) particles, reflecting the site's coastal location. At the inland sites, the sea-salt concentration is greatly reduced, and organic material and nitrates are second in concentration behind soil dust. The coarse-mode composition shows little variation from summer to winter, with absolute concentrations somewhat lower in the winter. The coarse-particle mode indoors was very small at the three sites with engineered HVAC systems and was dominated by soil dust and organic material. Coarse-mode concentrations were virtually undetectable at the Norton Simon Museum, where coarse-mass concentrations appeared to be $\leq$ 4 μg m^{-3}. At the other four sites, the measured species accounted for 46 to 74% of the measured indoor coarse-particle mass concentration in the summer, and 64 to 84% in the winter.

Indoor Sources

The observation that particulate organic matter concentrations inside at least two of the museums studied are often higher than those outdoors suggests that there may be indoor sources of organic particles. This possibility is particularly interesting because the usual activities associated with indoor organic particle generation, such as smoking and operation of combustion devices, are prohibited inside museums. From observations of the operations at these facilities, possible indoor sources include particles shed by the visiting public as well as maintenance operations such as floor waxing and vacuuming.

Particle Deposition

The slow rates of particle deposition indoors present an enormous challenge in terms of measurement because extremely sensitive analytical techniques and potentially long sample-collection times are required. Furthermore, in order to elucidate the fluid mechanical processes controlling indoor particle deposition, the particle deposition rates should be determined as a function of particle size. Deposition rates are usually reported in the form of a deposition velocity, which is not a physical velocity but rather the ratio of particle flux to a surface (number of particles per unit area per unit time) divided by the particle number concentration in the ambient

air adjacent to the surface of interest (number per unit volume), and thus has the dimensions of length per unit time.

Deposition velocities to vertical surfaces determined from the SEM analyses of deposited particles and airborne particle samples are presented in Figure 2.7a–c (pp. 45–47). These deposition velocities at all sites are in the range of 10^{-6} to 10^{-5} m/s. The vertical bars represent a $\pm$ 1σ confidence interval for the deposition velocity of the particles in the size interval surrounding that bar, considering the uncertainties in particle counting statistics, blank correction, filtration efficiency, and indoor ambient concentration variability from day to day. Also presented are the bulk-deposition velocities for sulfate determined by ion chromatographic (IC) analysis of extracts taken from the Teflon deposition surfaces. These values are presented in the form of boxes, where the vertical dimension again represents the $\pm$ 1σ confidence interval and the horizontal dimension represents the size range that contains 90% of the particles in the ambient samples that were classified by the SEM as sulfates. Because the bulk analyses were weighted by mass rather than by number, the sulfate deposition velocities would be expected to more closely represent the deposition velocities of the larger particles in the size range given.

Obtaining deposition velocities for the larger particles (0.6–2.1 μm) was difficult. Although such particles may represent a significant fraction of ambient aerosol mass, their number concentrations in both the ambient and vertical deposition samples were so low as to be statistically indistinguishable from the blanks in many cases. In Figure 2.7a–c (pp. 45–47), upper bounds for some deposition velocities in this size range are presented as dashed bars ending in an arrow at the lower end. The deposition velocities reported here for particles smaller than about 0.2 μm in diameter also should be considered uncertain due to particle losses during sample preparation. Because of this additional uncertainty, the deposition velocities for particles smaller than 0.2 μm in diameter are presented as dashed bars.

The Sepulveda House is located in downtown Los Angeles, where outdoor airborne particle concentrations are high. It is a partially restored, historic structure that has no central mechanical ventilation system for heating or cooling. Several large doors are left open during operating hours (10 a.m. to 3 p.m.) year-round. As a result, indoor fine-particle levels at this site are nearly as high as those outdoors, as shown in Figure 2.2 (pp. 38–39). In the presence of these high indoor particle concentrations, both the ambient and the deposition samples from the summer study were adequately loaded for analysis by the SEM technique, yielding the best set of data among the five sites studied on particle deposition velocities as a function of size.

At the Sepulveda House, the wall on which the deposition plates were located was made of brick, painted, and partially plastered. Although it is not an exterior wall, it adjoins an unoccupied, unheated building. Two vertical mica plates were analyzed from the summer experiment at this site. Results from the mica plate that was attached directly to the wall are presented in Figure 2.7a (p. 45), while the results from the mica plate that was attached to a

stretched, framed canvas and thus insulated from the wall by an air gap of approximately 1 cm are presented in Figure 2.7b (p. 46). The two plates were located within a meter of each other on the same wall and at approximately the same height. It is interesting that, the deposition velocities from the wall-mounted plate (Fig. 2.7a) are essentially constant with respect to particle size over the size range 0.05–0.6 μm, while the deposition velocities to the canvas-mounted plate (Fig. 2.7b) show a decreasing trend with increasing particle size over the same size range. The deposition velocity for sulfate as determined by ion chromatography from a plate that was in thermal contact with the wall is also presented in Figure 2.7a; it is in good agreement with the SEM-determined deposition velocities for the wall-mounted plate.

While the results from a single experiment should not be viewed as conclusive, the differences between the deposition velocities presented in Figure 2.7a (p. 45) are in accord with theoretical considerations based on the differences in the thermal environment experienced by the two plates. The canvas-mounted mica plate, which was in thermal equilibrium with the room air, exhibits the decline of deposition velocity with increasing particle size, which would be expected for diffusion-controlled particle deposition (Nazaroff and Cass 1989). In contrast, the wall-mounted mica plate was in thermal equilibrium with the masonry wall. During the summer sampling period, the wall temperature at the Sepulveda House was generally 0.5 °C to 1.0 °C cooler than the room air throughout the daylight hours. When the temperature of a surface is cooler than the temperature of the surrounding air, thermophoresis causes increased deposition of the larger particles (Goren 1977), thus tending to level the deposition velocity as a function of particle size and yielding a profile similar to that seen in Figure 2.7a (p. 45). The ambient and deposited particle concentrations obtained at the four other sites were lower than the corresponding values at the Sepulveda House by factors of two to ten. With fewer deposited particles available to be measured, the deposition velocities obtained for these sites (Fig. 2.7b–c, pp. 46–47) exhibit higher uncertainties.

Deposition velocities to vertical surfaces measured for winter and yearlong periods at the Sepulveda House site are shown in Figure 2.8 (p. 48). The winter and yearlong deposition velocities at this site show remarkable agreement in terms of dependence on particle size, although the magnitude of the deposition velocity is roughly a factor of two lower for the yearlong study than for the winter.

The measured deposition velocities to upward-facing horizontal surfaces during the summer period are presented in Figure 2.9 (pp. 49–50). The horizontal deposition plate at the Sepulveda House is believed to have been interfered with during the sample collection period, therefore no results are reported for that site. Because of the effects of gravitational settling, deposition velocities increase with particle size at all sites. Also presented for comparison are a calculated gravitational settling velocity, based on a particle density of 2.5 g cm^{-3}, and a shaded region representing the sum of the measured deposition velocity to vertical surfaces

(used as a surrogate for diffusional deposition to horizontal surfaces) and the gravitational settling velocity. At the Southwest Museum (Fig. 2.9, p. 49), this shaded region agrees well with the measured deposition velocity to horizontal surfaces. At the other sites, the measured deposition velocity to horizontal surfaces is larger than the sum of the gravitational settling velocity and the deposition velocity to vertical surfaces.

At most of the sites, the deposition velocity measured by IC for sulfate is somewhat larger than the SEM-measured deposition velocities for the submicron particles. This may be due to the presence of a small fraction of the ambient sulfate on supermicron particles which have very high deposition velocities (Wall et al. 1988). The measurement of the deposition velocities to horizontal surfaces for larger particle sizes was limited by the low number concentrations of these particles in the ambient samples.

Bulk deposition velocities for all ionic species measured are presented in Table 2.2 (p. 31). The most notable feature of Table 2.2 is the difference in magnitude of the deposition velocities to horizontal versus to vertical surfaces. With the exception of ammonium ion, the deposition velocities of all species to horizontal surfaces are one to two orders of magnitude larger than those to vertical surfaces at the same site, due to the additional deposition to horizontal surfaces caused by gravitational settling. It is possible that ammonium was lost from the deposition surfaces during the long exposure time, resulting in erroneously low ammonium deposition velocities. The four species studied range from chloride, which is associated primarily with coarse sea-salt particles; to nitrate, which has both a coarse and a fine component (Wall et al. 1988); to sulfate and ammonium, which are primarily associated with fine particles. The deposition velocities to horizontal surfaces in Table 2.2 are generally consistent with this, with chloride ion exhibiting the highest deposition velocities at all sites, ammonium the lowest, and sulfate and nitrate in between.

At the Sepulveda House, sufficient quantities of ionic material were available so that deposition velocities to vertical surfaces could be determined with a high degree of precision. The results indicate that deposition velocities of sulfate, nitrate, and ammonium ions were about 5×10^{-6} m/s. Little difference is found from summer to winter and among the three species. An upper limit was calculated for the deposition velocity of chloride ion to vertical surfaces, based upon the ambient chloride concentration and the detection limit for chloride on the deposition plates. This upper bound for chloride is a factor of two or more lower than the measured values for the other ions, indicating that at the Sepulveda House the deposition rate of coarse particles to vertical surfaces was significantly lower than the deposition rate of fine particles.

Site	Species[a]	Deposition velocity (10^{-6} m/s)				
		Vertical surfaces			Horizontal surfaces	
		Summer	Winter	Yearlong	Summer	Winter
Getty Museum	SO_4^{2-}	11.7 ± 3.7	9.8 ± 4.7	11.0 ± 1.9	200 ± 50	130 ± 20
	NO_3^-	7.4 ± 5.3	11.0 ± 5.2	9.4 ± 2.0	440 ± 110	260 ± 70
	NH_4^+	nd[b]	na[c]	8.0 ± 1.8	7.5 ± 1.8	na
	Cl^-	nd	nd	5.4 ± 2.2	710 ± 180	650 ± 190
Norton Simon Museum	SO_4^{2-}	7.4 ± 3.7	< 7.8	2.0 ± 1.1	64 ± 12	74 ± 15
	NO_3^-	< 25	< 18	11 ± 5	320 ± 140	90 ± 30
	NH_4^+	nd	na	8.0 ± 5.2	10.4 ± 2.0	na
	Cl^-	nd	nd	nd	670 ± 440	1000 ± 700
Sepulveda House	SO_4^{2-}	4.0 ± 0.9	5.9 ± 1.4	4.8 ± 0.7	290 ± 60	370 ± 80
	NO_3^-	3.8 ± 0.8	2.5 ± 0.7	3.3 ± 0.6	750 ± 130	120 ± 40
	NH_4^+	2.7 ± 0.6	na	4.9 ± 1.5	27 ± 5	na
	Cl^-	nd	nd	< 1.4	2100 ± 400	820 ± 250
Southwest Museum	SO_4^{2-}	2.9 ± 1.0	< 2.8	2.2 ± 0.4	53 ± 10	150 ± 20
	NO_3^-	< 5.6	< 2.7	4.7 ± 1.2	280 ± 60	190 ± 60
	NH_4^+	3.8 ± 0.8	na	6.0 ± 1.2	4.6 ± 1.0	na
	Cl^-	nd	nd	< 3.7	320 ± 140	1400 ± 300
Scott Gallery	SO_4^{2-}	3.0 ± 1.7	< 9.3	1.7 ± 0.6	38 ± 7	1060 ± 190
	NO_3^-	7.8 ± 4.3	< 8.8	6.3 ± 1.5	110 ± 30	220 ± 60
	NH_4^+	7.6 ± 1.5	na	5.1 ± 2.1	29 ± 6	na
	Cl^-	nd	nd	nd	550 ± 260	1700 ± 1300

a. Number of ambient samples: 11 (summer); 12 (winter) except for the Getty Museum (summer = 10), Scott Gallery (winter = 13).
b. nd = species not detected on deposition plates.
c. na = not analyzed.

Table 2.2. Deposition velocities for ionic species inside museums.

At the Getty Museum, the deposition velocities to vertical surfaces are quite consistent from summer to winter and, like the Sepulveda House, little difference is observed between the deposition velocities found for sulfate, nitrate, and ammonium ions. Measurements for these species indicate a deposition velocity to vertical surfaces of about 10^{-5} m/s, or twice the value found at the Sepulveda House. The deposition velocity for chloride was about half that found for the other three species, indicating that the deposition velocity to vertical surfaces does decrease at the Getty Museum for particles larger than those measured by single-particle analysis in this study.

At the Norton Simon Museum, both indoor ambient and vertical deposition plate samples exhibited very low levels of most of the ionic species measured. The deposition velocities obtained are highly uncertain: Some measurements suggest deposition velocities as high as those observed at the Getty Museum, while other measurements indicate much lower deposition velocities. The deposition velocities of ionic species to vertical surfaces at the Southwest Museum and the Scott Gallery appear to be comparable to those at the Sepulveda House. In both cases, the yearlong results suggest a lower deposition velocity for sulfate than for nitrate and ammonium. The deposition velocity of chloride ion appears to be lower than for the other species at the Southwest Museum, while an upper limit for the chloride deposition velocity could not be calculated for the Scott Gallery.

The results for sulfate deposition from Table 2.2 can be compared to the results of Sinclair et al. (1985), who also measured ionic species deposition indoors with an ion chromatographic method. Sinclair et al. found deposition velocities for sulfate to vertical and horizontal surfaces to be 2.8×10^{-5} and 7.5×10^{-5} m/s, respectively. The deposition velocities to vertical surfaces for sulfate from Table 2.2 are in the range of 0.16 to 1.1×10^{-5}, a factor of three or more lower than those found by Sinclair et al., while the deposition velocities to horizontal surfaces for sulfate in Table 2.2 ranged from 4 to 19×10^{-5}, roughly comparable to those found by Sinclair et al. The higher deposition rates to vertical surfaces found by Sinclair et al. could be due in part to the use of metallic surfaces as deposition substrates in that study, and to the lack of data on the indoor ambient concentrations of the species for most of the deposition period.

Predicting the Mean Particle Deposition Velocity

The rate of deposition of particles onto a vertical surface depends on particle transport in the fluid mechanical boundary layer near the wall, which in turn varies according to details of near-surface air movement. If the airflow regime (forced laminar flow, natural convection flow, etc.) is known, particle deposition velocities can be related to the mean air velocity along the wall and the surface-air temperature difference, parameters that were measured during this study. Neither the data obtained in this study, nor previous field work inside buildings, constitute a basis

for conclusively identifying the airflow regime that prevailed over all the surfaces investigated. However, calculations still can be performed for alternative flow regimes with velocities and temperature differences that are consistent with the data taken in this study.

For the present chapter, three model airflow conditions are considered: (1) forced laminar flow parallel to the wall (L), (2) laminar or turbulent natural convection induced by the temperature difference between the wall and the nearby air (NC), and (3) homogeneous turbulence induced by forced and/or convective air movement in the core of the room (T). Analyses of these cases are presented in detail in the final report on this project (Nazaroff et al. 1990).

For comparison against experimental data, calculations of particle deposition velocity were carried out for each site and for each sampling season using up to three alternative airflow regimes, as detailed in Table 2.3. For each simulation, the time-averaged deposition velocity was computed for thirty-one particle diameters in the range of 0.01–10 μm.

	Case A	Case B	Case C
Getty Museum	NC(00-08;18-24) T(08-18)	T	NC(00-08;18-24) L(08-18)
Norton Simon Museum	L	T	–
Scott Gallery	L	T	–
Sepulveda House	NC(00-10;15-24) T(10-15)	T	–
Southwest Museum	T	–	–

T ⇒ homogeneous turbulence; NC ⇒ natural convection; L ⇒ forced laminar flow. Parentheses, where present, contain time of day (hours) over which indicated condition applies; otherwise, the condition holds at all times.

Table 2.3. Airflow regimes used in calculating particle-deposition velocities.

Comparing Modeling and Measurement Results

Figure 2.10 (pp. 51–54) presents a comparison of particle deposition velocity predictions and measurements for each of the five study sites. While the bulk sulfate deposition data are shown as a horizontal bar over the diameter range 0.1–1.0 μm, it is noteworthy that the size distribution of Los Angeles outdoor sulfate aerosols typically peaks strongly within the diameter range 0.5–0.7 μm. The vertical bars for deposition velocities measured by single-particle analysis reflect estimates of the $\pm 1\sigma$ measurement uncertainty, incorporating factors such as the effect of substrate differences between air samples and deposition plates, and statistical variation due to the small numbers of particles detected. The particle concentrations within the Norton Simon Museum were very low.

A statistically significant number of particles were detected on the mica plate for only two size ranges at this site.

Considering the predictions alone, the highest particle deposition velocities are obtained for the homogeneous turbulence airflow regime, and the lowest values are obtained for the laminar forced-flow regime. For any particle size, the differences in deposition velocities among sites for a given flow regime are generally smaller than the differences that would occur for alternative flow regimes at a given site. This observation can be explained as follows: For a given flow regime, the particle-deposition velocity varies as a function of near-wall air velocities. The average near-wall air velocities for the five sites vary over a narrow range—less than a factor of three. However, for a given near-wall mean velocity, particle transport to the surface for the homogeneous turbulence flow regime is much more rapid—characteristically an order of magnitude—than for the laminar forced flow regime due to the contribution of eddy diffusion.

The differences between predictions for winter and summer arise from the thermophoretic effect. Seasonal differences are greatest at the Norton Simon Museum and at the Scott Gallery, where the mean value of $T_{wall}–T_{air}$ changes sign from summer to winter.

Available information on the factors driving airflow and the corresponding comparison between measured and predicted particle-deposition velocities may be combined as a basis for deciding the most likely flow regime for particle deposition onto the wall studied at each site. Our appraisal of the information produces the following results: Getty Museum—homogeneous turbulence from 0800–1800 hours and natural convection at other times; Norton Simon Museum—laminar forced flow; Scott Gallery—geometric mean of homogeneous turbulence and laminar forced flow; Sepulveda House—either homogeneous turbulence at all times or homogeneous turbulence during 1000–1500 hours daily with natural convection at other times; Southwest Museum—homogeneous turbulence. Best-estimate values of particle deposition velocity as a function of particle size, obtained from modeling predictions for these flow regimes, are presented for several particle sizes in Table 2.4. The range of deposition velocities among sites for a given particle size is approximately 15–30.

Further discussion is warranted regarding the comparison between measurement results and predictions corresponding to these best-estimate values. At the Getty and Southwest museums, measurement results shown for the size ranges of the smallest particles are lower than the predicted values. The measurement of particles in these size ranges may be more uncertain than is reflected in the error bars. A large evaporative loss of very fine particles may occur during vapor deposition of carbon onto a sample in preparation for SEM analysis. If the losses are not constant from one sample to another, then the measured deposition velocity will be inaccurate in general. Since the measurement is based on the ratio of particles detected on only one deposition plate to those detected on several filter samples, the occurrence of large error is more likely to yield a result that is too low rather than too high.

$d_p(\mu m)$	Southwest Museum	Getty Museum	Sepulveda House	Scott Gallery	Norton Simon Museum
0.05	20.0	17.0	4.1–18.0	10.1	1.3
0.10	11.0	10.0	2.0–8.4	4.7	0.6
0.20	7.0	6.6	1.1–3.9	2.3	0.3
0.50	4.3	4.4	0.6–1.8	1.2	0.2
1.00	3.1	3.3	0.5–1.2	0.8	0.1

Obtained as the mean predicted deposition velocity for summer and winter periods, using the following flow regimes: Southwest Museum—T; Getty Museum—NC/T; Sepulveda House—range of values with lower limit corresponding to NC/T and upper limit corresponding to T; Scott Gallery—geometric mean of L and T; Norton Simon Museum—L. See Table 2.3 for definition of flow regimes.

Table 2.4. Best-estimate values of the annual average particle-deposition velocity (x 10^{-6} m s^{-1}) to the wall studied at each museum site.

At the Norton Simon Museum, the deposition-velocity data based on single-particle analysis for the smallest particles agree well with predictions for forced laminar flow. This flow regime is consistent with the general flow conditions in that building: Air is discharged into the galleries through perforated ceiling tiles and returned to the mechanical ventilation system at low velocity through the hallways. The measured deposition velocity for sulfates and for particles of 0.3 mm diameter is higher than that predicted for a laminar flow regime alone. Information about the size distribution of sulfates within this museum is lacking; furthermore, because of the low sulfate concentrations generally present in this museum, the sulfate-deposition velocity is based on samples that are close to the detection limit.

At the Scott Gallery and the Sepulveda House, the agreement between best-estimate predictions and measurements is very good. The agreement is excellent for the deposition plate mounted on a stretched canvas frame at the Sepulveda House.

Summary

The concentration and chemical composition of airborne particulate matter inside and outside of five museums was measured. Indoor-outdoor ratios for fine particles ranged from 0.18 at the Norton Simon Museum to 0.94 at the Sepulveda House, while indoor-outdoor ratios for coarse particles were lower, ranging from 0.06 at the Norton Simon Museum to 0.49 at the Sepulveda House. At the Sepulveda House, which lacked an air-filtration system, indoor fine-particle concentrations were virtually as high as those outdoors, indicating that urban museums lacking environmental control systems can face indoor soiling hazards nearly as great as those found

outdoors. At the sites where ventilation systems included conventional HVAC- system particle filters, the indoor airborne particles were mostly fine (< 2.1 μm in diameter) and consisted largely of organic matter. At two sites, indoor concentrations of organic matter exceeded outdoor concentrations by an average of about 3 $\mu g\ m^{-3}$. Indoor-outdoor relationships for elemental (black) carbon particles and soil-dust particles in museums are of particular interest because those species are light-absorbing and can produce visible soiling deposits on works of art. Black elemental carbon particles and fine soil-dust particles are found in local museum environments at concentrations of about 20 to 50% of the outdoor levels at facilities with particle-filtration systems. For buildings that lack conventional particle filtration systems, both fine and coarse indoor elemental-carbon and soil-dust particle concentrations ranged from about 50 to 100% of the concentrations outdoors. This implies that museums should especially watch for indoor soiling problems caused by elemental carbon and soil-dust particles.

Particle deposition velocities were measured inside five Southern California museums by an automated SEM technique. These represent the first direct measurements of particle-deposition velocities as a function of particle size inside commercial and institutional buildings. Deposition velocities to vertical surfaces were in the range 10^{-6} to 10^{-5} m/s for particles 0.05 to 1.0 μm in diameter at all sites but varied from site to site in terms of their dependence upon particle size. Deposition velocities were also measured by IC for particulate sulfate, nitrate, ammonium, and chloride ions. Time periods of two months to a year were employed for the collection of particles deposited to walls; indeed, at some sites, even longer collection periods would have been desirable.

Deposition-velocity predictions based on long-term measurements of surface-air temperature differences, shorter-term measurements of near-wall air velocities, and idealized representations of complex airflow fields were compared against the deposition-velocity measurements. The general concurrence of modeling and measurement results is encouraging. In those cases where the range of measured deposition-velocity values overlaps the predictions for alternative airflow regimes, further work is required to refine both the measurement and modeling methods.

Figure 2.1. Ambient fine- and total-particle samplers.

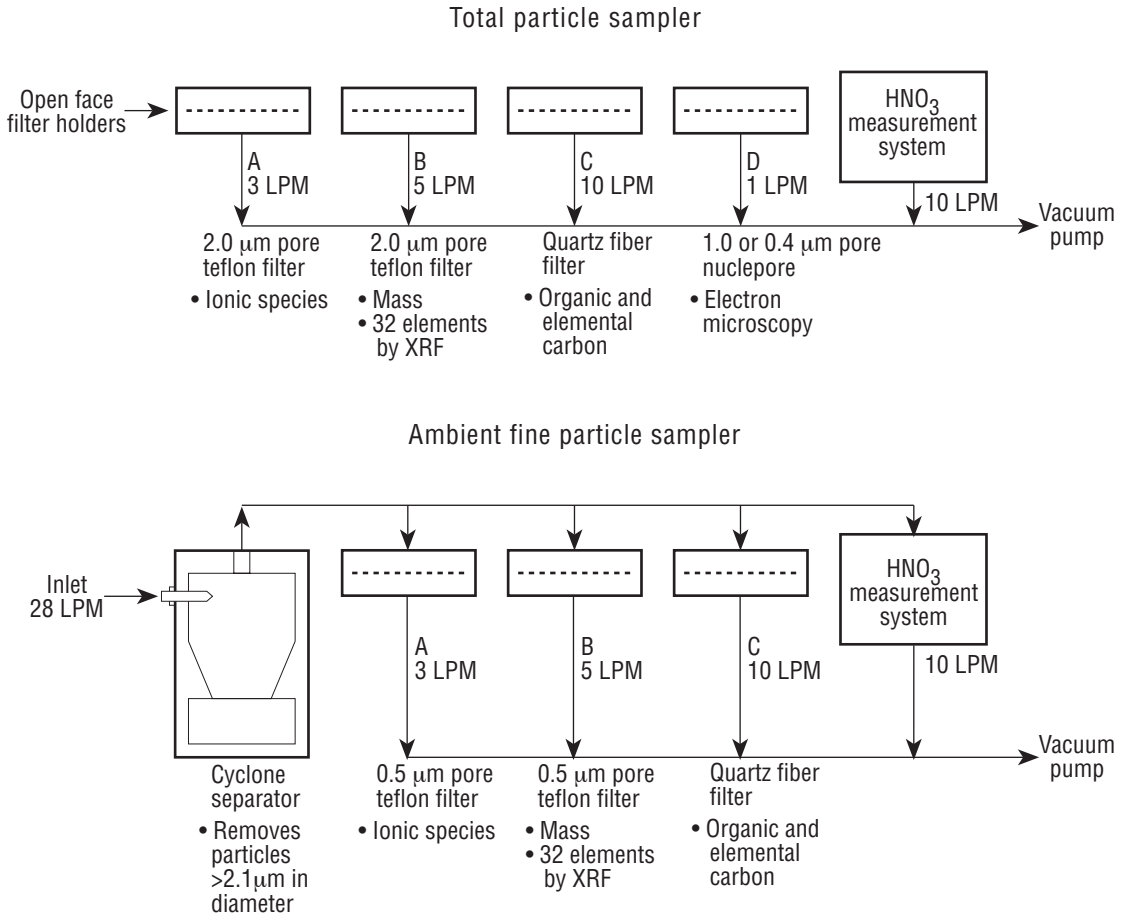

Figure 2.2. Time series of ambient fine-particle mass concentrations indoors and outdoors at five museums in Southern California.

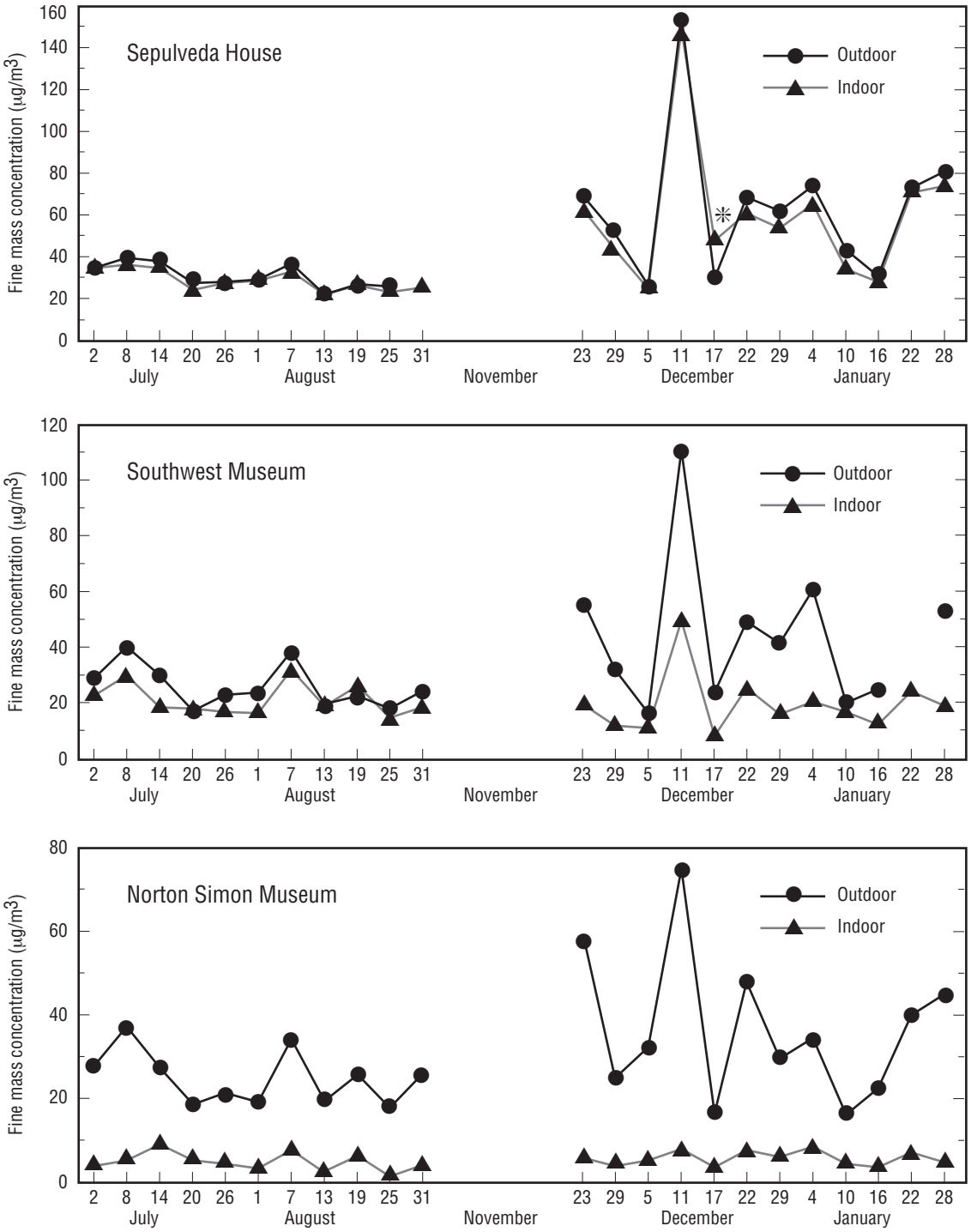

Figure 2.2. Continued.

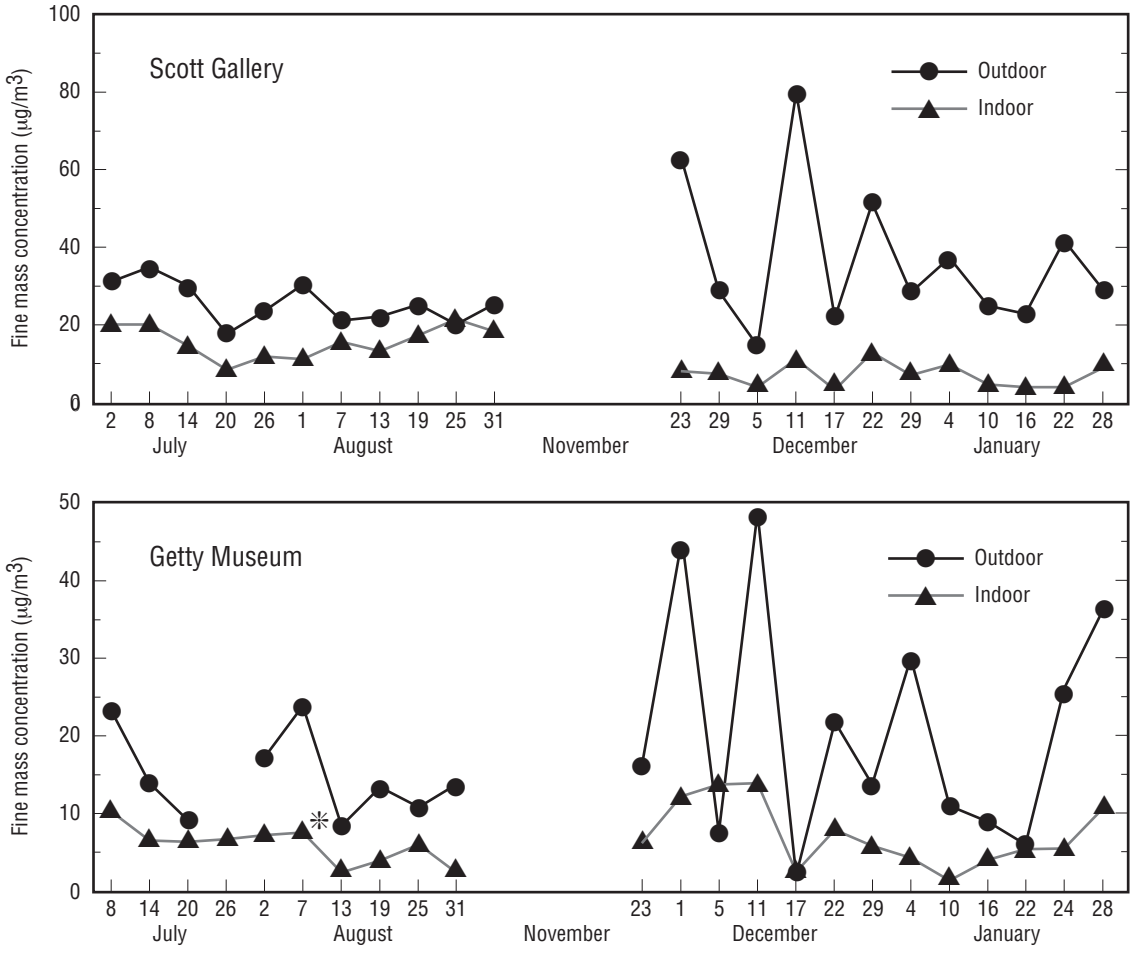

Figure 2.3. Time series of ambient coarse-particle mass concentrations indoors and outdoors at five museums in Southern California.

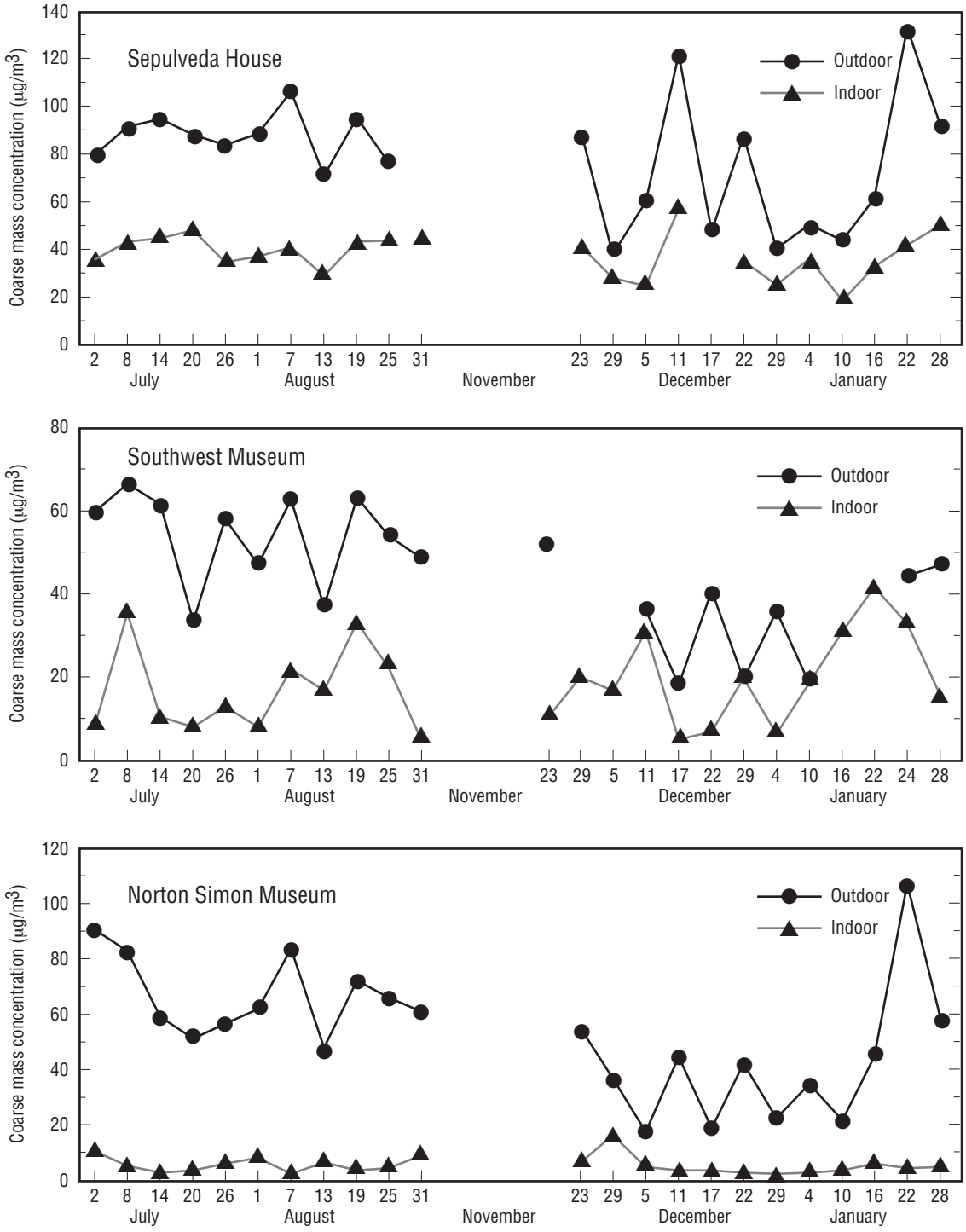

Figure 2.3. Continued.

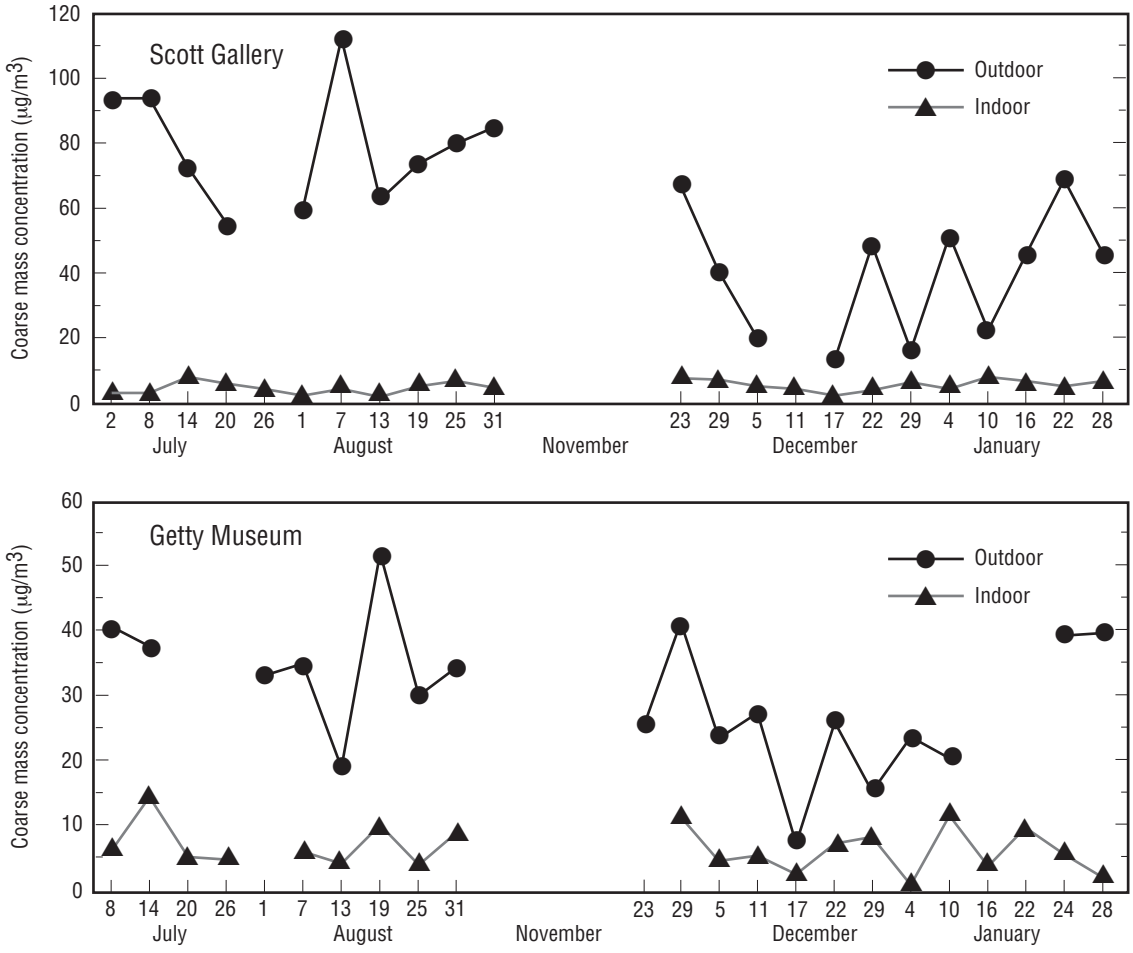

Figure 2.4. Seasonal mean indoor-outdoor concentration ratios for fine- and coarse-particle mass.

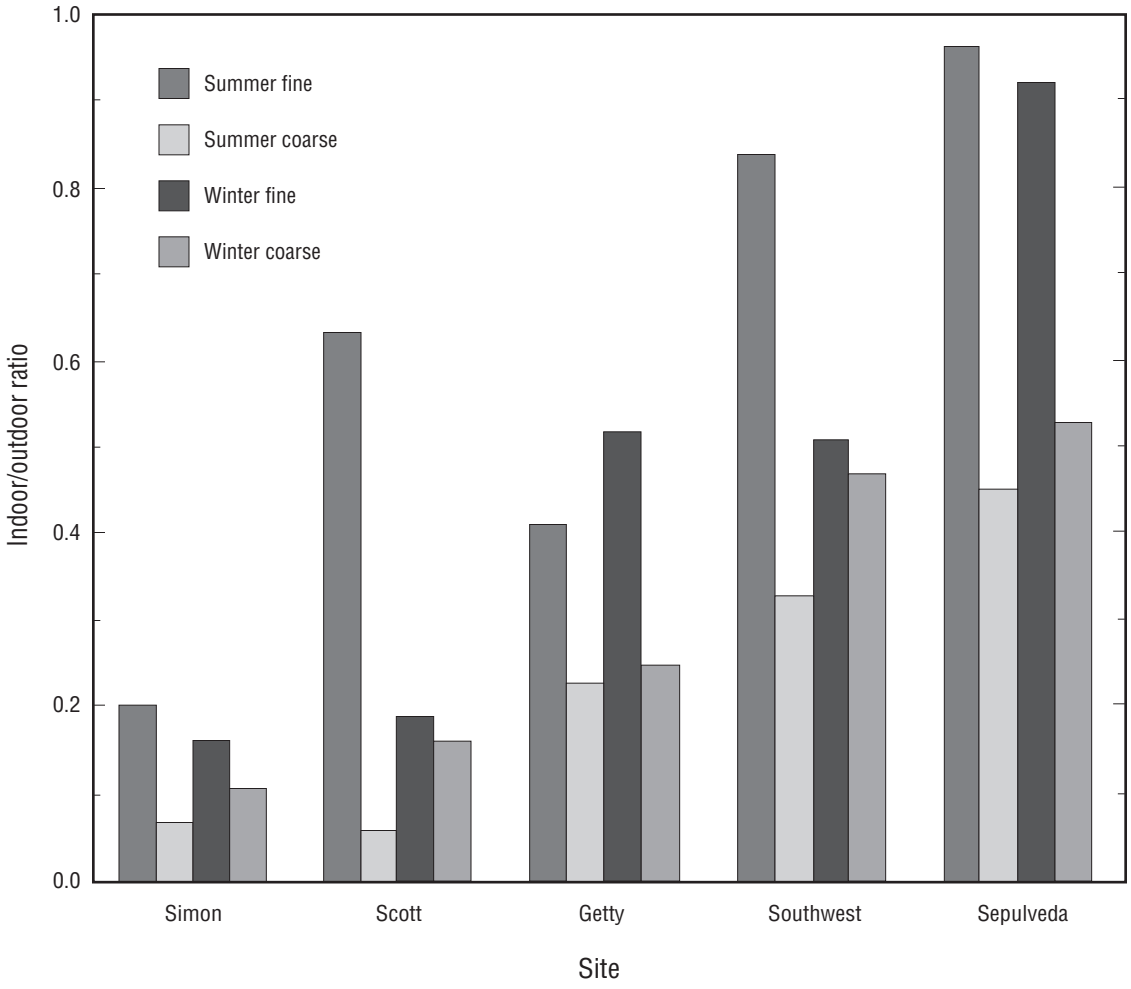

Figure 2.5. Seasonal mean chemical mass balances for outdoor and indoor fine particles.

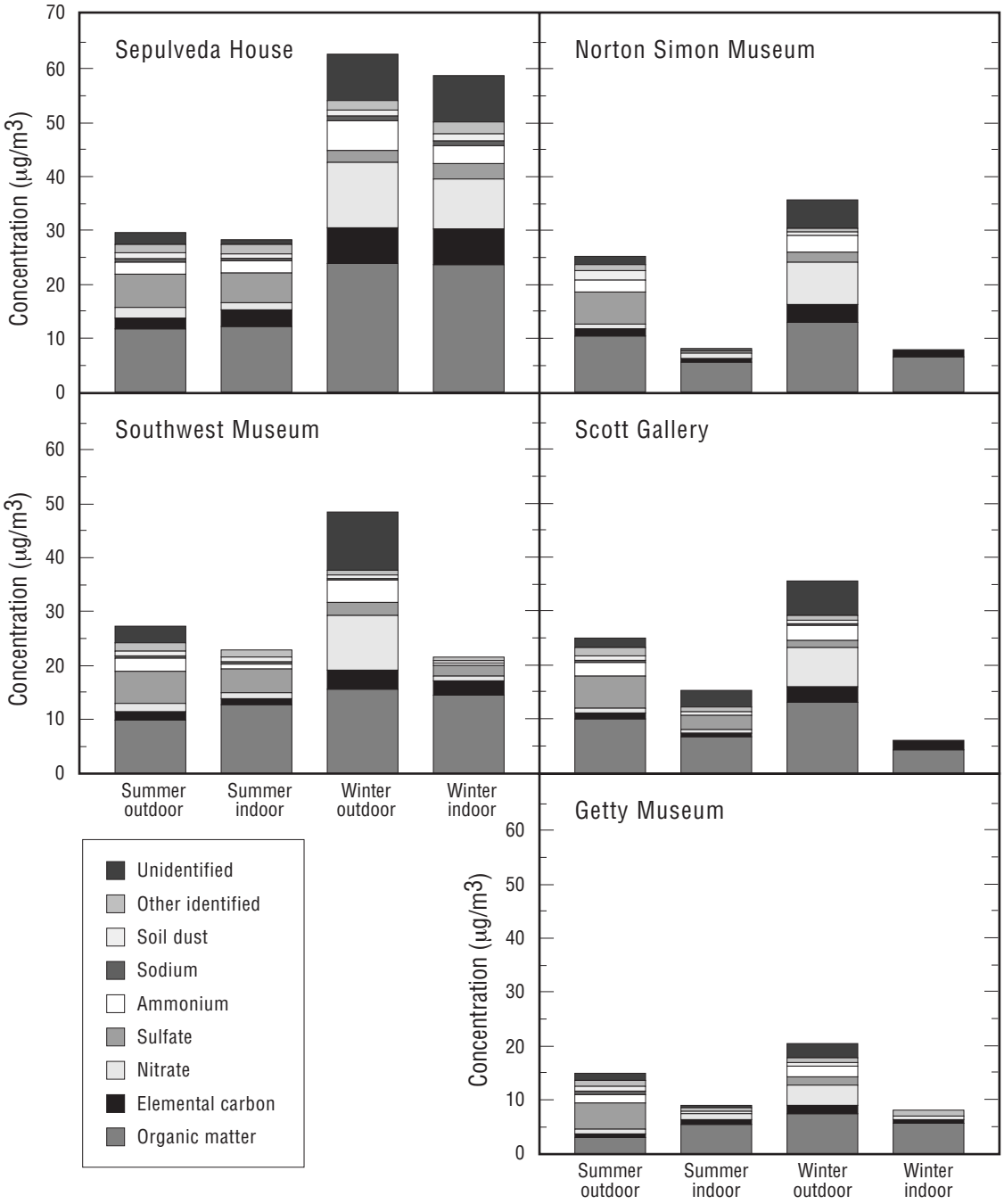

Figure 2.6. Seasonal mean chemical-mass balances for outdoor and indoor coarse particles.

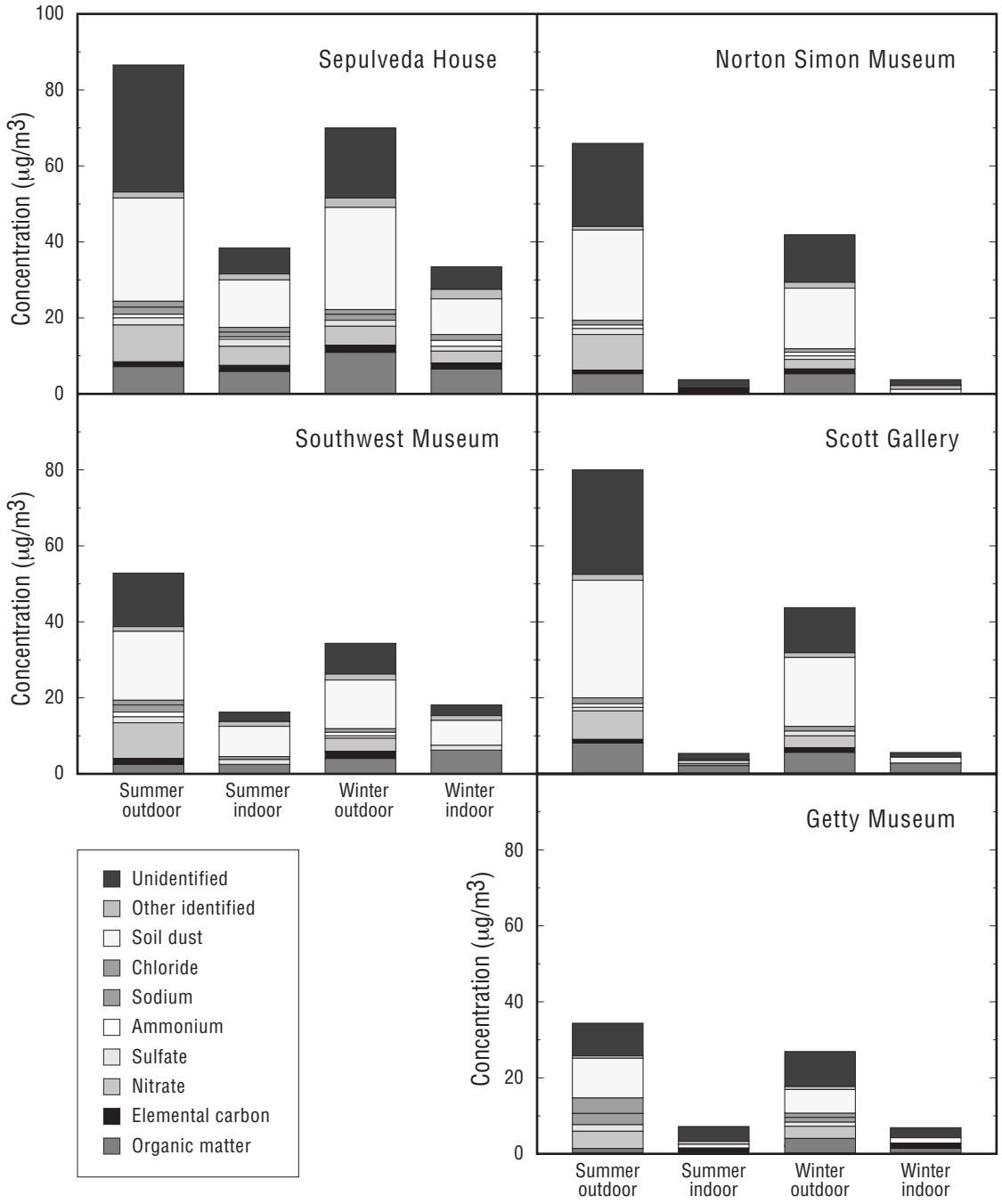

Figure 2.7a. Particle deposition velocities to vertical indoor surfaces at the Sepulveda House.

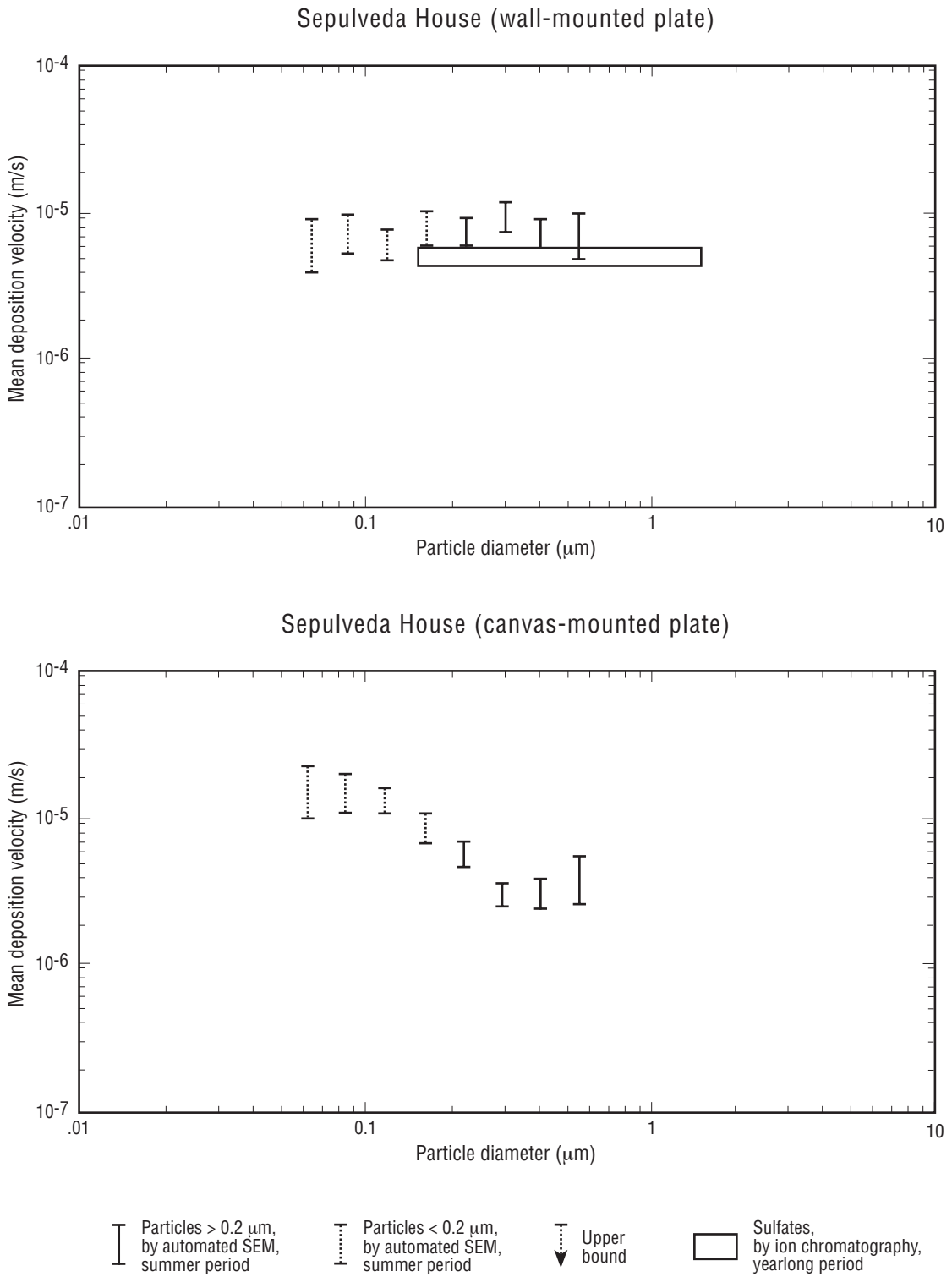

Figure 2.7b. Particle deposition velocities to vertical indoor surfaces at the Scott Gallery and the Southwest Museum.

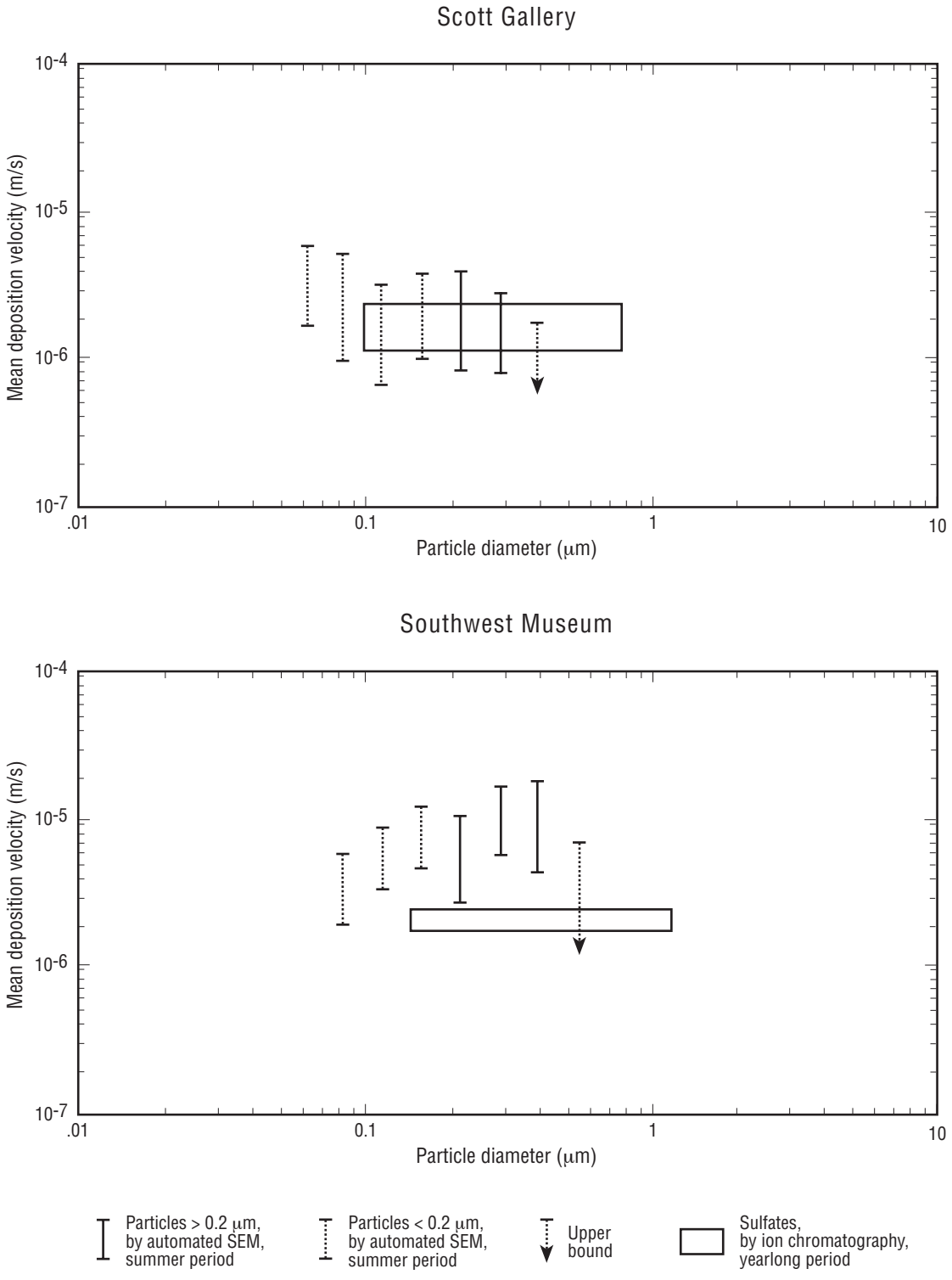

Figure 2.7c. Particle deposition velocities to vertical indoor surfaces at the Getty Museum and the Norton Simon Museum.

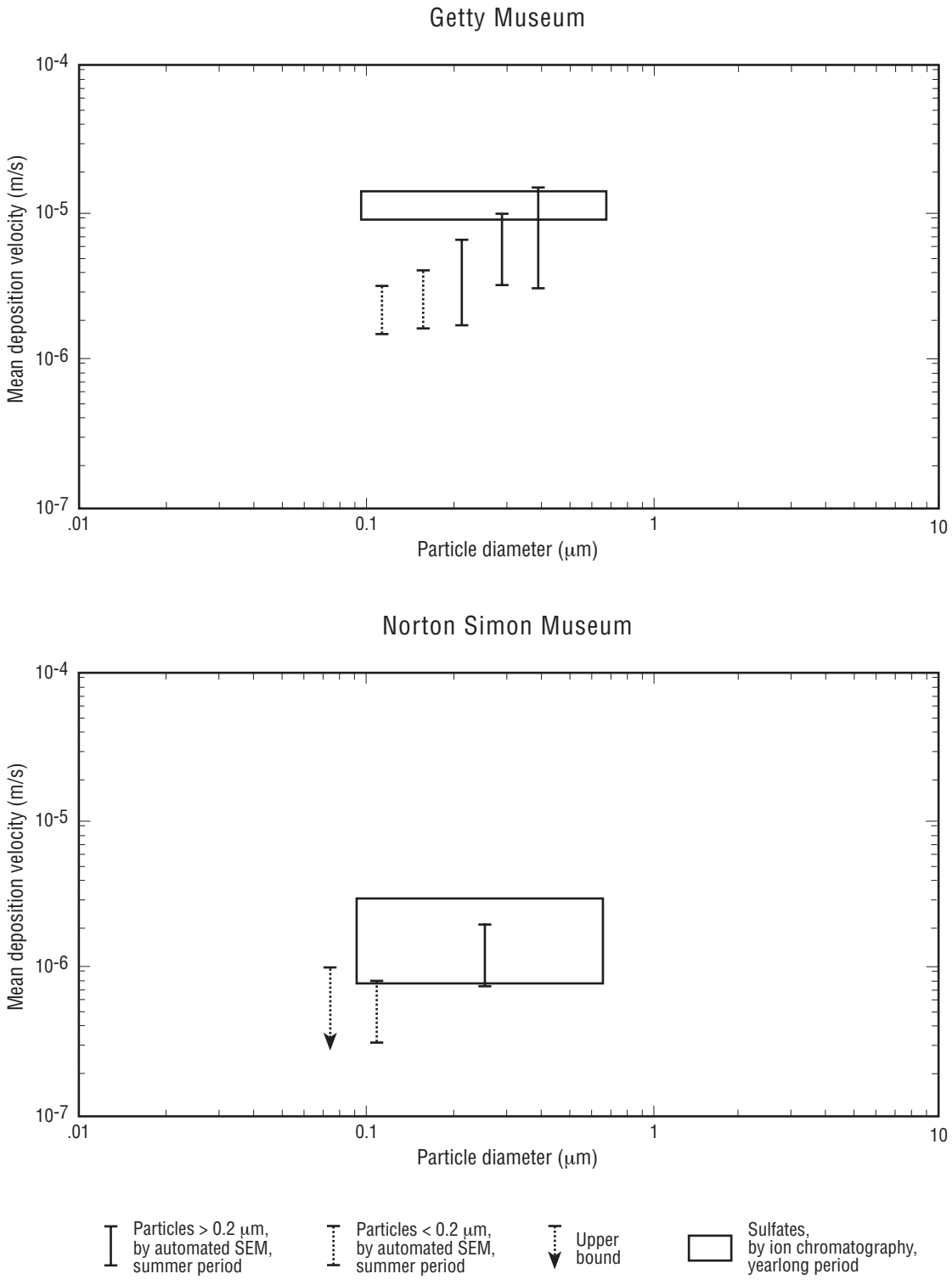

Figure 2.8. Particle deposition velocity estimates for vertical indoor surfaces during the winter and yearlong periods at the Sepulveda House, as measured by automated scanning electron microscopy.

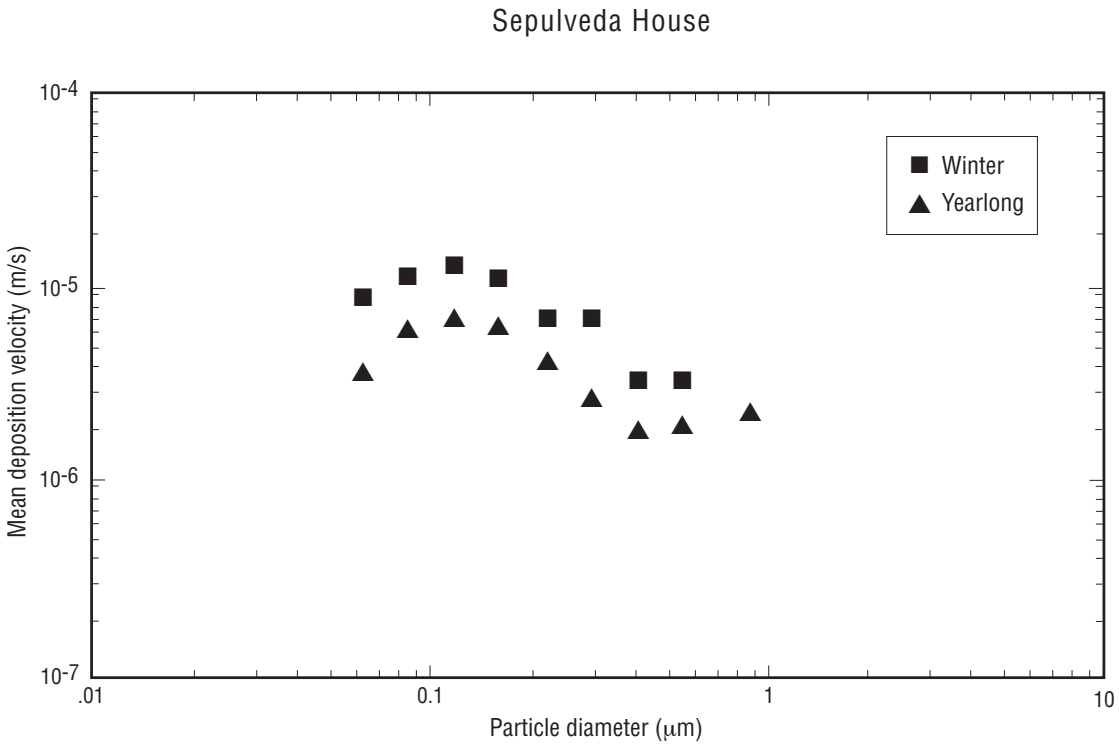

Figure 2.9. Particle deposition velocities to upward-facing horizontal indoor surfaces at four Southern California museums, and comparison to the sum of the measured deposition velocities to vertical surfaces and a calculated gravitational settling velocity.

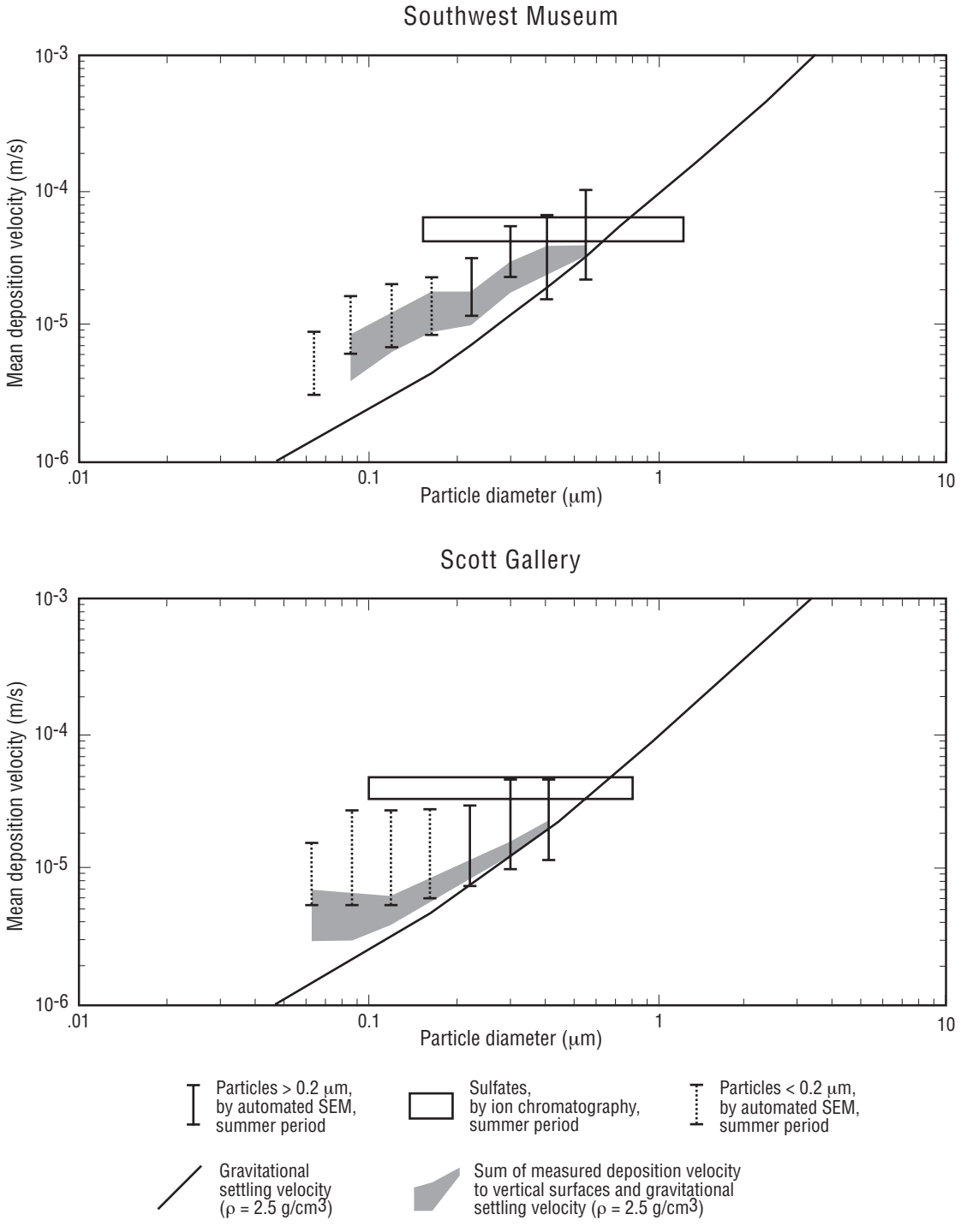

Figure 2.9. Continued.

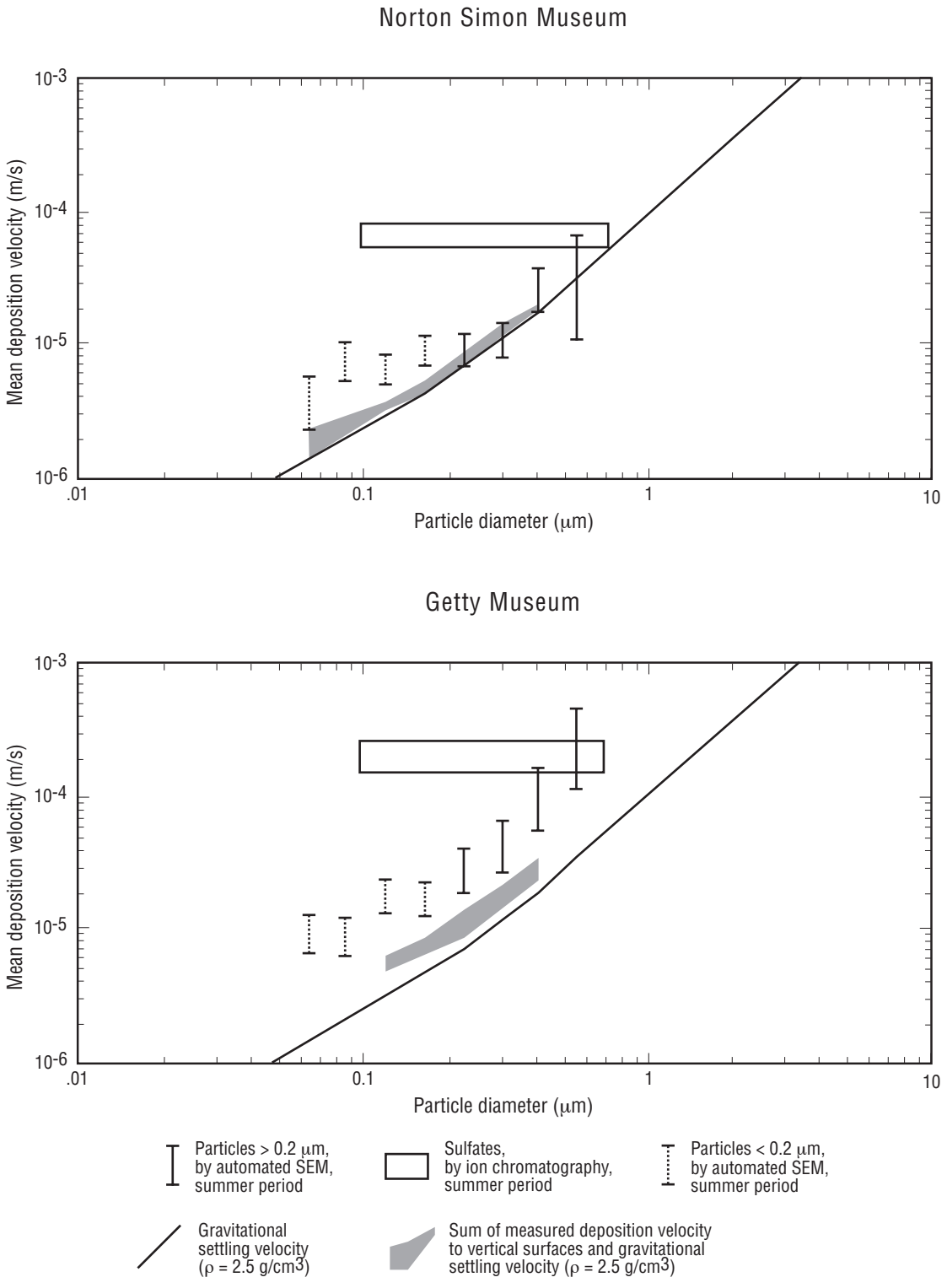

Figure 2.10. Comparison of predicted and measured particle deposition velocities versus particle diameter for the five study sites. See Table 2.3 for definition of the airflow regimes studied.

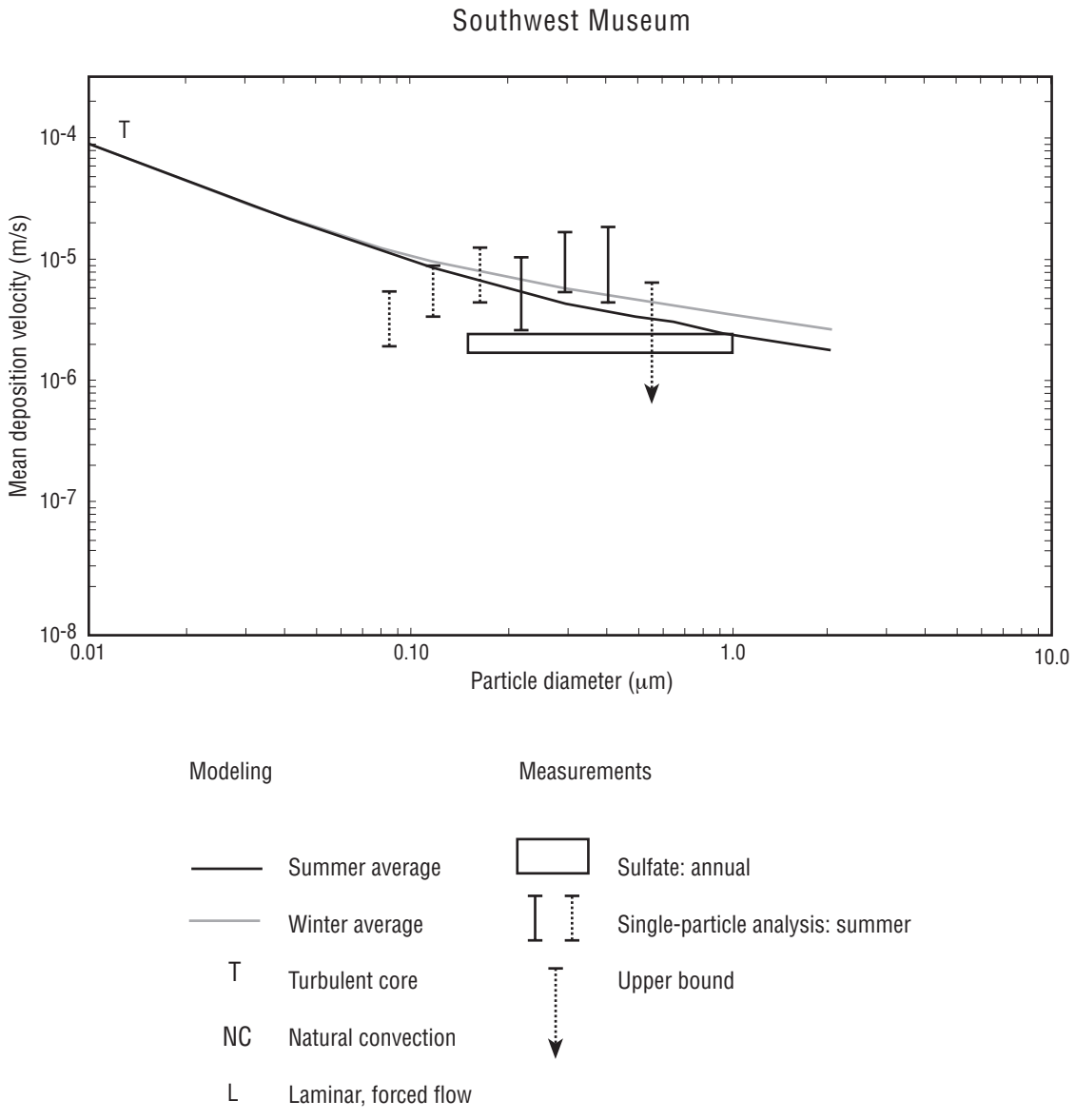

Figure 2.10. Continued.

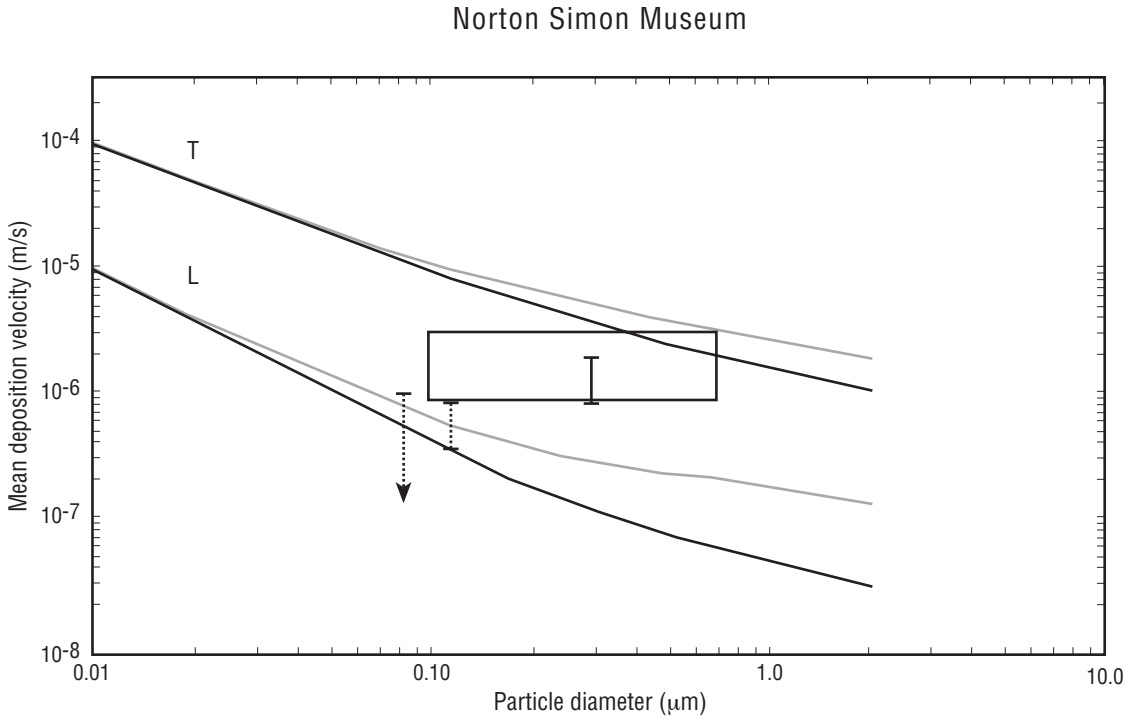

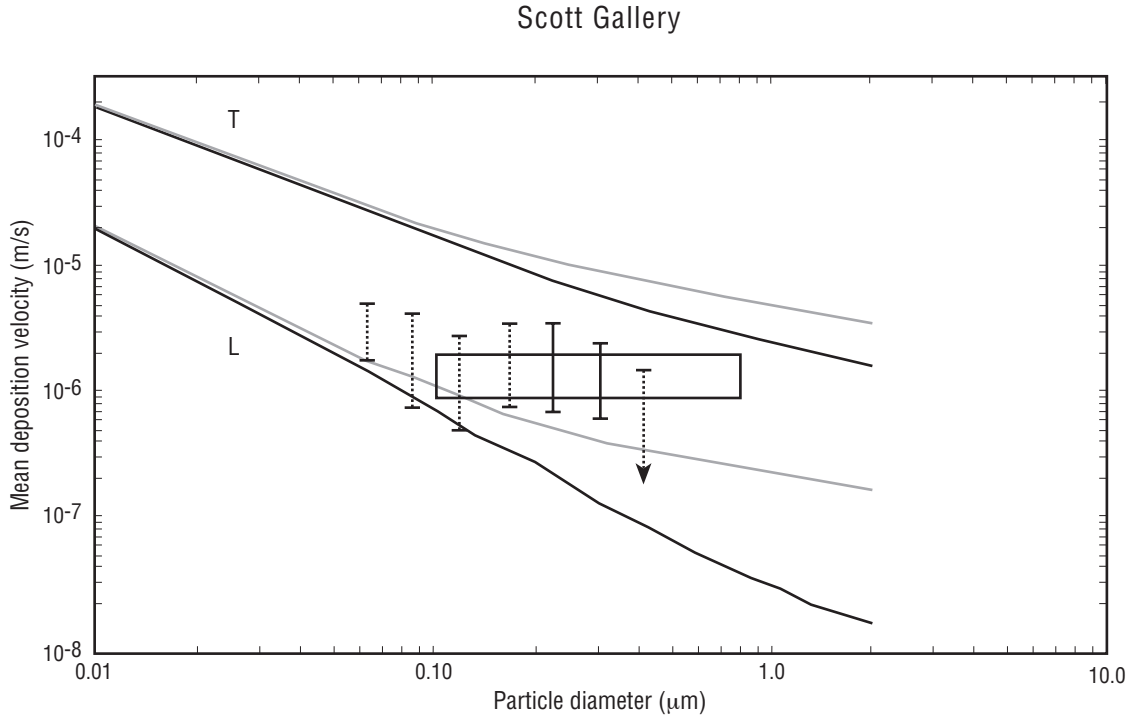

Figure 2.10. Continued.

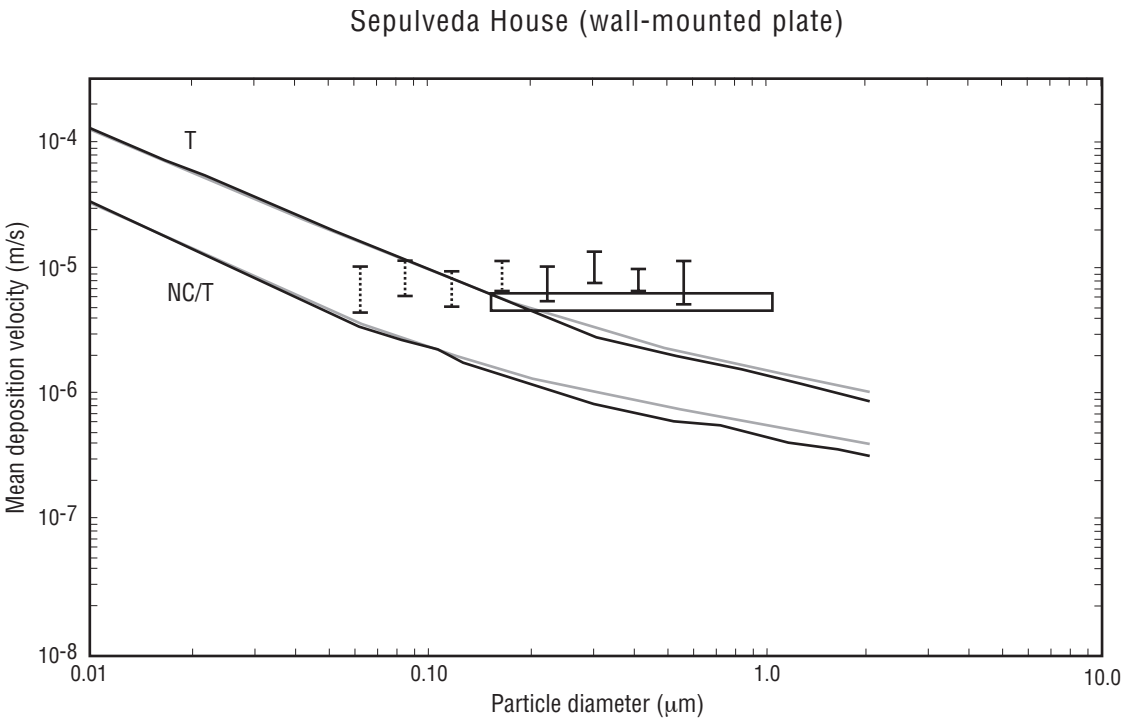

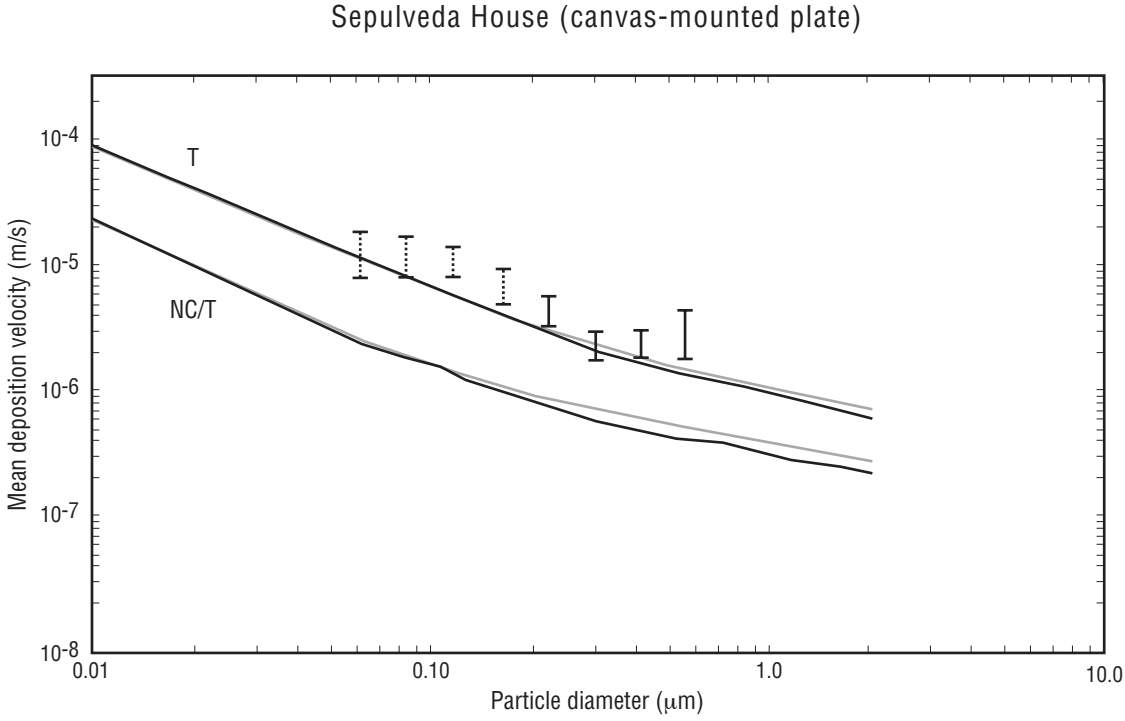

Figure 2.10. Continued.

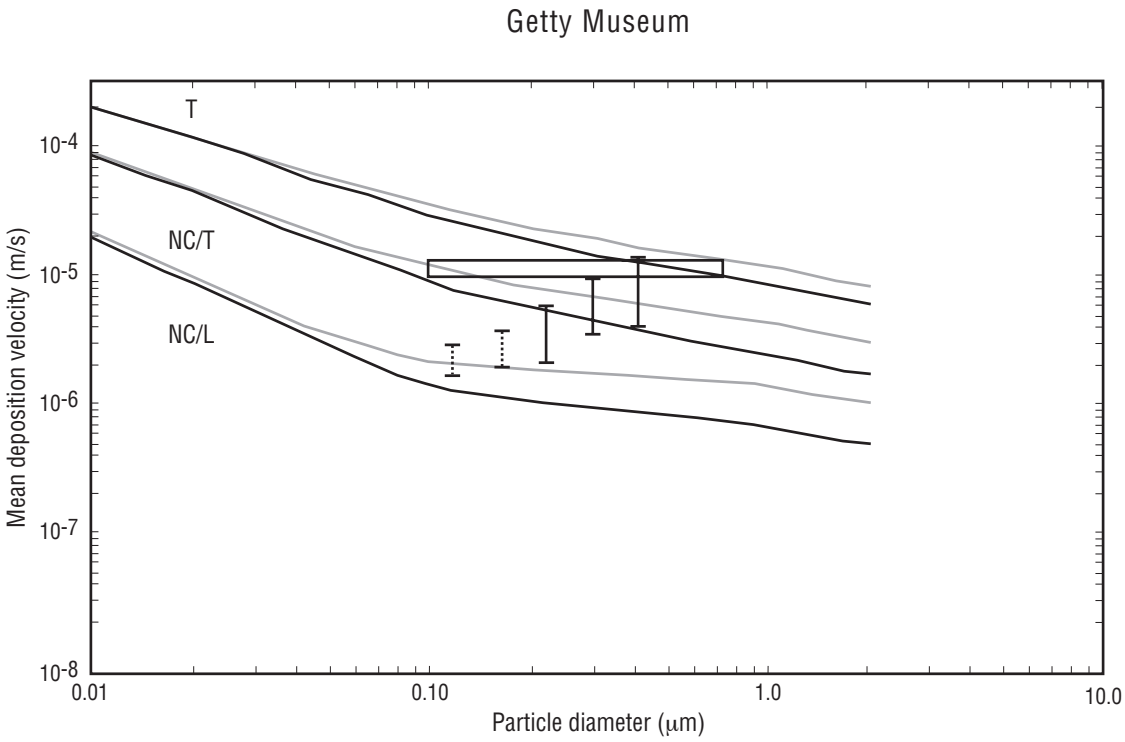

3 Mathematical Modeling of Indoor Airborne Particle Dynamics

To design effective strategies for protecting museum collections from soiling due to the deposition of airborne particles, it is important to develop engineering tools that can be used to predict the likely effect of building design changes on indoor soiling rates. As part of the present project, a computer-based simulation model has been developed that can estimate the indoor concentration of airborne particles, given data on outdoor conditions, and that can predict the resulting particle-deposition rates to indoor surfaces. Both particle-size distribution and chemical composition are simulated. Using a multichamber representation of a building, the model explicitly accounts for the effects of ventilation, filtration, deposition, direct indoor emission, and coagulation. The deposition calculations are especially detailed to permit simulation of soiling problems. The model is coupled with a previously described model for gaseous pollutants (Nazaroff and Cass 1986), permitting future calculations that account for both gas-phase and particle-phase pollutants within the museum environment.

In this chapter, the formulation of the model is described, then the model is tested to determine its ability to represent conditions observed in actual buildings. First, the model is used to explain the results of an experiment measuring the evolution of cigarette smoke in a poorly ventilated room (Offermann et al. 1985). That test of model performance is designed to examine the representation of size-dependent aerosol processes, such as coagulation and deposition, within the model. Next, in Chapter 4, the model is tested against air-quality and soiling data taken in Southern California museums. The model is shown to be reasonably successful in reproducing experimental observations.

Model Formulation

Airborne Particle Representation

For computational purposes, airborne particles are first grouped into contiguous narrow size ranges, called "sections," according to the formulation of Gelbard and Seinfeld (1980). A section of a given size might contain all the airborne particles with diameters that range between 0.1 μm and 0.2 μm, while an adjacent section might contain all particles with diameters between 0.2 μm and 0.3 μm, for example. This representation simplifies the problem; because millions of particles of all possible sizes are actually present in the atmosphere, this method facilitates the calculation of particle losses for a smaller number of particle groups of similar size. Within each section, the particles may be comprised of many different chemical components.

Ventilation and Filtration

The model is structured to represent the ventilation and filtration system of a typical museum, as shown schematically in Figure 3.1 (p. 59). Outdoor air, containing particles that are specified in terms of their size distribution and chemical composition, is brought into the building with the make-up air supply to the mechanical ventilation system. The air may be passed through particle filters before being introduced into the core of the building. The building is viewed as a series of adjacent rooms or chambers with possible air exchange between adjacent rooms. In the air within each room, particle coagulation processes are tracked as small particles collide in mid-air to produce agglomerates of larger effective particle size. Deposition of particles onto horizontal and vertical surfaces is computed. Indoor sources of new particles can be included in the model. Air can be recirculated back to the mechanical ventilation system, with or without further filtration. Infiltration of untreated air from outdoors through doors, windows, or cracks in the building is represented, as is exhaust from the building back to the outdoors. This approach is analogous to that previously developed for modeling gas-phase pollutants in museums (Nazaroff and Cass 1986) with one clarification: The filter efficiency may vary with particle size, but not particle composition. Thus, the efficiency for removing particles from each particle-size section may be specified independently for each filter.

Particle Deposition onto Surfaces

In determining indoor airborne particle concentrations, deposition is often of secondary importance, yielding a rate of removal from the atmosphere that is much smaller than is typically due to ventilation. However, accurate evaluation of particle-deposition rates is extremely important in cases where deposition itself is the concern, such as for the soiling of works of art. To address these problems meaningfully, the model is capable of making detailed calculations of particle-deposition rates.

The rate of particle deposition onto surfaces is related to the loss of airborne particles through the deposition velocity, v_d, which is defined as the ratio of the airborne-particle-mass flux to a surface to the airborne concentration in the core of the room. The model requires that each surface (ceiling, floor, walls, plus any items within the room) be designated in one of three orientations: (1) vertical, (2) horizontal upward-facing, or (3) horizontal downward-facing. For each orientation, the model contains three methods of evaluating v_d for each of three distinctly different mechanisms that may govern airflow along a surface: (1) natural convection driven by a temperature difference between the surface and the nearby air, (2) homogeneous turbulence in the core of the room, and (3) forced laminar flow parallel to a surface. The equations relating deposition velocity to particle size, surface orientation, and flow conditions are reported elsewhere (see the final project report, Nazaroff et al. 1990).

As an alternative to these calculational approaches, the model permits the user to specify the mean deposition velocity for each particle-size section. This approach allows direct utilization of experimental data on deposition rates.

In addition to accounting for the effect of deposition on the evolution of airborne particle concentrations in the core of a chamber, the model can report the time-integrated deposition to each surface of each aerosol chemical component within each size section of the particle size distribution. This capability is designed specifically for the investigation of soiling problems where the flux of black elemental carbon particles and brown soil dust particles to surfaces is of particular interest.

Test of Model Performance: Evolution of Cigarette Smoke

To develop confidence in the capabilities of the model, it is important to test its predictions against experimental data taken in rooms. Unfortunately, data on the evolution of indoor airborne particles are sparse, and no experiments had been reported prior to the start of the present research effort that include all of the important factors influencing the particle-size distribution. The most suitable experimental data available in the existing scientific literature for testing the model recount the decay of cigarette smoke in a room having a low air-exchange rate (Offermann et al. 1985). That experiment was carried out in a closed, unoccupied room of a research "house." A single cigarette was smoked by machine within the room at a rate of two puffs of 35 ml per minute for a period of six minutes, then automatically extinguished. The particle-size distribution was sampled continuously for 24 hours using a laser-based optical particle counter (PMS, Model LAS-X), with results reported seven times per hour. Simulations of this experiment are described below, and it is shown that by assuming reasonable values for unmeasured variables, reasonable agreement between the measured and predicted aerosol size distribution is obtained.

The fate of the cigarette smoke measured during the experiments of Offermann et al. (1985) was examined using the new indoor-air-quality model. The simulations were initialized at 30 minutes following cigarette ignition. The subsequent evolution of the particle-size distribution was simulated for 11 hours; at the end of 11 hours the measured airborne particle concentration had decayed to 23% of its initial value. Calculations were conducted for two different sets of assumptions about the fluid mechanics governing particle deposition: (1) that the deposition process is governed by natural convection flows that occur due to small wall-air temperature differences, or (2) that deposition is governed by air turbulence in the core of the room. Predicted particle-size distributions are compared against the experimental data in Figures 3.2 and 3.3 (pp. 60, 61). Both methods of predicting particle-deposition rates are seen to yield model results that agree reasonably with the experimental measurements. Thus, in these simulations the model accounts for 90–95% of the particle volume lost from the room air.

The fate of the cigarette smoke as predicted by the simulation used to generate Figure 3.2 (p. 60) is shown in Figure 3.4 (p. 62). For these circumstances, coagulation is an important loss mechanism for particles of less than approximately 0.2 μm in diameter, shifting their mass to particles having a diameter in the vicinity of 0.5 μm. Small particles are affected by coagulation to a greater degree than are large particles because of the greater number concentration of small particles and because of their higher mobility. Deposition to surfaces is an important loss mechanism for particles larger than approximately 0.4 μm in diameter in this simulation. The large depositional losses for the largest particles are due to gravitational settling. In other situations, loss of particles due to ventilation would be a more important sink, but in this case the air-exchange rate for the room is unusually low.

The predicted size distribution of particle mass deposited during the 11-hour period on different surfaces is shown in Figure 3.5 (p. 63) for the two alternative approaches used to calculate deposition fluxes. For the floor, most of the deposition is due to gravitational settling, and so the results are similar for the two airflow regimes. This is the dominant site of deposition for particles larger than about 0.2 μm in diameter. For the walls and ceiling, the deposition predictions depend strongly on assumptions concerning airflow. Using the natural convection model with the walls 1 K cooler than the air, uniformly smaller deposition rates are predicted than with the homogeneous turbulence model. Because of the competing effect of gravity, there is essentially no deposition onto the ceiling using the natural convection description; however, the assumed turbulence intensity is strong enough to overcome gravitational settling and cause some particle deposition onto the ceiling.

Figure 3.1. Schematic representation of the ventilation and filtration components of the indoor aerosol model.

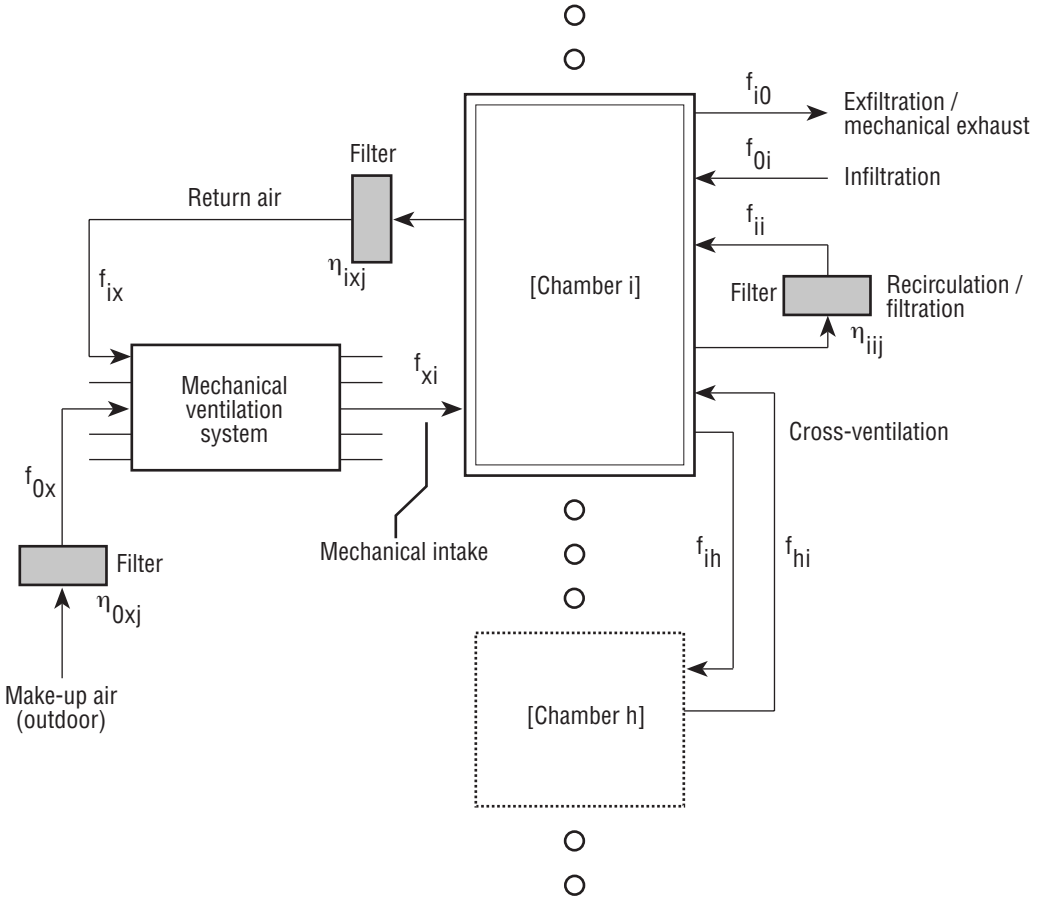

Figure 3.2. Evolution of aerosol size distribution following combustion of a single cigarette. Measurements were conducted in a 35 m^3 room with a ventilation rate of 0.05 h^{-1} (Offermann et al. 1985). In the simulation, the natural convection description of airflow was used to account for particle-deposition rates. All surfaces were assumed to be 1 K cooler than the air in the core of the room. Particle density was assumed to be 1.4 g cm^{-3}.

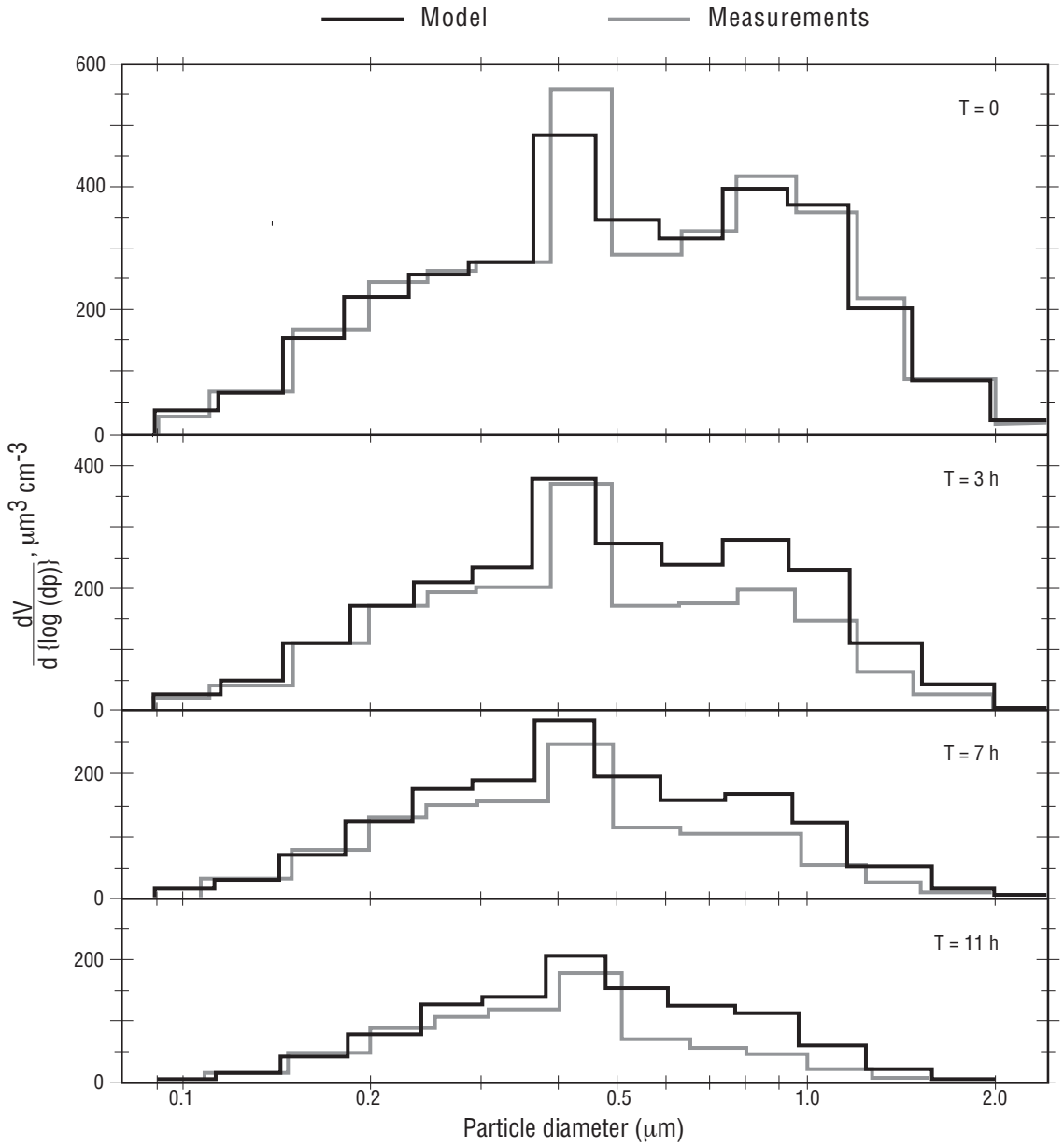

Figure 3.3. Evolution of aerosol size distribution following combustion of a single cigarette. Conditions are unchanged from those of Figure 3.2, except the homogeneous turbulence description of airflow, with $K_c = 0.3\ s^{-1}$ and $\Delta T = 0$, was used to determine the particle-deposition rates.

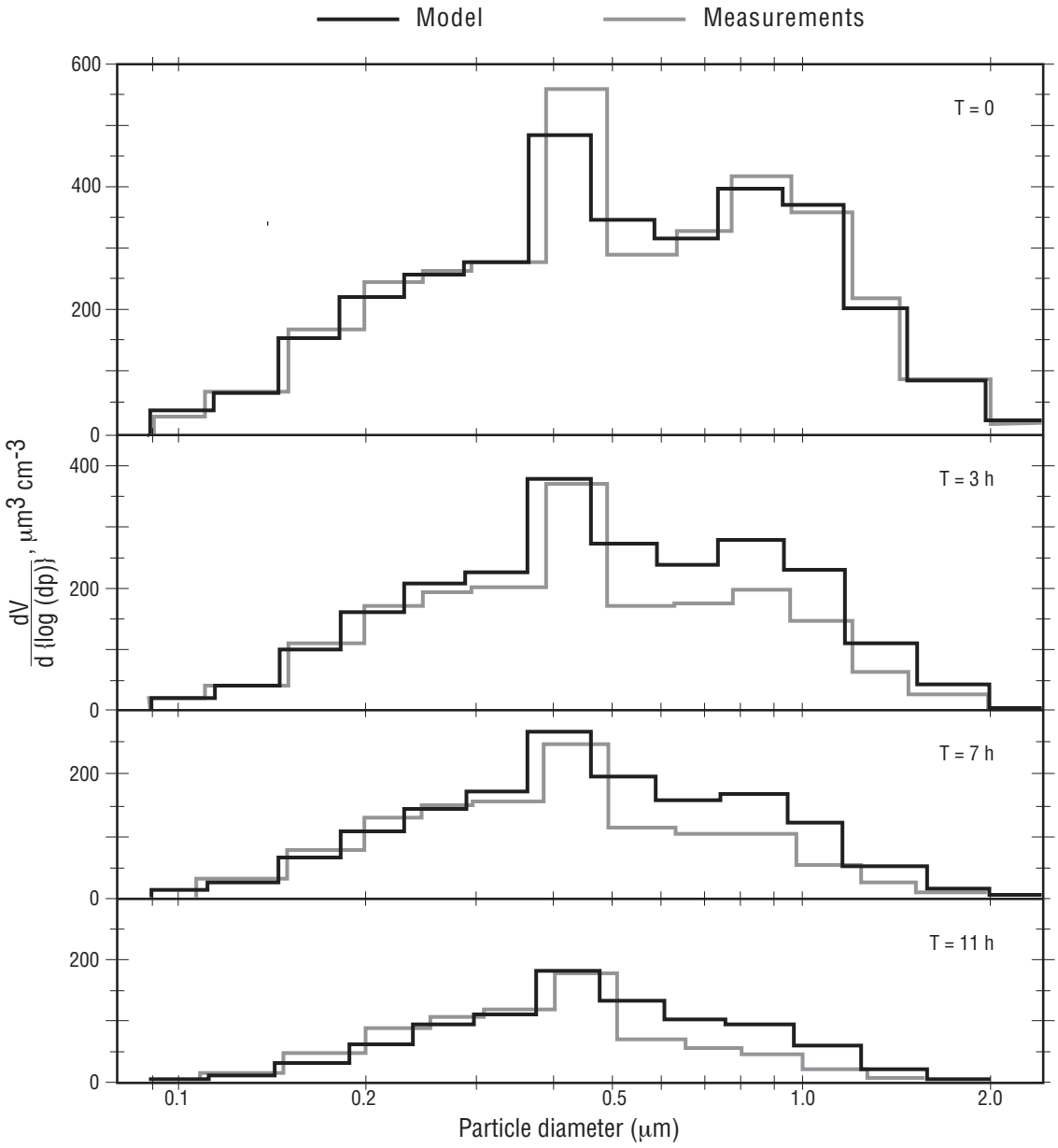

Figure 3.4. Predicted fate of cigarette smoke. The conditions of the simulation were the same as those used to generate Figure 3.2. Note that coagulation represents a net sink for particles in the four smallest sections and a net source of particles in the larger sections.

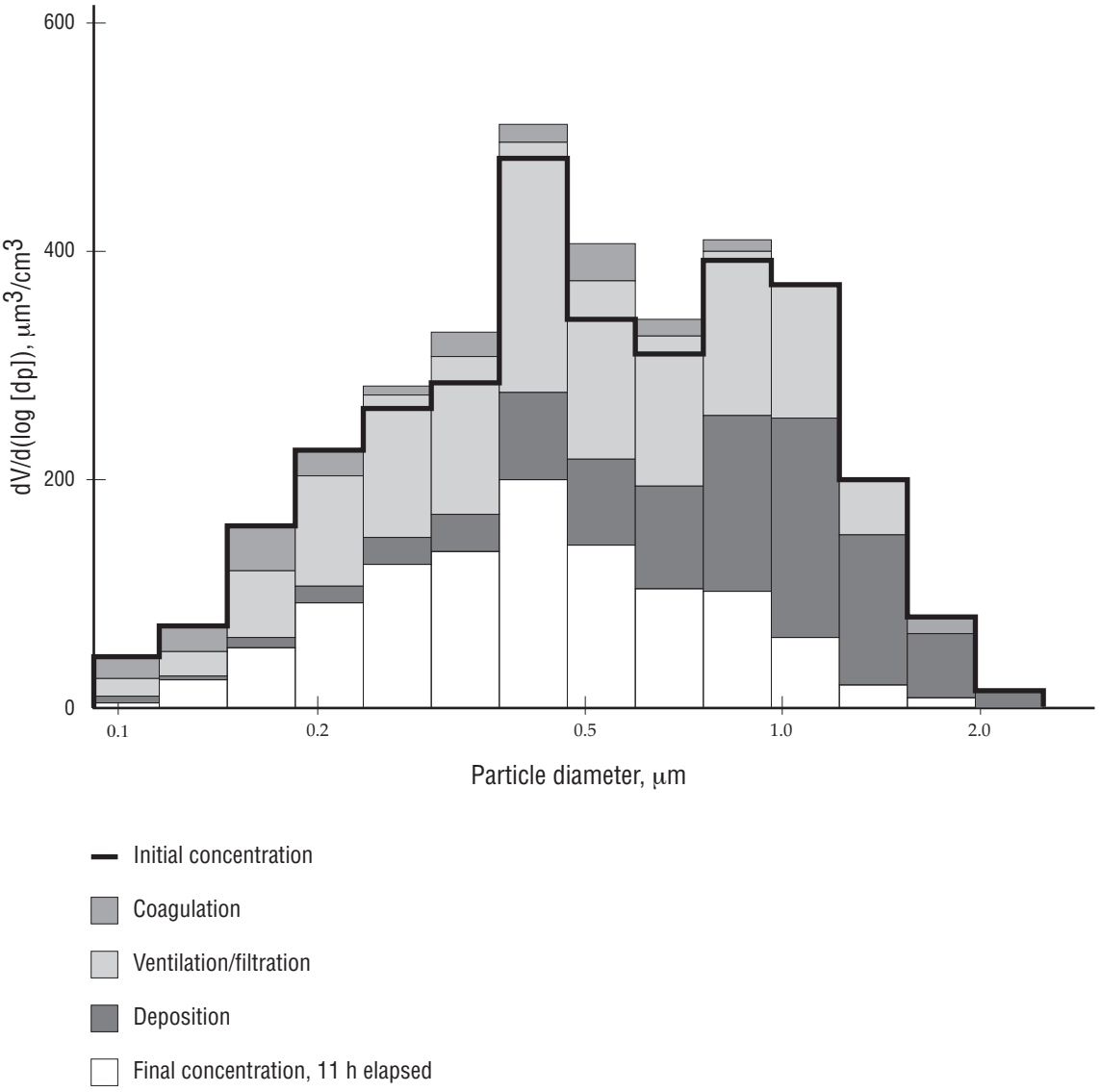

Figure 3.5. Predicted size distribution of cigarette smoke aerosol mass deposited per unit area to different surfaces of the test chamber, $dJ/d(\log d_p)$. The average deposited mass per unit area is plotted for each size section for the 11-hour period beginning 30 minutes after combustion of the cigarette. The simulation conditions correspond to those used to generate Figures 3.2 and 3.3.

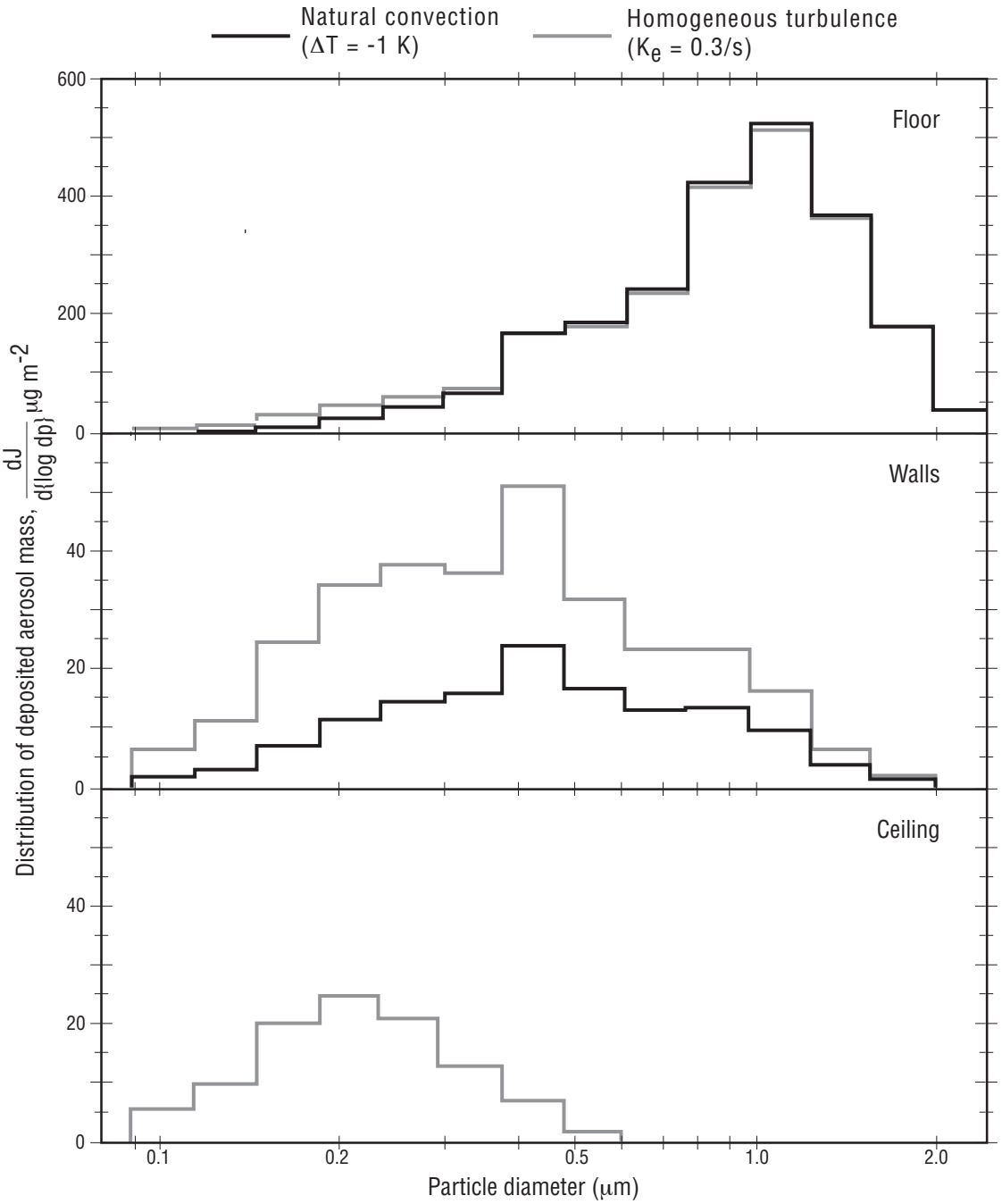

4 Concentration and Fate of Airborne Particles in Museums

Over periods of 24 hours at three of the Southern California museums described in Chapter 2, time-dependent measurements were made of the chemical composition and size distribution of the indoor and outdoor airborne particles. Building characteristics that influence particle concentrations and fates were measured: ventilation rate, temperature differences between a wall and the air, fluid velocities adjacent to a wall, and the particle-removal efficiency of filters in the mechanical ventilation system. From these data, the concentration and fate of the indoor airborne particles were computed for each site, using the mathematical model developed for use in this study (Chapter 3). To evaluate the performance of the model, the predicted indoor airborne particle properties—based on the outdoor particle concentration data and measured building characteristics—are compared against the results of the indoor measurements. The fate of particulate matter entering the museums is assessed through the use of the model, with emphasis on the deposition of particles—particularly those containing elemental carbon and soil dust—on indoor surfaces. The results show that the principal soiling hazard to smooth vertical surfaces and to downward facing surfaces results from the deposition of particles with diameters in the vicinity of 0.1 μm. For floors and other upward-facing surfaces, both fine and coarse particles contribute significantly to soiling.

Study Sites

Ventilation-system characteristics of the buildings studied are summarized in Table 4.1. The Norton Simon Museum and the Scott Gallery are modern buildings with custom-engineered heating, ventilation, and air-conditioning (HVAC) systems (Fig. 4.1, p. 78). At the Norton Simon Museum, make-up air from outdoors passes through a fibrous mat filter (F_{A1}), and an activated carbon filter (F_{A2}) before being blended with return air that has been passed through a fibrous mat filter (F_{A3}). The air mixture is then conditioned for proper temperature and humidity, and distributed to the building. The make-up airflow rate (Q_F) is lower than the original design value, because the supply-air blower (P_{A1}) has been shut off to improve temperature control. At the Scott Gallery, the building was originally operated with 25% make-up air, which was blended with the return air, passed through a fibrous filter, conditioned, and then distributed to the building (Nazaroff and Cass 1986). Recently, an activated-carbon filter was added to the system for ozone removal, and the flow rate of make-up air was reduced effectively to zero by closing the intake dampers (again to improve thermal control). At the time of the particular experiments discussed here, air-exchange between indoors and outdoors at the Scott Gallery occurred entirely due to infiltration through cracks in the building shell and through door openings.

	Norton Simon Museum	Scott Gallery	Sepulveda House
Dimensions			
Number of floors	2	1	2
Floor area (m^2)	4930	535	330
Wall area (m^2)	6950	1990	1050
Volume (m^3)	21540	2530	1200
Ventilation[a]			
Outdoor air exchange (h^{-1})	0.37[b]	0.28 ± 0.01	3.6 ± 1.4
Recirculation (h^{-1})	5.8	8.2	–
Monitoring period			
Start date	April 6, 1988[c]	April 24, 1988	March 30, 1988
Start time	1000 PDT	1800 PDT	2100 PST

a. Flow rate divided by building volume; mean ± one standard deviation of measurements for 24-hour period.
b. Based on hot-wire anemometry measurements of outdoor airflow rate into mechanical ventilation system. Tracer gas decay yielded 0.40 h^{-1} with 90% confidence bounds of 0.37–0.44 h^{-1}.
c. Boundary layer flow and temperature differences measured for 24 hours, commencing at 1200 PDT on April 4, 1988.

Table. 4.1. Characteristics of the study sites.

The Sepulveda House is an historical museum with no system for regulating the air temperature, humidity, or ventilation rate. Air exchange is provided by infiltration through relatively large openings in the building shell. When the building is open to the public (10 a.m.–3 p.m. daily, except Sunday) and the weather is warm, two downstairs doors are kept open.

At each site, one wall was selected for investigation of boundary-layer airflows and temperature gradients that influence particle-deposition rates. Measurements of particle-deposition rate, reported in Chapter 2, were made on the same walls. Briefly, an interior wall with a painted drywall surface was selected for investigation at the Norton Simon Museum; a painted plywood panel mounted on an interior wall with furring strips was selected at the Scott Gallery; and an outer brick wall with a painted, irregular plaster surface was chosen at the Sepulveda House.

Because these experiments would have been disruptive to normal museum operation, measurements at the Norton Simon Museum and at the Scott Gallery were conducted

while the buildings were closed to the public (although the museum staff was present). Consequently, this study does not fully incorporate the effects of occupancy on airborne particle properties. The Sepulveda House was open to the public as usual, from 10 a.m. to 3 p.m., on the day of monitoring.

Measurement and Modeling Results: Aerosol Size Distribution and Chemical Composition

Filter Efficiency

In order to support indoor air-quality model calculations, measurements were made first of the filtration efficiency (fraction of particles removed) of the filters now used in the museum facilities studied. The filtration efficiency is shown in Figure 4.2 (p. 79) as a function of particle size for a single pass through the building ventilation system filters F_{A3} and F_{B1}, located at the Norton Simon Museum and Scott Gallery as defined in Figure 4.1 (p. 78). At the Norton Simon Museum, filter F_{A1} is composed of the same material as filter F_{A3}. However, filter F_{A3} was sufficiently loaded with particulate matter to appear heavily soiled, whereas new filter material had recently been installed in F_{A1}. Very little difference (< 5%) between upstream and downstream particle concentrations was observed for all particle sizes measured in filter F_{A1}. (These observations are consistent with the general knowledge that particle filters become more efficient as the loading increases.) Measurements across the charcoal filter, F_{A2}, indicate that this type of filter also is ineffective in removing fine particles.

Temperature Differences and Boundary Layer Flows

The results of monitoring temperature difference and near-surface air velocity at the three sites are shown in Figure 4.3 (pp. 80–82). The prominent features of the temperature-difference profiles are clear. For example, the largest peak in the temperature difference T_{wall} to T_{air} at the Norton Simon Museum occurs in the late afternoon. At this time, the air temperature in this gallery increases, probably because of solar heating of the roof and of the south- and west-facing walls. The mechanical ventilation system supplies cool air to maintain the set-point temperature, thereby increasing T_{wall} to T_{air}. The large dip and rise in the profile at the Scott Gallery is associated with an inadvertent interruption in air conditioning for the building. (Apparently, the fans in the mechanical ventilation system continued to operate during this time, but the cooling function ceased for almost four hours.) The indoor air temperature rises rapidly at 1200 PDT and heat is transferred to the wall. At approximately 1545 PDT, the air-conditioning system resumes operation, rapidly cooling the air, and heat is transferred from the wall back to the air. At the Sepulveda House, which lacks thermal

control, the diurnal cycle is driven by the outdoor air temperature and the delayed thermal response of the brick wall. The maximum value of T_{wall} to T_{air} occurs just before dawn and the minimum occurs at 1400 PST, corresponding approximately to the peak outdoor air temperature.

At the Sepulveda House the near-wall air velocity is consistent with expectations for natural convection (Schiller 1984, Bejan 1984), driven by the temperature difference between the wall and the air, for the periods 0000–1000 and 1500–2400 PST, in other words, when the museum is closed. Note that during these periods, the maximum velocity occurs when the temperature difference is greatest; likewise, when the temperature difference is near zero, the air velocity is very low. When the museum is open, the airflow velocity adjacent to the wall is highly variable and appears to be driven predominantly by turbulent air movement in the core of the room.

At the Scott Gallery, the near-wall air velocity appears to be strongly dominated by the flow of air through the building because of the operation of its mechanical ventilation system. At this site, the supply- and return-air registers are located at the tops of the walls. The lower velocity observed during the period when air cooling failed was probably the result of buoyant, warm air entering the room from the ceiling registers, a condition that would not promote convective mixing in the core of the room. After cooling was restored, peak near-wall air velocities were observed. A similar correlation between the wall-air temperature difference and the near-wall air velocity is observed at other times during the monitoring period, most notably for the first seven hours. During this interval T_{wall} to T_{air} oscillated with an amplitude of ~0.3 K and a period of approximately 45 minutes; an envelope of the near-wall air velocity could be traced with an amplitude of approximately 5 cm s^{-1} and the same period. Some of the high-frequency fluctuations in the air velocity at the Scott Gallery may be because the sampling location was near a door that was opened and closed approximately ten times per hour during monitoring.

At the Norton Simon Museum, air is supplied to the gallery through perforated tiles that cover more than half the ceiling. Air is returned to the ventilation system through the interior hallways of the building. Combining this circulation pattern with a lower recirculation rate (Table 4.1, p. 66), it is not surprising that the measured near-wall air velocities are generally lower at this site than at the Scott Gallery.

Modeling Airborne Particle Characteristics

The indoor particle-size distribution and chemical composition were computed from measured outdoor aerosol properties for each site using the indoor air-quality model previously reported (Chapter 3). That model tracks the evolution of the indoor particle-size distribution and chemical composition as they are affected by ventilation, filtration, emission, coagulation, and deposition. For the present study, the particle-size distribution was represented by fifteen sections spanning the diameter range of 0.05 to 40 μm and by three chemical components—elemental carbon, soil dust, and "other."

For the model calculations, each site was represented as a single, well-mixed chamber, with building size and ventilation characteristics as indicated in Figure 4.1 (p. 78) and Table 4.1. A constant ventilation rate was adopted for the Norton Simon Museum, based on the apparent dominance of the constantly operated mechanical ventilation system over infiltration. Likewise, the rate of outdoor air-exchange at the Scott Gallery was taken to be constant, based on the small variance in results from tracer-gas decay measurements. At the Sepulveda House, tracer decay data were used to obtain hourly averaged air exchange rates, which were then applied in the model calculations.

Particle-removal efficiencies for filters F_{A3} and F_{B1} were based on measurements reproduced in Figure 4.2 (p. 79) or particles in the diameter range of 0.09 to 2.25 μm. The efficiencies for particles smaller than 0.09 μm and larger than 2.25 μm in diameter were estimated by extrapolation. The charcoal filters, F_{A2} and F_{B2}, were assumed to have no effect on particle concentrations, based on measurements of the penetration efficiency for F_{A2}. To best reflect the prevailing conditions on the day of monitoring for this study, the effectiveness of the newly replaced filter F_{A1} in removing particles was taken to be zero, based on measurements showing its effectiveness to be less than 5% at that time. An additional modeling run (Case C in Table 4.2, p. 70) was carried out with filter F_{A1} having the same effectiveness as filter F_{A3}. The latter case better represents ordinary conditions at the Norton Simon Museum. (The particle filter material is contained in large rolls. Routinely, the filters are advanced a small fraction [< 10%] of their exposed length, thereby maintaining a fairly uniform degree of particle loading. Just prior to the day of monitoring for this study, a new roll of material had been installed for filter F_{A1}.)

Particle-deposition rates were computed for idealized flow conditions using the data on wall-air temperature differences and near-wall air velocities shown in Figure 4.3 (pp. 80–82). These data were used to determine the hourly average temperature difference between the wall and the air. The temperature differences were then assumed to apply to all surfaces of the building. For the Sepulveda House, particle deposition was computed using the natural convection description of airflow during the periods of 0000–1000 and 1500–2400 PST. Homogeneous turbulence in the core of the building was assumed to dominate deposition processes for the remaining period at this site. At the Norton Simon Museum and at the Scott Gallery, deposition calculations were carried out for two representations of near-wall airflows. As shown in Table 4.2 (p. 70), the base case (A) calculations were made assuming laminar forced flow parallel to the surfaces. Case B calculations were made assuming that the near-wall flows were dominated by homogeneous turbulence in the core of the rooms. A comparison of model and measurement results for particle-deposition velocity at these two sites suggests that the actual deposition rates lie between the values predicted for Case A and Case B conditions at the Scott Gallery and closest to the results for Case A conditions at the Norton Simon Museum.

Norton Simon Museum	Case A	Deposition: forced laminar flow; filter F_{A1}: ineffective
	Case B	Deposition: homogeneous turbulence in the core of the room; filter F_{A1}: ineffective
	Case C	Deposition: forced laminar flow; filter F_{A1}: same efficiency as filter F_{A3}
Scott Gallery	Case A	Deposition: forced laminar flow
	Case B	Deposition: homogeneous turbulence in the core of the room
Sepulveda House	Case A	Deposition: natural convection flow (0000–1000 and 1500–2400 h), homogeneous turbulence in the core of the room (1000–1500 h)

Table 4.2. Deposition and filtration conditions simulated at study sites using the indoor air-quality model.

For each site, a comparison is presented in Figure 4.4 (pp. 83–85) of the results of outdoor measurements, indoor measurements, and the indoor model predictions (under Case A conditions) for the total fine-particle concentration as a function of time and for the 24-hour-average airborne particle size distribution. At both the Norton Simon Museum and the Scott Gallery, the fine-particle-mass concentration indoors is reduced to 15 to 20% of the outdoor value, and the coarse aerosol mass present indoors is less than 5% of the outdoor value. The agreement between the indoor model and measurement results ranges from excellent to good: the size distribution and total fine aerosol concentration is predicted accurately for the Scott Gallery, while at the Norton Simon Museum the agreement is good except that the aerosol mass concentration for particles with a diameter in the range of 0.18 to 0.35 μm is overpredicted by the indoor-air-quality model.

At the Sepulveda House, there is little difference between the indoor and outdoor fine-particle concentrations. The model reflects this fact. However, the high-frequency fluctuations in the indoor concentration, which result from the high air-exchange rate, are smoothed in the model calculations, an artifact of using hourly averages for outdoor concentrations in the model. (Although the model as used here employs outdoor particle concentration data on an hourly averaged basis, this method does not preclude using data with finer time resolution.) One does not need a detailed mathematical model to predict the indoor concentrations of fine particles based on outdoor values if the building has a high air-exchange rate and no filtration. However, the estimates of particle flux to the walls and other surfaces of the Sepulveda House are complex and utilize the indoor-air-quality model's capabilities.

Table 4.3 (p. 71) compares measurements and predictions of the particle chemical constituents, sorted according to particle size into coarse and fine modes. Again, the agreement is good, particularly for the fine particles for which the input data are more detailed.

	Fine			Coarse[a]		
	E. carbon	Soil dust	Total	E. carbon	Soil dust	Total
Norton Simon Museum						
Outdoor, measured	3.90	1.50	50.0	2.7	30.0	81.0
Indoor, measured	0.67	0.15	9.3	0.09	0.25	-2.0
Indoor, modeled, Case A	0.83	0.36	12.5	0.10	1.0	2.9
Indoor, modeled, Case B	0.82	0.36	12.4	0.10	1.0	2.9
Indoor, modeled, Case C	0.62	0.30	10.1	0.004	0.04	0.11
Scott Gallery						
Outdoor, measured	1.5	0.75	26.0	0.95	6.9	37.0
Indoor, measured	0.16	0.09	4.1	0.01	0.13	2.3
Indoor, modeled, Case A	0.23	0.08	3.7	0.05	0.32	1.8
Indoor, modeled, Case B	0.22	0.08	3.6	0.05	0.32	1.8
Sepulveda House						
Outdoor, measured	5.0	2.6	34.0	1.3	41.0	117.0
Indoor, measured	5.6	0.86	24.0	0.75	23.0	57.0
Indoor, modeled, Case A	4.9	2.5	22.0	0.49	14.0	40.0

a. Coarse data are obtained by difference between mass concentration determined for filters in open-faced holders and filters downstream of cyclones with ~2.0 μm diameter cut-point. The negative measured value at the Norton Simon Museum results from subtraction of two small and nearly identical measurement results.

Table 4.3. Average mass concentrations ($\mu g\ m^{-3}$) of aerosol components for study periods from filter-based measurements and simulations.

Overall, the agreement between model calculations and measurement results justifies the use of the model with confidence to further consider the dynamics of indoor aerosols. The next two sections explore the fate of particles and the magnitude of the soiling hazard in museums.

Fate of the Particles Entering from Outdoor Air

The design of effective measures to control indoor particle deposition can be facilitated by examining the relative strengths of particle sources and sinks. For the three sites considered in this chapter, the overwhelming source of indoor airborne particles during these experiments was the entry

of outdoor air. This observation is substantiated by the agreement between measurement and model results. The relative strength of the particle sinks may now be considered as follows: filtration, removal by ventilation, and deposition on interior surfaces. Coagulation, which serves as a sink for very fine particles, transferring their mass to larger particles, is also considered.

For each simulation and for each particle size section, the mean rate of removal of airborne particle mass by the various sinks was computed, then normalized in each case by the mean rate of supply of aerosol mass in the section from outdoor air. The results for Case A, shown in Figure 4.5 (pp. 86–87), indicate that at the Norton Simon Museum and the Scott Gallery the dominant fate of particles smaller than approximately 10 μm in diameter is removal by filters. This result is obtained despite the moderately low particle-filtration efficiencies because during its residence time within these museums, air makes a large number of passes through the filters in the recirculating air ducts. At the Sepulveda House, particles of this size are predominantly removed by ventilation. Surprisingly, at all three sites the dominant fate of larger particles is deposition on surfaces, almost entirely by gravitational settling on the floor. This result demonstrates the importance of an effective filter for removing coarse particles from the ventilation supply air. Under ordinary conditions at the Norton Simon Museum, with filter F_{A1} partially loaded with particles rather than clean, it is expected that 95% of coarse particles are removed from the air entering the building.

Deposition constitutes a much smaller sink for fine particles; for example, of particles 0.1 μm in diameter that enter the buildings, only 0.1 to 0.5% will ultimately deposit on a surface. This indicates that detailed calculations of deposition rates are not necessary to obtain accurate predictions of the indoor airborne concentrations of fine particles in these particular buildings.

At all three sites, and for all particle sizes, coagulation is seen to be of little importance. It is not correct to conclude, however, that particle coagulation is never important in indoor air. The study conditions at these three sites tend to minimize the rates of coagulation: low particle concentrations at the Norton Simon Museum and at the Scott Gallery imply low particle collision rates, and the high air-exchange rate at the Sepulveda House does not allow sufficient time for coagulation to have a significant effect. On the other hand, previous analysis of the fate of cigarette smoke in a room having a low air-exchange rate showed that coagulation was an important sink for particles smaller than 0.2 μm in diameter (Chapter 3).

Particle Deposition onto Indoor Surfaces

Even though only a small fraction of the fine particles that enter a building deposit onto surfaces, the soiling hazard posed by particle deposition may still be significant. To assess the magnitude of the problem, the rates of particle accumulation on the floor, walls, and ceiling of each of the three

sites were computed for the 24-hour study periods using the indoor-air-quality model. The results are displayed in Figure 4.6 (pp. 88–90) in terms of the rate of mass accumulation per unit surface area, J, as a function of particle size and composition. Table 4.4 (p. 74) gives the total rate of accumulation of elemental carbon, soil dust, and of the total aerosol on the walls, floors, and ceilings for each of the three sites. Before considering the significance of the results, it is important to emphasize that the calculations at each site represent predictions for a single day. Thus, extrapolations to longer time periods must be regarded only as estimates. In particular, differences in the deposition rates between sites may reflect differences in the outdoor conditions on the particular days studied, rather than differences in the long-term average rates of soiling. Note, also, that although the calculations are made specifically for the floor, walls, and ceiling, the results are indicative of expected values for other surfaces, such as those of art objects, which have corresponding orientations.

The computed total rate of accumulation of elemental carbon particles on the walls of the three sites is in the range 0.02–0.7 $\mu g\ m^{-2}\ day^{-1}$. The corresponding rates for the ceilings are smaller, 0.002–0.5 $\mu g\ m^{-2}\ day^{-1}$, and are very sensitive to the assumed nature of near-surface airflow. For forced laminar flow conditions (Case A), gravitational settling is effective in reducing deposition of ~0.1 μm particles onto the ceiling. For homogeneous turbulence (Case B), however, eddy diffusivity dominates gravitational settling for the very fine elemental carbon particles, and the deposition rate is about the same for the ceiling as for the walls. The rates of accumulation of elemental carbon onto the floors are much larger, 2–50 $\mu g\ m^{-2}\ day^{-1}$, for the Norton Simon Museum. The particle sizes associated with volume-weighted elemental carbon deposition onto these surfaces are quite distinct: predominantly 0.05–0.3 μm for the walls and ceiling, compared with 4–40 μm for the floor. However, considered in terms of the rate of accumulation of projected particle cross-sectional area (probably the appropriate scale for assessing the rate of soiling [e.g., Carey 1959]), the deposition of fine particles onto the floor has a significance comparable to the deposition of coarse particles.

Because of its lower rate of accumulation, soil dust appears to pose a smaller soiling hazard than elemental carbon for the ceiling and walls at the Norton Simon Museum and at the Scott Gallery. However, the rates of accumulation of soil dust onto the floor at those two sites are seven to ten times larger than those of soot. These differences are a consequence of the fact that soil dust, being mechanically generated, is found predominantly in the coarse-particle mode and settles on upward-facing surfaces under the influence of gravity, whereas elemental carbon, produced in combustion systems, is found primarily in fine particles for which deposition occurs to surfaces of any orientation by a combination of advective diffusion and thermophoresis.

		E. carbon	Soil dust[a]	Total
Norton Simon Museum, Case A	Ceiling	0.003	(0.000)	0.003
	Walls	0.050	(0.010)	0.30
	Floor	52	560	1540
Norton Simon Museum, Case B	Ceiling	0.54	(0.10)	3.6
	Walls	0.64	(0.23)	6.2
	Floor	53	560	1540
Norton Simon Museum, Case C	Ceiling	0.002	(0.000)	0.002
	Walls	0.039	(0.007)	0.24
	Floor	2.4	23	67
Scott Gallery, Case A	Ceiling	0.015	(0.001)	0.036
	Walls	0.017	(0.008)	0.22
	Floor	19	130	710
Scott Gallery, Case B	Ceiling	0.26	(0.08)	3.0
	Walls	0.29	(0.13)	3.9
	Floor	19	130	710
Sepulveda House	Ceiling	0.40	(0.32)	1.4
	Walls	0.69	(0.70)	2.8
	Floor	280	8500	24,000

a. The soil dust results for walls and ceilings represent lower limits. Inertial effects, which may be important for coarse-particle deposition to these surfaces, are not included in the model predictions of deposition.

Table 4.4. Average deposition rate of aerosol mass ($\mu g\ m^{-2}\ day^{-1}$) to indoor surfaces based on simulations of study periods at each site.

The much higher flux density of particle mass to the floor compared with values for the ceiling and walls points to a limitation of the calculations employed here in assessing the soiling hazard for certain surfaces. In these calculations, vertical surfaces are assumed to be smooth; however, many real surfaces are rough. Through gravitational settling, large particles will deposit preferentially on the upward-facing portions of surface roughness elements. Because contrast is readily detected, nonuniform deposition of particles by such a process would probably lead to noticeable visual degradation of the object more rapidly than an equivalent rate of deposition spread uniformly over the surface.

To gain perspective on the significance of these results in the context of protecting museum collections, a characteristic time interval for soiling was computed. Previous studies have shown that a white surface is perceptibly darkened when 0.2% of its area is effectively covered by either black dots that are too small to be distinguished individually (Carey 1959) or by black particles (Hancock et al. 1976). Since the light-absorbing properties of elemental carbon particles differ from those of soil dust, the degree of surface coverage needed to produce perceptible soiling probably differs for the two components. The information needed to combine the accumulation rate of the two components into a single soiling rate is lacking, and so, for the present study, the characteristic times for soiling by elemental carbon particles ($\tau_{s;\,EC}$) and by soil dust ($\tau_{s;\,SD}$) were estimated as the time required to achieve 0.2% coverage of a surface by these components independently. These times were computed for each surface orientation and each model case, given the deposition rates as a function of size (as displayed for Case A in Figure 4.6, pp. 88–90), and assuming that, within each particle size section, the deposited elemental carbon or soil dust can be considered to exist as spherical particles with a diameter equal to the logarithmic mean for the particle size section.

The resulting values for $\tau_{s;\,EC}$ for the three sites are given in Table 4.5 (p. 76). For smooth, vertical walls and ceilings, deposition of elemental carbon particles constitutes a greater soiling hazard than the deposition of soil dust. Characteristic soiling times associated with elemental-carbon-particle deposition are in the range of 1 to 40 years for walls. For ceilings, the corresponding predictions are in the range of 1 to 35 years; except for the Norton Simon Museum under the assumption of forced laminar flow, for which the estimated characteristic soiling time is two centuries. For floors (and other horizontal surfaces), predicted characteristic soiling times due to soil-dust deposition are more rapid than those due to elemental carbon deposition. The values of $\tau_{s;\,SD}$ range from as short as three days at the Sepulveda House to as long as three years for the Norton Simon Museum with an effective intake filter (Case C). Among the three surface orientations, predictions for the ceilings must be regarded as the least certain, since, as with the walls, the deposition rates critically depend on near-surface airflows, and no measurements of flows near ceilings were made in this study.

With the exception of the few large values of τ_s for the ceiling of the Norton Simon Museum, these soiling periods are short relative to the periods over which museum curators wish to preserve their collections. In some respects, these estimates are conservative. The degree of effective area coverage by black particles needed to produce perceptible soiling would be at a minimum for completely white surfaces for which the 0.2% result applies. The surfaces of heavily pigmented paintings, however, could probably accrue a greater deposit before soiling became perceptible.

	Ceiling		Walls		Floor	
	$\tau_{s;\,EC}$	$\tau_{s;\,SD}$	$\tau_{s;\,EC}$	$\tau_{s;\,SD}$	$\tau_{s;\,EC}$	$\tau_{s;\,SD}$
Norton Simon Museum						
Case A	180	–	12	(170)	1.2	0.2
Case B	1.2	(12)	1.1	(8.4)	0.6	0.2
Case C	230	–	16	(210)	4.7	3.0
Scott Gallery						
Case A	35	(720)	40	(240)	2.9	0.6
Case B	2.5	(19)	2.4	(16)	1.4	0.6
Sepulveda House						
Case A	1.5	(6.2)	0.9	(4.1)	0.15	0.01

Based on the predicted deposition rates for the single study day at each site. The characteristic soiling time is computed as the time required for the accumulation of sufficient elemental carbon particles (τs; EC) or soil dust particles (τs; SD) on a smooth surface to effectively cover 0.2% of the surface area. For black particles on a white surface, this degree of coverage has been shown to yield perceptible soiling (Carey 1959, Hancock et al. 1976).

Predictions of particle-deposition rate do not include inertial effects, which may be important for coarse-particle sizes where most of the soil dust is found. Therefore, the characteristic times for perceptible soiling to occur on walls and ceilings due to soil-dust deposition represent upper limits. For floors, deposition of coarse particles is dominated by gravitational settling, and so the estimates are believed to be accurate.

Table 4.5. Characteristic time (years) for perceptible soiling to occur.

As expected, the soiling problem is most acute at the Sepulveda House because of its high ventilation rate and lack of particle filtration. Taking the geometric mean of the results for Cases A and B as a representative estimate of the true soiling rates at the Norton Simon Museum and the Scott Gallery, soiling rates due to elemental carbon deposition at these sites are approximately five to ten times lower than at the Sepulveda House.

For soil dust deposition on upward surfaces, the difference between the characteristic soiling time at the Sepulveda House and at the other two sites is even greater. It is noteworthy that the effectiveness of the supply-air filter at the Norton Simon Museum in lengthening the soiling periods (compare Cases A and C) is not large for soiling by elemental carbon particles. This result is obtained because the deposition of fine particles on the floor contributes significantly to $\tau_{s;\,EC}$, and the inlet filter is relatively ineffective in removing these particles. On the other hand, an effective supply-air filter at the Norton Simon Museum does significantly extend the characteristic soiling time for the floor, associated with soil-dust deposition.

Discussion

The results of this study serve several purposes. First, they substantially increase the basis for confidence in the ability to predict the size distribution and chemical composition of indoor airborne particles using the indoor air-quality model described in Chapter 3. Second, they provide considerable information beyond that previously available about the indoor-outdoor airborne-particle-concentration relationship for two types of buildings. (The Norton Simon Museum and the Scott Gallery are representative of modern commercial buildings, apart from their relatively high ratios of recirculated air to outdoor make-up airflow rates and the presence of activated carbon filters. The Sepulveda House is representative of many older buildings, at least of those in temperate climates.) Third, the results constitute, to our knowledge, the first detailed estimates of the cause-and-effect relationships that lead to soiling of indoor surfaces. Information about the size of particles that contribute to soiling is crucial in designing efficient control measures. Estimates of the rate of soiling will help concerned officials make informed decisions about how much of their limited resources to devote to control measures.

Figure 4.1. Schematic representation of the ventilation and filtration systems for the three study sites showing the flow rates (Q), fans (P), and filters (F) in each system. For airflows, subscripts L, F, and R represent leakage (infiltration), forced supply (make-up), and recirculation, respectively. Filters F_{A2} and F_{B2} contain activated carbon for ozone removal; the other filters are mat-fiber type for removing particles.

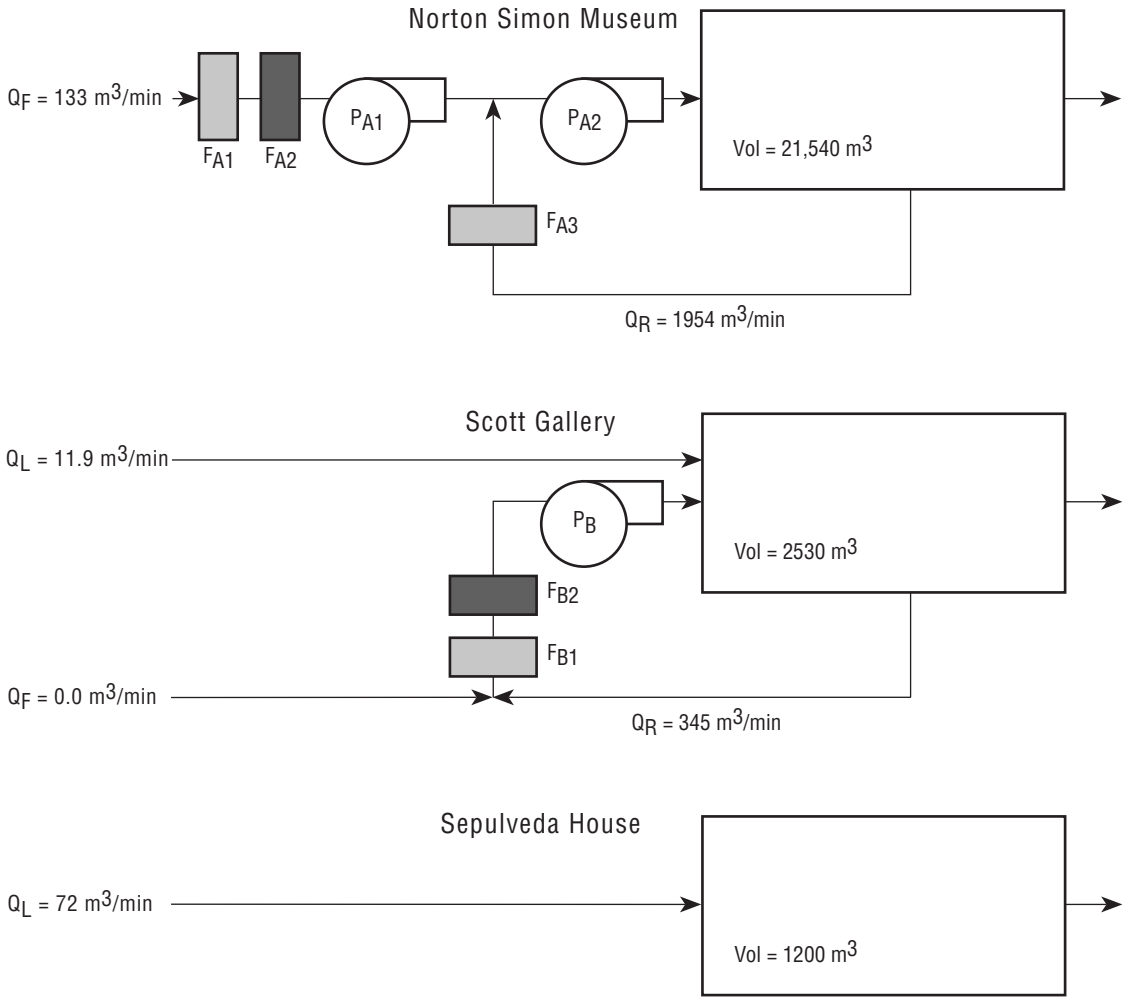

Figure 4.2. Filtration efficiency of particle filters as a function of particle size. The results are based on 21 and 4.5 hours of data for filters F_{A3} and F_{B1}, respectively. The corresponding operating flow velocities across the filter faces are 0.44 and 1.7 m s^{-1}. Filter media: filter F_{A3} is Servodyne type SR-P1L; filter F_{B1} is Servodyne type Mark 80. Filter F_{A1} was found to have less than 5% removal efficiency when new for particles smaller than 2.3 μm in diameter.

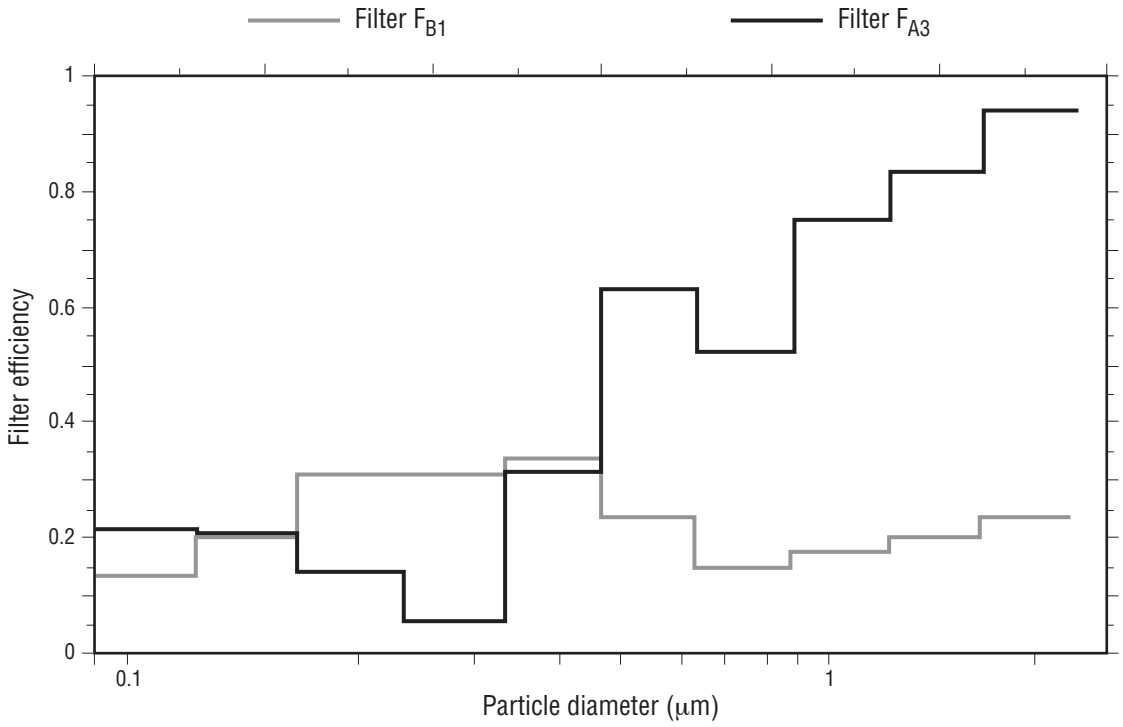

Figure 4.3. Temperature difference between the surface of a wall and the air, and the air velocity near the same wall versus time for 24-hour periods at each site. The air-velocity probe was located at a distance of 1.05 cm from the wall at the Norton Simon Museum, 1.3 cm at the Scott Gallery, and 1.2 cm at the Sepulveda House.

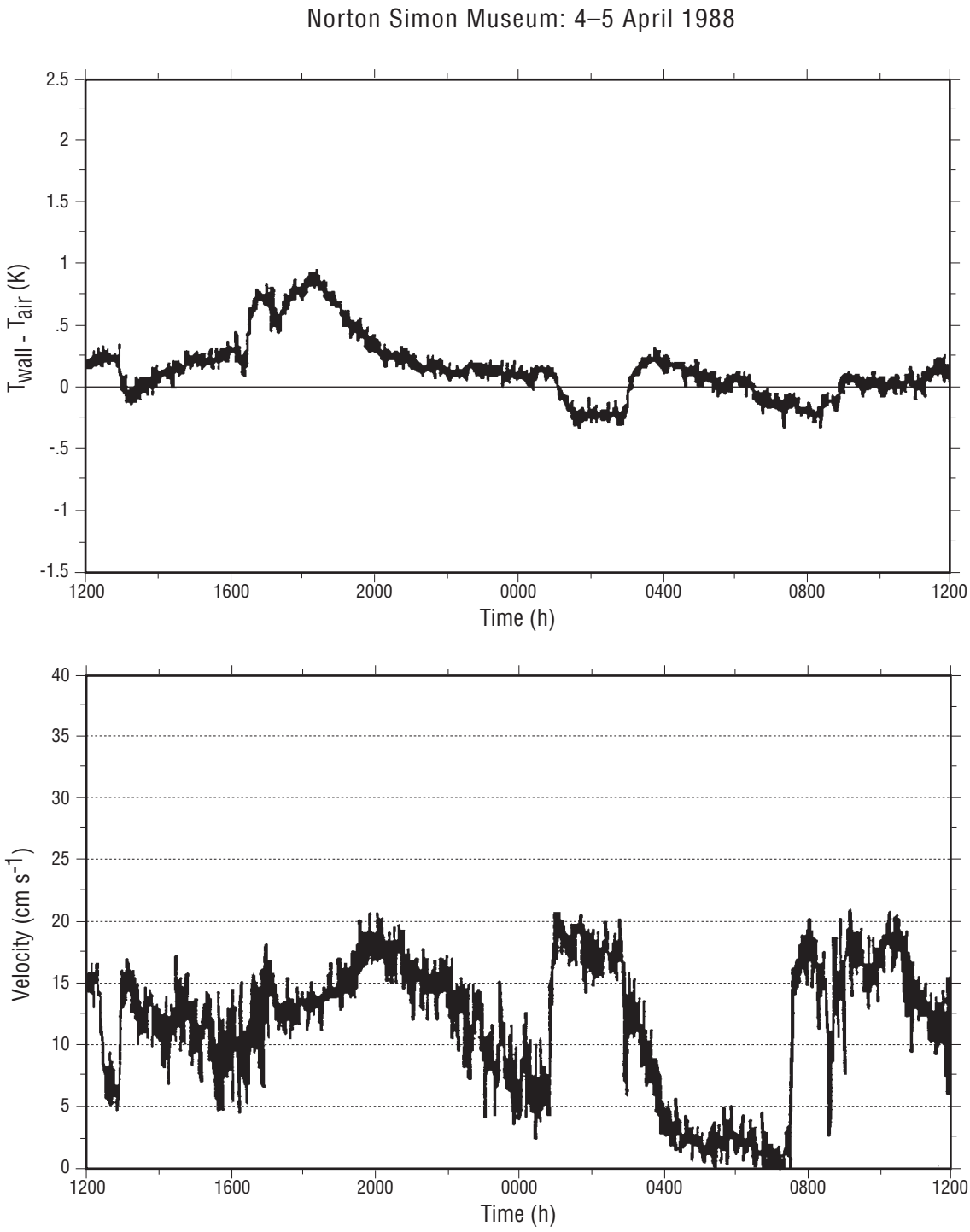

Figure 4.3. Continued.

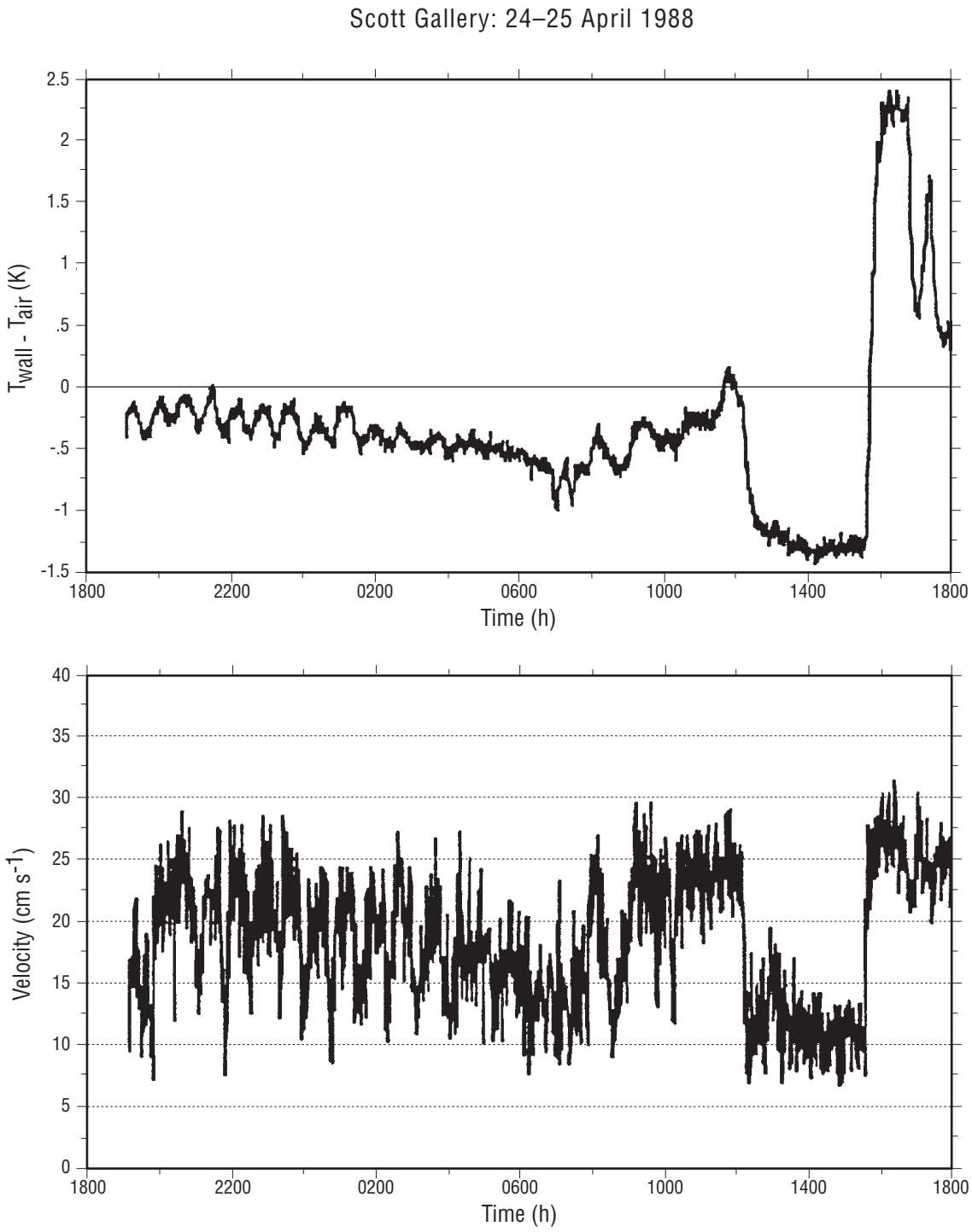

Figure 4.3. Continued.

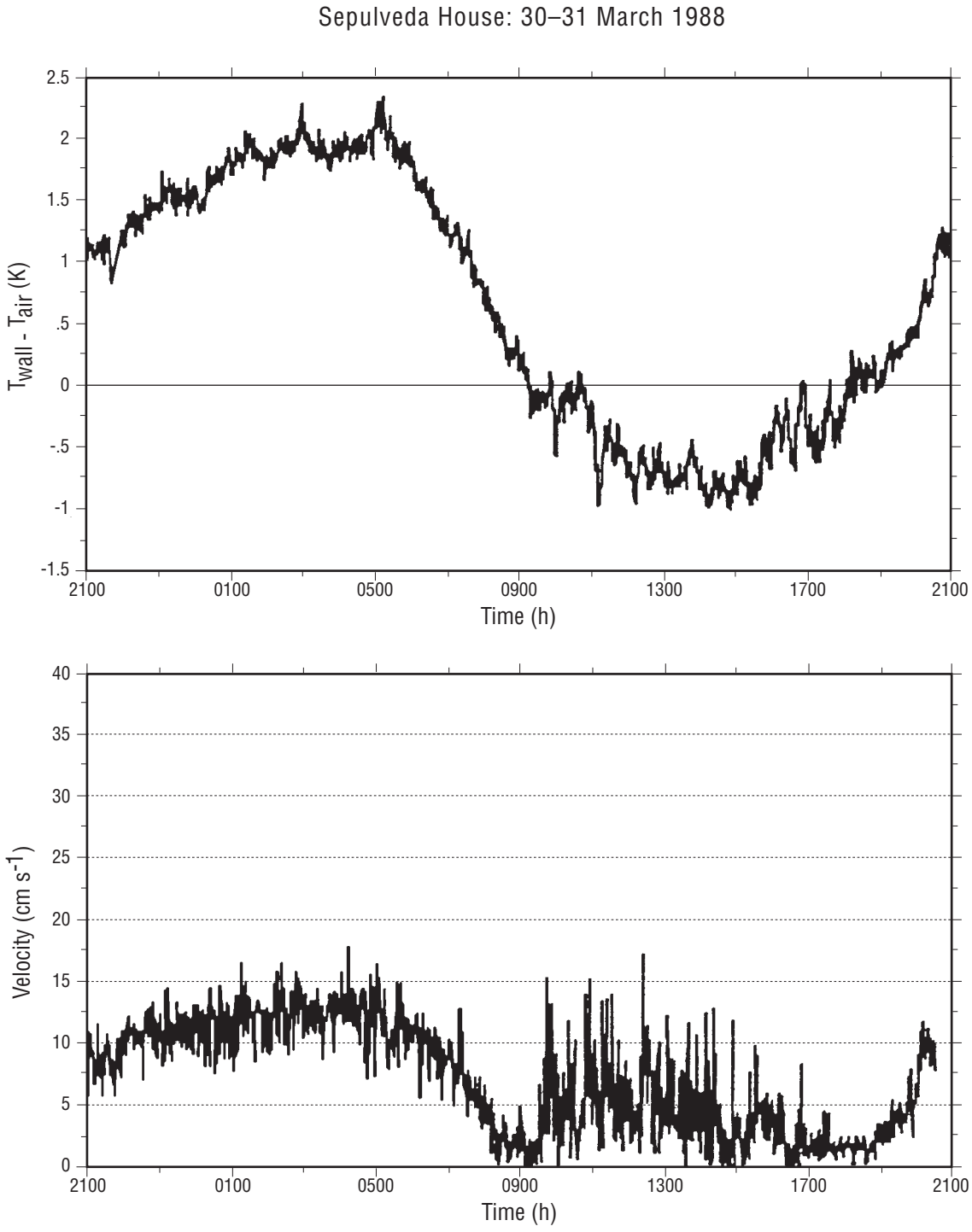

Figure 4.4. Fine-particle mass concentration versus time and 24-hour-average aerosol size distribution for the three study sites. The figure compares outdoor measurements, indoor measurements, and indoor modeling results. The measured fine-particle concentrations are based on midrange optical particle counters. The coarse component and the mass in the smallest section of the size distribution are based on analysis of filter samples. The modeling results for the Norton Simon Museum and the Scott Gallery reflect Case A conditions, defined in Table 4.2.

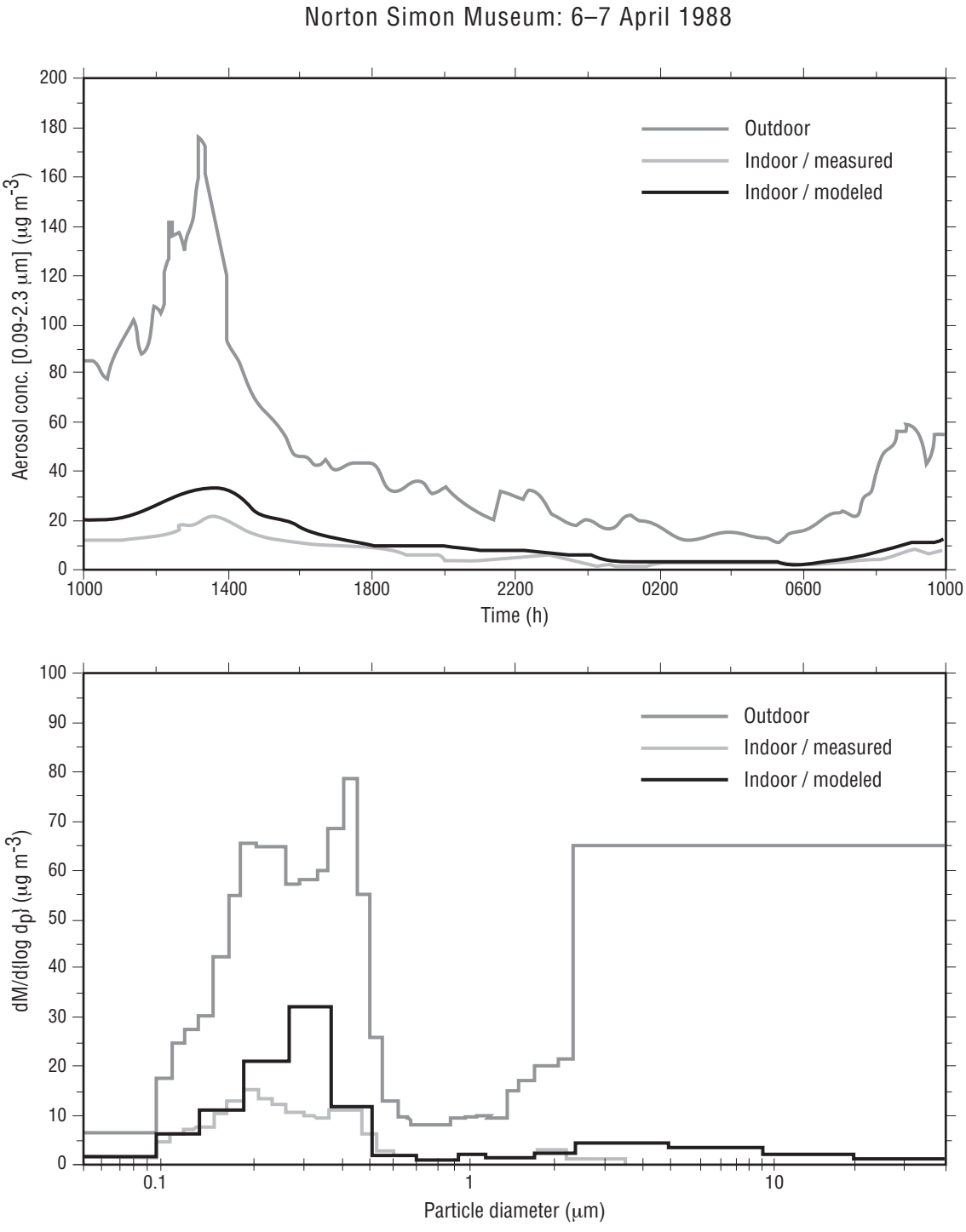

Figure 4.4. Continued.

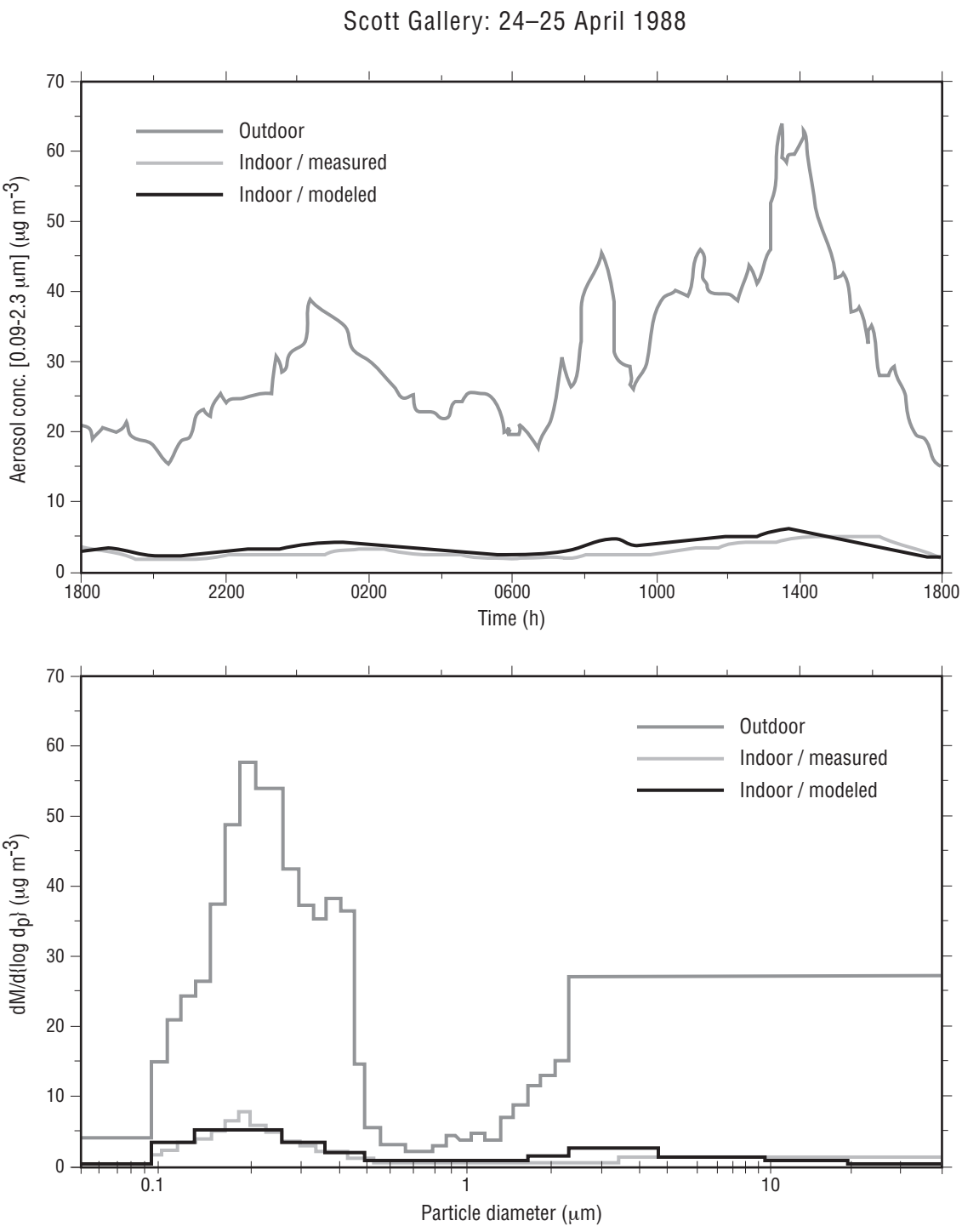

Figure 4.4. Continued.

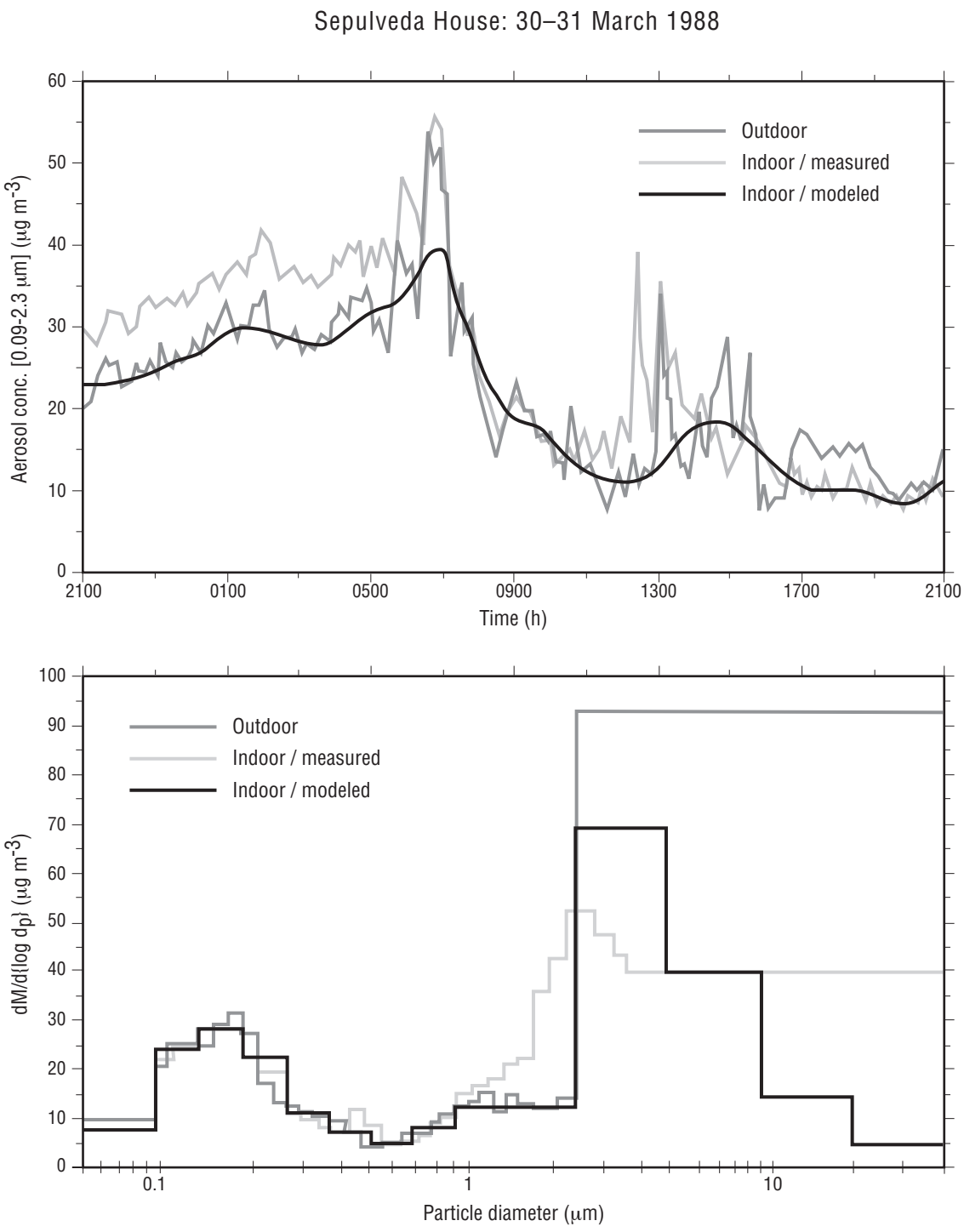

Figure 4.5. The predicted fate of particles introduced into the buildings from outdoors. The ordinate of each point represents the 24-hour-average fraction of the mass in that section brought in from outdoors that is removed by the indicated process. The abscissa reflects the logarithmic midpoint of the range of diameters in the size section. Coagulation (-) indicates a net loss of aerosol mass in the section due to particle coagulation, and Coagulation (+) indicates a net gain. The results shown for the Norton Simon Museum and the Scott Gallery reflect the Case A conditions defined in Table 4.2.

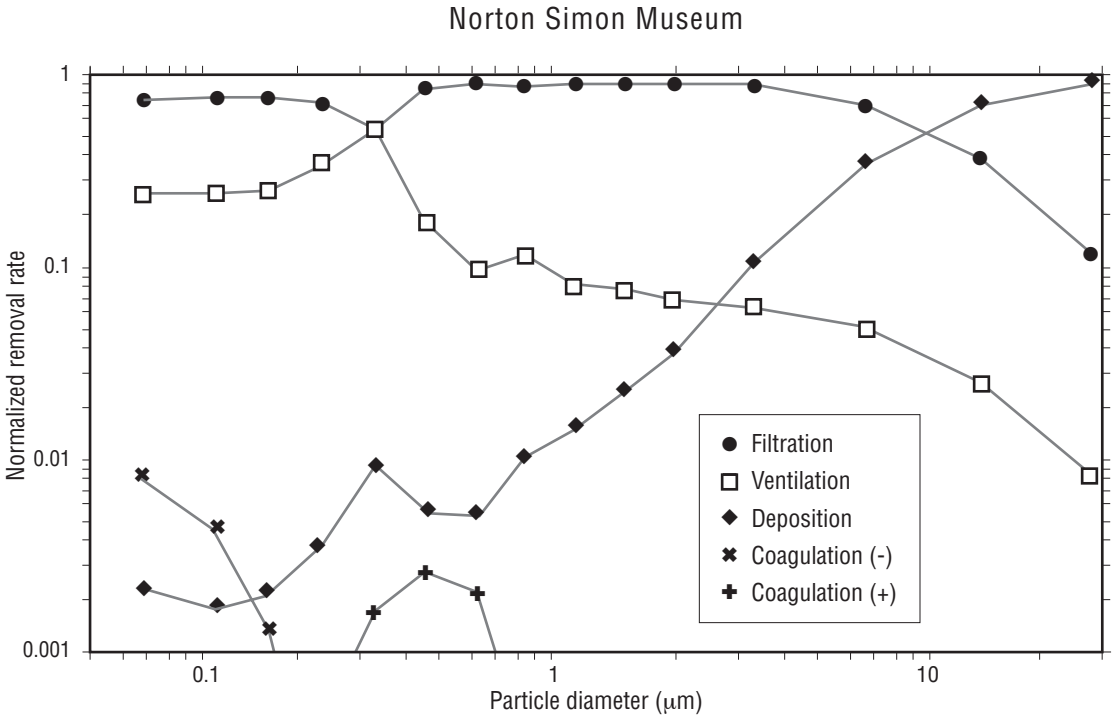

Figure 4.5. Continued.

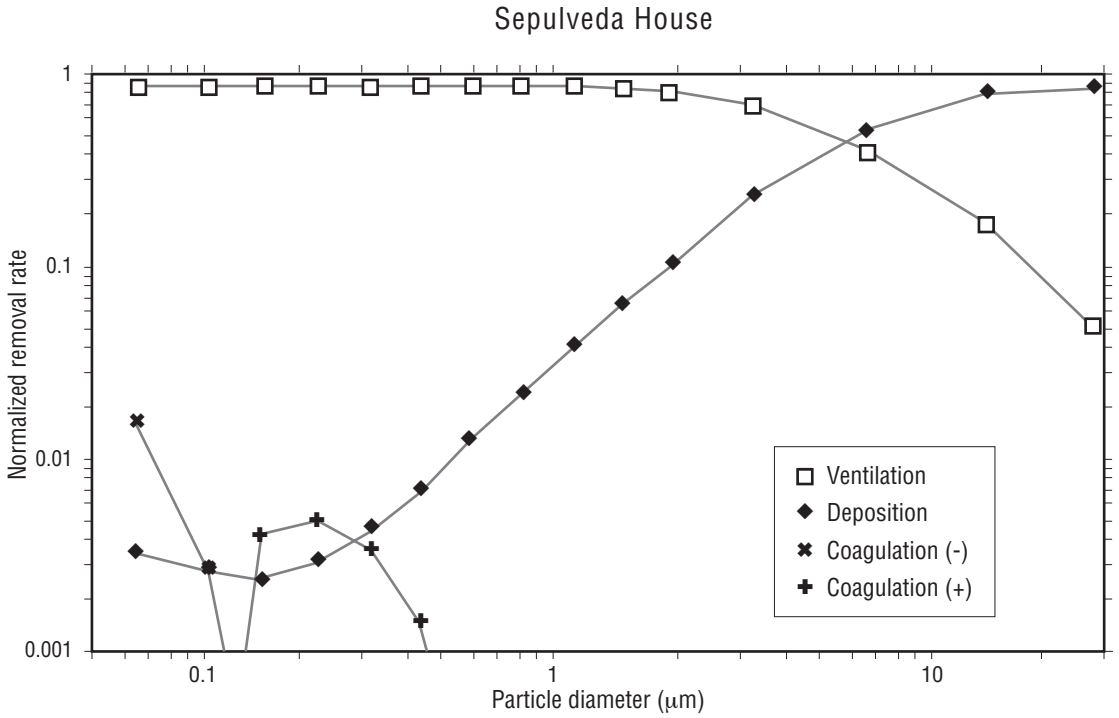

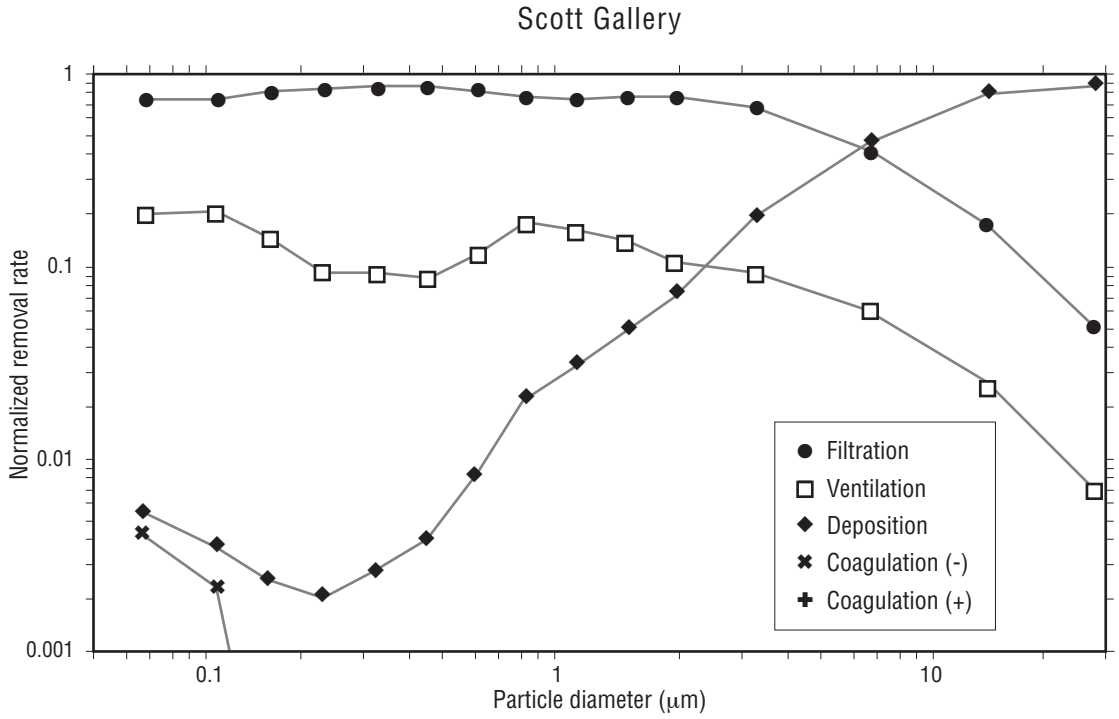

Figure 4.6. Predicted rate of accumulation, based on the single study day, of aerosol mass as a function of particle composition and size for three major surface orientations. Note that the vertical axes have different scales; in particular, the mass unit for the floors is mg, compared with μg for the other surfaces. The results shown for the Norton Simon Museum and the Scott Gallery reflect the Case A conditions defined in Table 4.2.

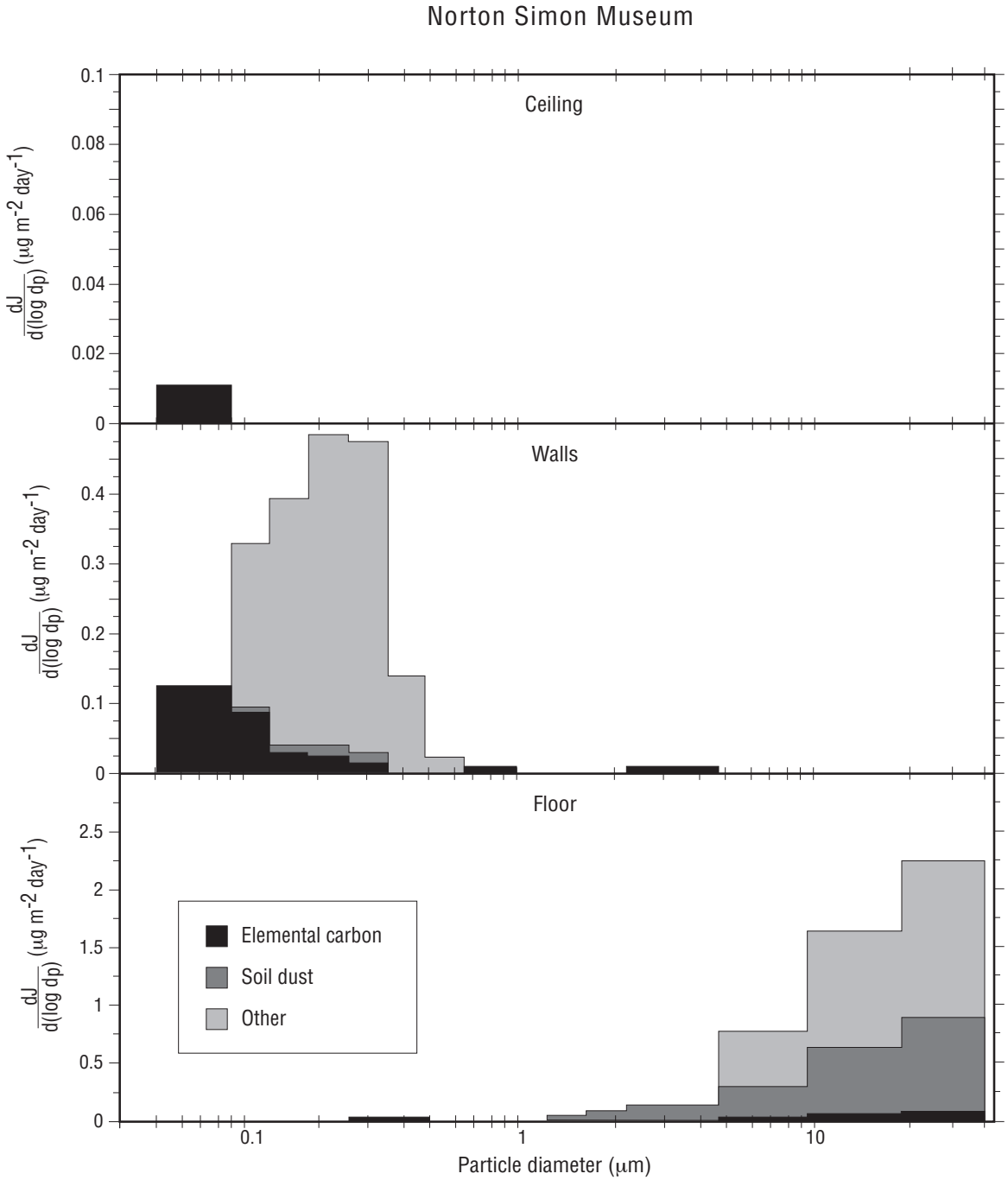

Figure 4.6. Continued.

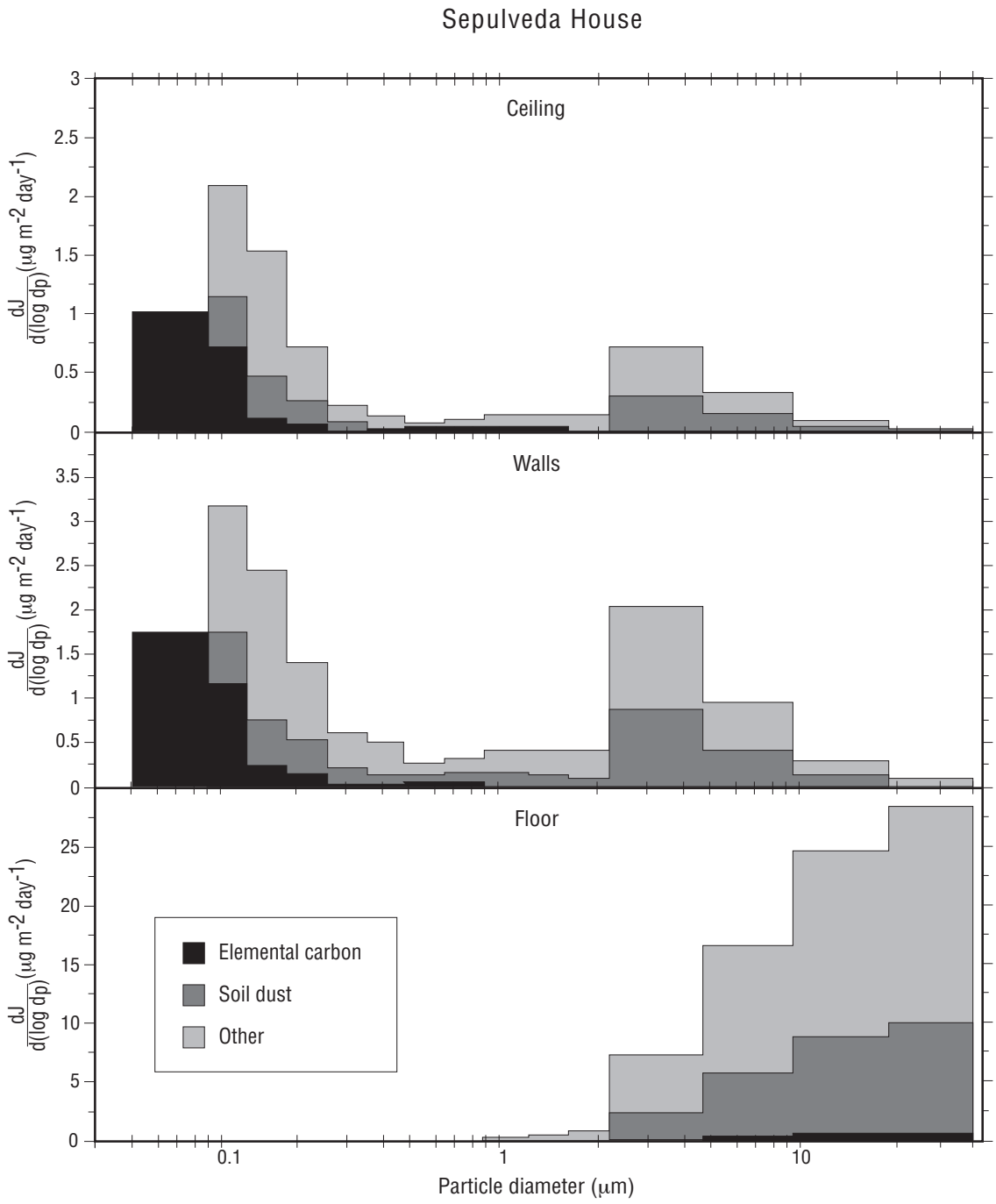

Figure 4.6. Continued.

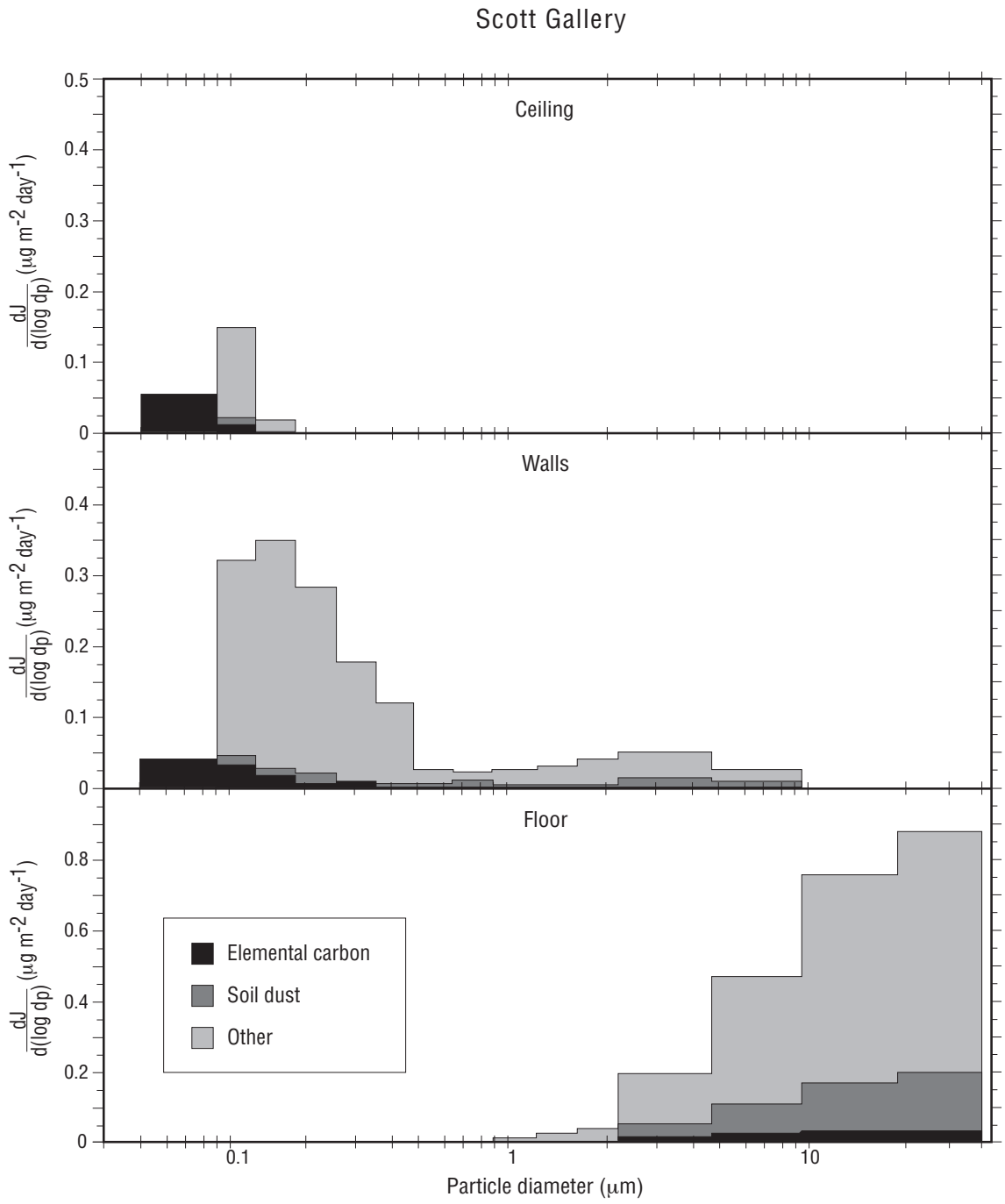

5 Measurements of the Rates of Soiling Inside Museums Due to Deposition of Airborne Particles

To understand the potential for the soiling of artifacts, it is necessary to consider not only the particle concentrations in the indoor air and the rates at which airborne particles deposit onto surfaces, but also the optical characteristics of the accumulated deposit of particulate matter. The quantity of black material that must be deposited onto a surface in order for the darkening to be perceived by the human eye has been studied by Carey (1959) and Hancock et al. (1976). Carey found that a white surface covered by fine black dots at a coverage density of 0.2% could be distinguished from a pure white surface by an average observer. For a surface that is initially grey, a black dot density of 0.4% was required in order for the difference to be perceived. Hancock et al. determined that at a fractional coverage of 0.7%, the degree of darkening was considered offensive by a panel of observers.

While much of the airborne particulate matter complex consists of light-colored ionic material, several types of airborne particles can be expected to contribute to the color of deposits. Elemental or black carbon particles are derived from combustion processes (such as diesel engine soot) and are generally associated with particles of a few tenths of a micrometer in diameter. Soil-dust material, which is usually brown in color, is generally associated with particles of a few micrometers in diameter or larger. Organic matter, which is often yellow in color, can be associated with large or small particles. Of these, particles containing elemental carbon are of particular concern, because their small size allows them to penetrate the filters in many commercial HVAC systems; once lodged in the pores in surfaces, these very fine black particles cannot be removed easily.

It is possible to measure the mass flux of particles to surfaces and to measure the darkening of surfaces by optical methods. A method is needed to tie together the information provided by these two analyses and to relate the results to the visual appearance of a soiled surface. One possible approach consists of the following steps:

1. Measure the mass flux of particles to a surface over a given period of time.
2. Determine the elemental composition and size distribution of the deposited material.
3. From (1) and (2), calculate the fraction of the surface of interest that is covered by colored particles that have significant soiling potential.
4. Measure the change in optical characteristics of the surface over the same period of time.
5. Develop a method for predicting visual appearance based upon surface coverage and compare that prediction to the results of the optical analysis.

In this chapter, data from the experiments reported in Chapter 2 are combined with measurements of the deposition rate of elemental carbon particles. Also considered are optical measurements of the rate of darkening of white paper and canvas surfaces to test the procedure described above for estimating the rates at which artifacts in urban museums may become soiled.

Experimental Methods

Sample Collection

Deposition surfaces for optical analysis that were included in the Southern California museum experiments described in Chapter 2 consisted of white artists' canvas and Whatman 42 filter paper. Some of the paper and canvas samples were clamped into aluminum frames, similar to those described in Chapter 2 for the quartz cloth deposition plates. Those quartz cloth deposition surfaces will be used here as the basis for measurement of black carbon-particle deposits. The quartz deposition surfaces were left in place for one full year, beginning in June 1987. Sets of the canvas and paper deposition surfaces were left in place for a summer period (July 2 through August 31, 1987), a winter period (November 23, 1987, through January 30, 1988), and for the entire year. During the summer and winter periods, airborne particle samples were collected over 24-hour periods every sixth day.

Measurements of the diffuse reflectance spectra of the canvas and paper deposition surfaces were made before and after use with a Diano Match-scan II reflectance spectrophotometer (Diano Corp., Woburn, Mass.). The measurements were made at three specific, recorded positions on the sample surface in order to maximize the ability to detect slight color changes. Each sample was analyzed a few days prior to placement at the sampling site, then reanalyzed after removal. Measurements were made in triplicate to determine the variability of measurements taken at the same position on the sample, at different positions on the sample, and at the same position but on different analysis days. Field blanks also were analyzed and used to correct for instrument drift over the sample collection period. The initial color of the samples and the color after exposure were calculated in terms of the tristimulus values X, Y, and Z, and also the L*, a*, b* color scale (CIE 1978, Billmeyer and Saltzman 1981) for the CIE 2 ° standard observer (CIE 1931) using illuminant C. Small changes in the white deposition surfaces associated with slight degrees of soiling are easily interpreted using this system. The ΔE value, indicating the overall color change of a sample over the course of the experiment, also was determined.

The minimum color change detectable was determined by the variability in the samples and blanks. The largest variability was found for the L* coordinate and for the paper samples. In general, ΔE values as small as 0.2 units were found to be statistically significant when

measurements were taken of the canvas samples, while ΔE values of 0.5 units or greater were found to be statistically significant when measurements were taken of the paper samples.

Results and Discussion

Over the sampling periods of three months to a year, the canvas and paper surfaces experienced a measurable color change at every site. In most cases, the color change consisted of a combination of darkening and yellowing of the surface. At all sites, there was a greater color change observed with the horizontally oriented samples than with the vertically oriented samples. The Sepulveda House and the Southwest Museum are the only two sites studied at which darkening of the vertically oriented surface was detected during a one-year exposure period. These optical data are presented in detail in the final project report (Nazaroff et al. 1990).

Canvas-covered deposition plates that had been placed inside a display case at the Southwest Museum and inside the isolated display bedroom at the Sepulveda House also were analyzed optically. The nearly airtight enclosure used at the Sepulveda House to protect the artifacts both from pollutants and from temperature and humidity fluctuations was extremely effective in reducing the darkening of horizontally oriented white surfaces. By contrast, the display cases at the Southwest Museum were not airtight. Air gaps of approximately 4 mm existed between each of the panels of glass that enclosed the display case. The color change experienced by the horizontally oriented canvas deposition plates inside the display case after one year was roughly twice those present on the horizontally oriented canvas samples placed in the main portion of the same building after 22 weeks. Thus, the display cases at this site afforded no significant protection from soiling.

The fluxes of black elemental-carbon particles to indoor horizontal surfaces, as measured by combustion analysis applied to the quartz fiber cloth deposition surfaces, are presented in Table 5.1 (p. 94) for four of the five sites. (The horizontal deposition plate at the remaining site, the Norton Simon Museum, was inexplicably removed from the museum during the course of the study.) The fluxes of elemental carbon were highest at the two sites lacking in particle filtration equipment. Deposition velocities (v_d) for elemental carbon also are presented in Table 5.1. These deposition velocity values are computed from the following expression:

$$V_d(m/s) = \frac{\text{(flux to surface } (\mu g/m^2 \cdot s)}{\text{airborne concentration } (\mu g/m^3)}$$

using the indoor yearlong average of airborne elemental carbon concentrations measured during the experiments described in Chapter 2.

	Elemental Carbon	
Site	**Flux ($\mu g/m^2 \cdot day$)**	**Deposition velocity (10^{-4} m/s)**
Getty Museum	< 3	< 0.7
Scott Gallery	7 ± 3	0.9 ± 0.4
Southwest Museum	19 ± 3	1.0 ± 0.2
Sepulveda House	21 ± 3	0.39 ± 0.1

Table 5.1. Fluxes and deposition velocities of elemental carbon to horizontal surfaces inside museums.

At all sites, the quantity of elemental carbon deposited to vertical surfaces in a one-year period was below the detection limit of the analytical method. Using that information, an upper limit in $\mu g/(m^2$ day) can be placed on the elemental carbon flux to vertical surfaces, based upon the elemental-carbon detection limit of 0.1 $\mu g/cm^2$. This value yields an upper limit to the elemental-carbon deposition velocity at the Sepulveda House of 5×10^{-6} m/s. By comparison, the measured deposition velocities for sulfate, nitrate, and ammonium ions to vertical surfaces at the Sepulveda House were 4.8, 3.3, and 4.9×10^{-6} m/s, respectively. This comparison indicates that the deposition velocity of elemental carbon on vertical surfaces at that site was not appreciably larger than the velocities of ionic species measured. The upper limits for the elemental carbon deposition velocities at the other sites are higher and less informative, due to lower indoor elemental-carbon concentrations. However, the deposition velocity for other submicron-size particle species (e.g., sulfates) at these sites is known from ion chromatographic analysis of airborne particle concentrations and resultant deposition fluxes (Chapter 2). The size-dependent deposition velocities for the overall aerosol also are known as a result of SEM analysis of airborne and deposited particles (Chapter 2). These deposition velocity data were combined with a knowledge of the size distribution of airborne elemental-carbon particles in Pasadena and Los Angeles (Ouimette 1981) to arrive at a best-estimate value for the elemental-carbon deposition velocity at all sites. These values, when multiplied by the measured ambient elemental-carbon concentrations, give an estimate of the elemental carbon deposition flux to vertical surfaces. These estimated fluxes and deposition velocities for elemental carbon are presented in Table 5.2. (p. 95).

Site	Flux ($\mu g/m^{-2} \cdot day$)	Deposition velocity (10^{-6} m/s)
Norton Simon Museum	0.08	1.5
Scott Gallery	0.15	2.1
Getty Museum	0.20	5.5
Southwest Museum	0.55	3.0
Sepulveda House	2.7	5.0

Table 5.2. Estimated fluxes and deposition velocities of elemental carbon to vertical surfaces inside museums.

Estimates of the Time Required for Soiling to Occur

To calculate the rate of surface area coverage by dark elemental-carbon or soil-dust particles, the size distribution of the particles must be known. Size distributions of outdoor fine elemental-carbon particles are available for downtown Los Angeles and for Pasadena (Ouimette 1981). The elemental-carbon size distribution for Los Angeles is representative of the size distribution near vehicular sources, with predominantly small (0.1 μm) particles, while the Pasadena data represent an aged size distribution. The Los Angeles size-distribution data were used to represent elemental carbon at the Getty Museum and Sepulveda House sites, while the Pasadena size-distribution data were used to represent elemental carbon at the Norton Simon Museum and the Scott Gallery. An arithmetic mean of the two size distributions was used to represent elemental carbon at the Southwest Museum. The assumption was made that the elemental-carbon size distribution indoors was the same as that outdoors. These size distributions were scaled to match the measured fine elemental-carbon concentrations inside these museums as reported in Chapter 2. The measured elemental carbon deposition rates to horizontal surfaces reported in Table 5.1 and the best-estimate deposition velocities from Table 5.2 then were used to calculate elemental carbon mass fluxes. These fluxes were converted into projected area coverages by assuming a monolayer coverage of spherical particles of density 2.3. The time required for the accumulation of a 0.2% surface coverage by elemental carbon alone was calculated. The results are presented in Table 5.3 (p. 96) for both vertical and horizontal surfaces.

Table 5.3 indicates that soiling of horizontal surfaces due to black elemental-carbon particles takes place rapidly, even inside the museums with particle filtration. The times required for a perceptible elemental carbon deposit to accumulate ranges from about one month to one-and-a-half years. If the additional effects of deposited organic matter and soil dust are taken into account, the computed times before perceptible soiling occurs are even shorter.

Site	Vertical	Horizontal
Norton Simon Museum	18	1.4
Scott Gallery	7.2	0.9
Getty Museum	4.8	1.3
Southwest Museum	2.0	0.3
Sepulveda House	0.3	0.1

Perceptible soiling defined as 0.2% surface coverage by elemental carbon.
Deposition of other colored particles (e.g., soil dust) will act to further decrease the time to reach the onset of perceptible soiling.

Table 5.3. Best estimate of the time (years) required for perceptible soiling to occur on indoor vertical and horizontal white surfaces due to elemental-carbon deposition.

As expected, the estimated time required for perceptible soiling is longer for the three sites with particle filtration systems than for the two sites without them. Among the sites studied, the greatest protection from soiling exists at the Norton Simon Museum, where nearly two decades are required for perceptible soiling of vertical surfaces by elemental carbon particles. At both the Getty Museum and Scott Gallery, deposition fluxes are higher than at the Norton Simon Museum, in part because these facilities have higher infiltration rates of unfiltered air through open doors in the building.

The soiling time estimates presented in Table 5.3 on the basis of experimentally determined deposition velocities and indoor elemental carbon concentrations are in good agreement with estimates made for three of the same sites on the basis of the indoor air-quality modeling calculations discussed in Chapter 4. Furthermore, these estimates are in excellent agreement with visual observations of the deposition surfaces. The treatment in Table 5.3 predicts that horizontal surfaces at the Sepulveda House and Southwest Museum will become visibly darkened in much less than one year, that horizontal surfaces of the Scott Gallery will be just barely darkened in a year, but that deposits at the Getty and Norton Simon museums will not be visible at the end of a year. Further, Table 5.3 predicts that Sepulveda House is the only site at which visible deposits will be seen on vertical surfaces within a one-year period. Recorded visual observations of the quartz deposition surfaces after exposure for one year were as follows: For the horizontal surfaces, reports indicated Sepulveda House with “deposit quite dark (grey)”; Southwest Museum with “grey, visible deposit”; Scott Gallery with “deposit faintly visible”; and the Getty Museum with “no visible deposit.” For the vertical surfaces, reports indicated “no visible deposit except Sepulveda House.”

6 Protecting Museum Collections from Soiling Due to Deposition of Airborne Particles

The aim of this chapter is to explore the options available to museum conservators to reduce soiling rates within museums. The potential effectiveness of several control options—reducing ventilation, improving filtration, and reducing particle-deposition velocities—is assessed by computing the effects of these methods on the soiling rate of surfaces in a specific Southern California museum: the Sepulveda House. For these calculations, the indoor air-quality model of Chapter 3 is applied, using data on outdoor airborne-particle concentrations and building parameters from the experiments discussed in Chapter 4. Assessment of other control options—using display cases, managing a site to achieve low outdoor aerosol concentrations, and limiting indoor aerosol sources—are obtained through additional modeling calculations and measurements for this site. The results demonstrate that the rate of soiling of surfaces may be reduced by two to three orders of magnitude relative to uncontrolled conditions through the application of practical control measures.

The work in this chapter complements a recent examination of control options for protecting works of art from damage by atmospheric ozone (Cass et al. 1988). However, because the chemical and physical properties of soiling particles are distinct from those of reactive gases, the control options are somewhat different in the two cases, and the effectiveness of a particular control measure may be quite different.

Factors Governing the Soiling Rate of Indoor Surfaces Due to Particle Deposition

In Chapter 3, a detailed mathematical model was developed to predict the time-dependent chemical composition and size distribution of indoor aerosols. That model accounts in detail for the effects of emission, filtration, ventilation, coagulation, and deposition. As shown in Chapter 4, the model is capable of making accurate predictions of the airborne particle characteristics in Southern California museums based on building parameters and data on outdoor particle properties. Predictions of the rate of particle deposition to surfaces in museums were shown to be reasonably consistent with measurement results (Chapters 2 and 5). In the present chapter, that model is applied to evaluate the effectiveness of control measures aimed at reducing the soiling rate.

Several approximations are employed for this purpose. First, only two chemical components of the airborne particulate matter—elemental carbon and soil dust—are considered. Elemental carbon is directly associated with the blackness of the airborne particulate matter (Cass et al. 1984), and so this material is a major concern as a soiling agent. Soil dust contributes

much of the brown color seen in coarse airborne particle samples and thus may also lead to soiling. Elemental carbon is predominantly found among fine particles with a mass-median diameter in the vicinity of 0.1 μm (Ouimette 1981). Airborne soil dust, by contrast, occurs primarily as coarse particles, larger than 2 μm in diameter (see Chapter 4, Table 4.3, p. 71). Because of the relatively large particle size of this material, the dominant mechanism for soil-dust deposition indoors is gravitational settling onto surfaces with an upward orientation; the soiling of vertical and downward-facing surfaces by soil dust is minimal. By contrast, the gravitational settling velocity of particles with 0.1 μm diameter, such as those of elemental carbon, is less than typical deposition velocities for particles of that size due to convective diffusion and thermophoresis; as a result, surfaces with any orientation may be soiled by the deposition of elemental carbon particles.

For the purposes of this chapter, a characteristic time for soiling, τ_s, associated with the accumulation of a soiling deposit is defined as the time necessary to accumulate an effective surface-area coverage of 0.2% by the particles of interest. As explained in Chapter 5, a 0.2% surface coverage by black particles represents the approximate point at which soiling of a white surface first becomes apparent to an observer. The actual point at which soiling becomes perceptible may well depend on additional factors, such as the chemical composition and morphology of the particles and the optical properties of the surface of interest. Since the light-absorbing properties of elemental carbon differ from those of soil dust, the degree of surface coverage needed to produce perceptible soiling probably differs for the two components. The information needed to combine the accumulation of the two components into a single soiling rate is lacking, so the control objective shall be to increase the value of τ_s associated with both soiling components of the atmospheric aerosol to as great an extent as possible for all surfaces of interest.

Evaluating the Effectiveness of Measures to Control Soiling Inside Museums

In this section, methods for controlling soiling rates inside museums are evaluated using the indoor airborne particle dynamics model of Chapter 3. That model computes the total deposited mass of particles onto a given surface as a function of particle size and chemical composition, includes coagulation, and captures the full effect of the particle-size distribution on deposition velocities and filtration efficiencies. As discussed in Chapter 4, the total rate of effective area coverage of a surface by a given particulate chemical component may be computed by summing the rates for that component over each particle-size section. In applying the model, characteristic soiling times are computed for the floor, the walls, and the ceiling. These results indicate soiling times for other exposed surfaces, such as those of art objects with corresponding orientations.

A case study based on data taken at an historical museum in downtown Los Angeles is presented below for purposes of illustration. First, a retrofit of the building to add a conventional mechanical ventilation and particle-filtration system is analyzed. Then, further measures to control the rate of soiling of indoor surfaces are considered.

Site Description and Baseline Soiling Conditions

The two-story Sepulveda House historic museum has no mechanical ventilation or indoor climate control system. Air exchange is provided by uncontrolled leakage through openings in the building shell. A large gap (~0.35 m^2 total area) around the perimeter of a carriage door downstairs, coupled with skylight vents in the upstairs ceiling, leads to a frequently strong buoyancy-driven flow through the building. The average (± one standard deviation) of hourly air-exchange rates, measured by tracer-gas decay for a 24-hour period on March 30–31, 1988, is 3.6 (± 1.4) h^{-1}.

Within a few city blocks of the downtown location of this museum are major aerosol sources, including the intersection of two major freeways, the main railroad station for Los Angeles, and numerous routes for diesel trucks and buses. The high concentration of airborne particulate matter in outdoor air, in combination with the high air-exchange rate and lack of particle filtration within the building, leads to high indoor particle concentrations, including the highest indoor elemental-carbon and soil-dust concentrations observed from among the five museums examined during this study (Chapter 2). In turn, the rate of soiling of surfaces within this museum is large. Modeling calculations indicate that the deposition of elemental-carbon particles on walls would lead to perceptible soiling within a year (Chapters 4 and 5). This prediction is confirmed by observations showing that the rate of color change of white quartz filter material mounted on a wall within this site was perceptible within one year (Chapter 5). Soiling of upward-facing horizontal surfaces is even more rapid. Thus, the deposition of airborne particles constitutes a soiling hazard for objects in this museum. The Sepulveda House provides a challenging case against which the effectiveness of control options to reduce the soiling rate may be judged. This site is also very interesting as it may closely approximate the situation at many small, older urban museums and churches.

For the purposes of this evaluation, detailed experimental results from the Sepulveda House on outdoor aerosol characteristics and factors governing particle deposition rates are used as input data to the indoor aerosol dynamics model (see Chapter 4 for a discussion of these data). The Sepulveda House is configured, for modeling purposes, as a single-building volume (V), exposed to outdoor pollutant concentrations (C_o), air infiltration at a given flow rate (f_{oi}), with indoor concentrations (C_i), and particle deposition velocities (v_d) to each of the interior surfaces (A), as shown in Figure 6.1 (p. 115) . Provision is made in the model for the future addition of a mechanical ventilation system with an outdoor air-supply rate (f_{ox}), and an indoor air-

recirculation rate (f_{ii}), with filters of a given efficiency (η) placed within that ventilation system. The building parameters are changed for each case to reflect the successive adoption of control techniques (Table 6.1, p. 101). The characteristic soiling rate associated with each case is computed based on modeling calculations for a 24-hour period beginning on March 30, 1988, at 2100 hours PST, with input data provided on an hourly averaged basis. The 24-hour averages of the outdoor airborne particle-size distribution and chemical composition are presented in Figure 6.2 (p. 116). For the day of study, the total mass concentration of elemental carbon associated with fine particles was 5.0 $\mu g\ m^{-3}$, essentially the same as the annual mean for this site (Table 6.2, p. 102). Most of the mass of elemental-carbon particles is in the size range of 0.05–0.2 μm. The total mass concentration of coarse soil-dust particles on this day was 41 $\mu g\ m^{-3}$, three times larger than the annual mean value for this site. The characteristic times for soiling associated with soil dust, based on the March 30–31, 1988 data, are therefore shorter than those that would result from annual-average conditions; assuming that the size distribution is unchanged, results for the annual mean conditions may be obtained by linear scaling. Information on the time dependence of the outdoor aerosol concentrations may be found in Figures 4.4 and 6.3 (pp. 83–85 and 117).

Baseline conditions	
Case 1	No filtration or mechanical ventilation; mean infiltration rate: $f_{oi} = 1.2\ m^3\ s^{-1}$; deposition according to homogeneous turbulence 1000–1500 hours, mean turbulence intensity parameter: $K_e = 0.56\ s^{-1}$; deposition according to natural convection model 000–1000 and 1500–2400 hours, surface-air temperature difference as shown in Figure 4.3 (pp. 80–82).
Standard mechanical ventilation retrofit	
Case 2	Same as Case 1 with the following exceptions: infiltration rate reduced; $f_{oi} = 0.06\ m^3\ s^{-1}$; mechanical ventilation added: $f_{ox} = 0.6\ m^3\ s^{-1}$ and $f_{ii} = 2\ m^3\ s^{-1}$; all air in mechanical ventilation system passed through filter with efficiency of 15–30% ($\eta_{ox} = \eta_{ii} = 0.15$–$0.3$), varying according to particle size as shown for filter F_{B1} in Figure 4.2 (p. 79).
Reduce ventilation rate	
Case 3	Same as Case 2 with the following exception: reduce mechanical ventilation make-up airflow rate to design occupancy while holding total flow rate constant: $f_{ox} = 0.167\ m^3\ s^{-1}$, $f_{ii} = 2.43\ m^3\ s^{-1}$, and $f_{oi} = 0.06\ m^3\ s^{-1}$.
Case 4	Same as Case 3 with the following exception: eliminate mechanical ventilation make-up airflow when building is closed to public: $f_{ox} = 0.0$, $f_{ii} = 2.6\ m^3\ s^{-1}$, and $f_{oi} = 0.06\ m^3\ s^{-1}$ during 000–1000 and 1500–2400 hours.
Improve filtration effectiveness	
Case 5	Same as Case 4 with the following exception: improve filter efficiency: $\eta_{ox} = 0.99$ for coarse particles ($d_p > 2\mu m$) and 0.88 for fine particles, and $\eta_{ii} = 0.95$ for coarse particles and 0.875 for fine particles.
Case 6	Same as Case 3 with the following exceptions: improve filter efficiency: $\eta_{ox} = 0.99$ for coarse particles ($d_p > 2\ \mu m$) and 0.88 for fine particles, and $\eta_{ii} = 0.95$ for coarse particles and 0.875 for fine particles; eliminate infiltration: $f_{oi} = 0.0$.
Reduce particle deposition velocities	
Case 7	Same as Case 6 with the following exception: natural convection flow regime assumed to hold at all times for computing particle deposition rates with $T_{surface} - T_{air} = 1K$.
Case 8	Same as Case 6 with the following exception: laminar forced flow regime assumed to hold at all times for computing particle deposition rates with free stream airflow rate and surface-air temperature differences corresponding to conditions at the Norton Simon Museum, Case A, in Chapter 4.
Basic building data: volume = 1200 m^3; floor area = 330 m^2; wall area = 1050 m^2. Airflows (f_{oi}, f_{ox}, f_{ii}) and filtration efficiencies (η_{ox} and η_{ii}) are defined in the text and illustrated schematically in Figure 6.1 (p. 115).	

Table 6.1. Building conditions for modeling the effect of control measures at the Sepulveda House.

		Fine elemental carbon			Coarse soil dust		
City	**Museum**	**Summer[a]**	**Winter[b]**	**Mean**	**Summer[c]**	**Winter[d]**	**Mean**
Malibu	Getty Museum	0.3	1.3	0.8	5.8	5.9	5.9
Los Angeles[e]	Sepulveda House	2.6	7.3	4.9	15.0	9.8	12.4
Los Angeles[f]	Southwest Museum	1.5	3.3	2.4	17.2	22.0	19.6
Pasadena	Norton Simon Museum	1.5	3.3	2.4	12.3	12.5	12.4
San Marino	Scott Gallery	1.3	2.8	2.1	20.3	12.9	16.6

a. Average of 10–11 24-hour samples collected at six-day intervals during July 2–August 31, 1987.
b. Average of 12 24-hour samples collected at approximately six-day intervals during November 23, 1987–January 28, 1988.
c. Average of 9–11 24-hour samples collected during July 2–August 31, 1987.
d. Average of 5–9 24-hour samples collected during November 23, 1987–January 28, 1988.
e. Located in the downtown area.
f. Located in Highland Park, roughly 10 km north of downtown.

Table 6.2. Mean outdoor concentrations ($\mu g\ m^{-3}$) of aerosol components measured at museum sites in Southern California.

For the baseline conditions, the rates of particle deposition on indoor surfaces are computed as in Chapter 4: Homogeneous turbulence in the core of the building is assumed to govern deposition rates during 1000–1500 hours, when the museum is open to the public, and natural convection flow adjacent to the surfaces is assumed to govern deposition rates at other times.

The indoor air-quality model of Chapter 3 was run for base-case uncontrolled conditions at the Sepulveda House, and the results are reported in Chapter 4 (Fig. 4.4 , pp. 83–85; Table 4.3, p. 71). The characteristic soiling times are three days for the accumulation of a perceptible deposit of soil dust on upward-facing surfaces, and 0.9 and 1.5 years for the accumulation of a perceptible deposit of elemental carbon particles on walls and ceilings (Table 4.5, p. 76; Table 6.3, p. 103).

	Aerosol concentration (μg m^{-3})				Mass deposition rate (μg m^{-2} day^{-1})						Characteristics soiling time (y)					
	Coarse		Fine		Floor		Walls		Ceiling		Floor		Walls		Ceiling	
Case	SD	EC	SD	EC	SD	EC	SD	EC	SD	EC	SD	EC	SD	EC	SD	EC
Outdoor	41.6	1.34	2.51	4.92												
1	14.4	0.49	2.47	4.92	8500	280	0.70	0.69	0.32	0.40	0.01	0.2	4.1	0.9	6.2	1.5
2	6.3	0.21	1.18	2.79	3600	118	0.32	0.41	0.15	0.24	0.02	0.3	7.8	1.4	12	2.4
3	2.71	0.093	0.62	1.59	1400	47	0.16	0.24	0.077	0.14	0.05	0.7	14.3	2.4	21	4.0
4	1.49	0.052	0.33	0.74	680	23	0.14	0.18	0.074	0.13	0.1	1.2	16.6	3.3	23	4.5
5	0.46	0.015	0.069	0.13	350	11	0.022	0.021	0.010	0.013	0.24	4.8	126	29	190	45
6	0.014	0.0007	0.022	0.043	9.9	0.41	0.003	0.006	0.002	0.003	7.4	34	490	100	740	170
7	0.016	0.0008	0.022	0.043	8.5	0.31	0.000	0.003	0.000	0.000	10	90	3100	220	—	—
8	0.016	0.0008	0.022	0.043	8.5	0.32	0.001	0.003	0.000	0.001	10	48	1650	180	—	930

Outdoor aerosol properties and baseline data on building characteristics measured over 24-hour period beginning at 2100 hours PST on March 30, 1988.

Table 6.3. Predicted effect of control measures for reducing soiling rates at the Sepulveda House resulting from the deposition of soil dust (SD) and elemental carbon (EC) particles onto indoor surfaces.

Preliminary Renovation: Adding a Conventional Mechanical Ventilation and Particle Filtration System

To achieve reduced soiling rates for all surfaces within the building, the first step to be considered is the addition of a mechanical ventilation system with particle filtration. The parameters of this first system studied, summarized in Table 6.1 (Case 2, p. 101, reflect the properties of a typical installation in a modern commercial building. To achieve the retrofit, the rate of uncontrolled leakage of air into the building must be reduced. Closing the skylight vents and the large perimeter gaps around the downstairs carriage doors would substantially reduce the effective leakage area of the building shell. Airflow through other leakage pathways also can be reduced. A conventional mechanical ventilation system could be designed to maintain the building at a slightly higher air pressure than outdoors, so that most of the air entering the building would pass through the mechanical ventilation system rather than through the remaining leaks and openings in the building shell. However, some uncontrolled leakage into the building is likely to persist as, for example, when visitors open doors to enter the museum.

For the baseline retrofit assumptions, the mechanical ventilation system provides 1.8 building volumes per hour of outdoor air, which constitutes 23% of the total airflow rate through the mechanical ventilation system, the remainder being recirculated from the building itself. The rate of uncontrolled air leakage into the building is taken to be 10% of the outdoor air-supply rate of the mechanical ventilation system, or 0.18 building volumes per hour. All of the air handled by the mechanical ventilation system, both make-up and recirculated, passes through a fibrous mat filter with filtration efficiency characteristics corresponding to the filters now used at a new museum in the Los Angeles area (Scott Gallery, Filter F_{B1}, Fig. 4.2, p. 79); i.e., 15–35% removal, depending on the particle size.

Model calculations show that the installation of such a mechanical ventilation and particle-filtration system would lead to a moderate improvement in the characteristic soiling times (Table 6.3, p. 103). The accumulation of either soil-dust or elemental-carbon particles onto upward-facing surfaces still would lead to perceptible soiling in a period of less than three months. Characteristic times for perceptible soiling of walls and ceilings due to deposition of elemental carbon particles would be extended to only 1.4 and 2.4 years, respectively.

Clearly, a conventional air-conditioning system at this location would be insufficient to control the soiling problem. Measures that lead to more dramatic improvements in the characteristic times before soiling becomes apparent are discussed in the following section.

Evaluation of the Effectiveness of Further Control Measures

Several control opportunities exist that could be used to reduce the rate of soiling. These may be grouped into six categories: (1) reducing ventilation rates (making $f_{oi} + f_{ox}$ small), (2) improving particle filtration (making η_{ox} and/or η_{ii} large), (3) reducing the deposition velocity to the surface to be protected (making v_d small), (4) using display cases or framing to reduce the rate of particle deposition onto the surfaces of an art object, (5) managing a site in a way that maintains lowered outdoor aerosol concentrations (making C_o small), and (6) limiting indoor aerosol sources (making S_k small).

In this section, the effect of applying these control measures for the Sepulveda House case study is considered. The first three measures are applied as further measures to improve the soiling-control performance of the preliminary renovation just discussed. The last three measures are considered independently, without presuming the existence of a mechanical ventilation system for the building.

Reducing Ventilation Rates

In the absence of significant indoor emissions, the indoor concentration of airborne particles, and consequently the soiling rate, may be reduced by lowering the rate at which outdoor air enters the museum. The effect of reducing the outdoor air-exchange rate from the nominal value for the conventional mechanical ventilation system design described above is examined below. In adopting this control measure, it is first necessary to ensure that adequate ventilation is provided for the occupants of the building. The recommended lower limit for the supply of outdoor air to a building is 8.5 $m^3\ h^{-1}\ person^{-1}$, based on the need to prevent accumulation of CO_2 produced by the building's occupants (ASHRAE 1985). In a system in which the building is pressurized relative to outdoors, the flow rate of the mechanically induced outdoor air supply must exceed the mechanically induced exhaust flow rate, as, for example, from restrooms. Furthermore, reducing the supply rate will reduce the degree to which the building operates at a higher air pressure than outside. To avoid concomitantly increasing the infiltration rate, it may be necessary to further reduce the leakiness of the building shell.

The occupancy of a museum gallery may be highly variable. With many conventional mechanical ventilation systems, the rate of supply of outdoor air is fixed according to the size of the building to a level sufficient for the maximum expected occupancy. If, instead, the ventilation rate were varied according to the actual occupancy, the average ventilation rate would be much lower, and the rate of soiling could be considerably reduced. Outdoor air-supply rates are generally controlled by the position of dampers at the inlet register. By equipping the inlet register with dampers that are easily adjusted, the ventilation rate could be changed in response to changing occupancy.

Model predictions of characteristic soiling times indicate the reduction in soiling rates that can be achieved by reducing outdoor air-exchange rates. Two situations (Cases 3 and 4) are examined in Table 6.1 (p. 101). For Case 3, the baseline retrofit mechanical ventilation system is retained, but the outdoor air make-up flow rate is reduced to a constant lower level ($f_{ox} = 0.167$ m^3 s^{-1}). This flow rate corresponds to 8.5 m^3 h^{-1} $person^{-1}$ at a design occupancy of 20 persons per 1,000 square feet of floor area. In Case 4, the reduced make-up flow rate stated for Case 3 is used during the hours when the museum is open to the public, but it is assumed that the intake dampers are closed at other times of the day. The mechanical ventilation system fans continue to operate, causing air recirculation through the particle filters. Table 6.3 (p. 103) indicates that these measures extend the characteristic soiling times to 0.05–0.1 years for soil dust settling on upward-facing surfaces and to a range of two to five years for elemental-carbon deposition on the walls and ceiling.

Benefits beyond reduced soiling rates may be realized by implementing this control measure. Reducing the ventilation rate reduces operating costs by lowering the amount of energy required to control the indoor air temperature and relative humidity. An improvement in the stability of indoor air temperature and relative humidity may also be realized, reducing the mechanical stresses experienced by objects that would otherwise expand and contract as temperature and relative humidity fluctuate. Improved climate control therefore constitutes an important additional benefit toward preservation of museum collections.

Improving Particle Filtration

Indoor particle concentrations may be reduced by improving the particle filters that are otherwise customarily specified for commercial air-conditioning systems. The filters found in many conventional mechanical ventilation systems are designed primarily to protect the ventilation system components, rather than to deliberately control the level of air pollution in the indoor environment. Air filters commonly used in commercial buildings are generally efficient at removing very large particles from the air stream, but have only a modest single-pass efficiency (commonly 20 to 30%) for removing fine particles, such as those containing elemental carbon.

The efficiency of commercial air filters is commonly specified according to one or more of three rating tests. The "synthetic dust weight arrestance" rating refers to the effectiveness of a filter in removing a suspended mass of coarse artificial dust from an air stream (ASHRAE 1976). The "atmospheric dust spot efficiency" rating refers to the effectiveness of a filter in reducing the opacity of atmospheric particulate matter (ASHRAE 1976). The "DOP efficiency" rating refers to the effectiveness of the filter in removing from an air-stream liquid droplets of dioctyl phthalate having an approximate median diameter of 0.3 μm (U.S. Department of Defense 1956).

Fibrous air filters may be obtained with a wide range of rated particle-removal efficiencies. A recent discussion of the efficiency of particle filters used in general ventilation

applications (Rivers 1988) indicates that the least effective filters commonly employed (home furnace, room air-conditioner) have an atmospheric dust-spot efficiency of 20 to 25%. Rigid, pleated paper filters and pocket bag filters have an atmospheric dust-spot efficiency of 60 to 95%. High-efficiency particle (HEPA) filters[1] with a 99.97% DOP efficiency rating also are available. An important consideration in selecting an air filter is its resistance to airflow, which generally increases with increasing filtration efficiency. The design choice involves balancing the goal of removing particles from the air against the additional equipment and operating cost of high filtration efficiency.

In addition to fibrous filters, an electrostatic precipitator may be used to remove particles from an air stream. These devices operate with much lower pressure drop than a fibrous filter; however, they may be a source of ozone (Sutton et al. 1976, Allen et al. 1978).

The effect on soiling rates of incorporating higher efficiency filters into the baseline retrofit mechanical ventilation system at the Sepulveda House (along with reduced outdoor airflow conditions) is considered in Cases 5 and 6 (Table 6.1, p. 101). The particle-removal efficiencies adopted in this example—0.99 for coarse-particle removal by the intake filter (η_{ox}), 0.95 for coarse-particle removal by the filter in the recirculating line (η_{ii}), and 0.875 for fine-particle removal by both filters—represent the minimum dust weight arrestance and dust spot efficiency, respectively, recently specified in a draft ANSI standard for the storage of library and archival documents (ANSI 1985, Baer and Banks 1985, Committee on Preservation of Historical Records 1986). To achieve these overall efficiencies, a sequence of several filters of progressively higher efficiency is recommended (ANSI 1985). Results for Case 5 (Table 6.3, p. 103) indicate that the characteristic soiling time associated with soil dust settling on upward-facing surfaces is increased to three months, and that the soiling time associated with elemental-carbon deposition on the walls and ceiling is extended to thirty to forty-five years.

For high-efficiency filtration to be effective, it is essential that the leakage of untreated air directly into the building be reduced to the greatest extent possible. This is demonstrated by comparing the results for Cases 5 and 6. The most significant difference between these cases is that infiltration is entirely eliminated in Case 6. With this combination of high-filter efficiency, no infiltration, and a low rate of outdoor air supply, the characteristic times before soiling is apparent are increased by more than two orders of magnitude relative to the base-case assumptions (Table 6.3, p. 103).

1. A HEPA filter unit with $\eta_{ii} f_{ii} = 300\ m^3\ h^{-1}$ was commercially available for $400 in 1983; replacement filters cost $80, and the unit consumed less than 70 W of power (Offermann et al. 1985). The reader is cautioned that not all devices marketed as air cleaners are effective. Five of the ten devices tested in the same study had effective cleaning rates ($\eta_{ii} f_{ii}$) in the range 0–12 $m^3\ h^{-1}$, insignificantly low values for almost all applications. Furthermore, ion generators are particularly to be avoided in museum environments: these devices reduce airborne concentrations by electrically charging particles and causing them to deposit more rapidly on indoor surfaces.

In historical buildings and other sites that lack a mechanical ventilation system, air filtration may still be provided to reduce the rate of soiling due to fine-particle deposition. Unducted console units designed to filter the air in a single room are commercially available. The more effective of these devices combine an efficient air filter with a fan, and are capable of removing 0.45 μm-diameter particles from the air at an effective rate (corresponding to the product $\eta_{ii}\, f_{ii}$) of 100 to 300 $m^3\, h^{-1}$ (Offermann et al. 1985). For a building lacking both mechanical ventilation and significant indoor sources of particles, the introduction of a recirculating filtration device will substantially reduce the indoor particle concentration only if the effective filtration rate is significantly greater than the sum of the ventilation rate and the total particle-deposition rate. This condition will seldom be met for coarse particles (because the coarse-particle deposition rate is so high), but may be achieved for fine particles if the infiltration rate is low. Consider, for example, a room having dimensions of 8 m by 12 m, a ceiling height of 3 m, and an average infiltration rate of 0.3 h^{-1}. Assume, for the purposes of illustration, that the particle-deposition velocities are near the middle of the range corresponding to typical conditions in Southern California museums. A console filtration unit having $\eta_{ii}\, f_{ii}$ equal to 300 $m^3\, h^{-1}$ for both fine and coarse particles is introduced into the room. The concentration of fine particles will be reduced to 23% of the prior value, but the concentration of coarse particles will only be reduced to 86% of the value in the absence of the filtration unit. Thus, the soiling rate of vertical and downward-facing surfaces would be reduced by approximately a factor of four. This improvement is not large relative to the potential improvement of two orders of magnitude for a high-efficiency, low outdoor-air exchange, ducted ventilation and filtration system. However, employing an unducted filtration unit at least provides some improvement in cases where finances will not permit a complete building retrofit.

Reducing Particle Deposition Velocities

The soiling control measures just discussed act by reducing indoor particle concentrations. Soiling rates depend not only on ambient particle concentrations but also on the rate of particle transport to surfaces. That transport phenomenon is parameterized by the deposition velocity, which is calculated as the particle flux to the surface divided by the airborne concentration. Calculations described in Chapter 2 indicate that, for a given particle size, the deposition velocity to the walls of five Southern California museums differ by as much as a factor of 30 among different sites. By controlling the factors that govern the deposition velocity, a substantial reduction in the soiling rate may be achieved without reducing the indoor particle concentration.

The soiling of vertical and downward-facing surfaces is predominantly due to the deposition of fine particles. The rate of deposition of these particles onto a surface is governed by the rate of particle migration across the thin concentration boundary layer adjacent to the surface. The particle flux to the surface varies with the gradient of the particle concentration

at the wall, which increases as the particle concentration boundary layer becomes thinner. The deposition rate can be reduced by increasing the thickness of the concentration boundary layer or by reducing the migration velocity toward the surface. For a given distance downstream along a flat surface, the concentration boundary-layer thickness is relatively large if the near-surface airflow is laminar and if the air velocity is low; conversely, high velocities and turbulent flow conditions lead to a relatively smaller boundary-layer thickness. A simple means of limiting soiling rates that employs this principle is to avoid placing works of art near doors, windows, or mechanical ventilation registers, where local air velocities are likely to be higher than the average for the room as a whole. Likewise, the more precious works in a collection should not be placed on or near exterior walls, as heat transfer through these walls can lead to large local flow velocities due to natural convection and, if the surface is cooler than the air, enhanced deposition due to thermophoresis. For example, particle-deposition velocities at the Getty Museum were among the highest of the five sites studied (Chapter 2). An exterior, concrete wall that was generally cooler than the air in the room was investigated at this site. Even though the mechanical ventilation system operated less than 50% of the time, the mean near-wall airflow velocity (0.19 m s^{-1} at 1 cm from the wall) was the highest observed among the five sites. The high particle-deposition velocities resulted from a combination of the large near-wall velocity and the relatively cool surface. In contrast, near-wall air velocities were lowest at the Norton Simon Museum (0.08 m s^{-1} at 1 cm from the wall, despite continuous operation of a forced-air mechanical ventilation system.

The design and operation of the mechanical ventilation system are vital factors governing the near-wall airflow regime. In much conventional ventilation system design, air is discharged into a room at high velocity through small-area registers. From the standpoint of thermal control, this approach offers the benefit of good mixing. However, this approach also promotes particle deposition by producing relatively high turbulence intensities: for example, streaks of soot on building surfaces near a ventilation discharge register are common sights. An alternative approach is low-velocity air discharge from large-area diffusers. To be effective for thermal control, the return-air path for this approach must be at a different elevation; otherwise, the discharged air may not be distributed throughout the room, but instead follow the return-air path directly. Ideally, if the air-supply diffusers are located at ceiling level, the entrance to the return-air path would be near the floor. At the Norton Simon Museum, this approach is successfully employed by using perforated ceiling tiles to discharge air into the galleries, with the return air flowing back to the mechanical ventilation system through the hallways. At this site, the particle deposition velocities onto walls were the lowest observed among the five museums studied.

To minimize near-wall airflows and to avoid enhancing deposition by thermophoresis, it is important that the building shell of a museum gallery is constructed for low ther-

mal conductivity. It is common in museums to find works of art, such as paintings, hanging from a display panel (for example, a sheet of plywood mounted to the wall with furring strips) or from a false wall. That the surface-air temperature difference is generally smaller for the display panel than for the wall itself is beneficial in reducing deposition velocities.

Further reductions in near-wall air velocity appear possible through the use of a "displacement" ventilation system. Full implementation of this technique might employ two sets of mechanical ventilation system registers, one each at floor and ceiling levels, that can be switched from discharging air into the gallery to returning air to the mechanical ventilation system. When the indoor thermostat calls for cooling, air would be discharged from the register at floor level and removed from the register at ceiling levels. When the indoor thermostat calls for heating, the role of each register is reversed. This ventilation strategy promotes a stable thermal stratification of the air in the room, which suppresses turbulent mixing. The paired mechanical supply and exhaust provide for a slow upward or downward net airflow sufficient to prevent air stagnation in the presence of this thermal stratification. In the ideal case, each parcel of air discharged into the room remains there for a constant period before being removed. This approach has attracted attention as a means of maximizing the effectiveness of ventilation (Sandberg 1981, Skåret and Mathisen 1982). From the perspective of preventing soiling, this approach minimizes the contribution of the mechanical ventilation system to the near-wall air velocity and also minimizes the turbulence due to buoyancy-induced mixing in the core of the room. A hint of the effect of displacement flow on reducing near-wall air velocities can be seen in the case of the Norton Simon Museum during periods when warm air is being discharged through the ceiling tiles and removed down the halls. For a pure displacement flow, the net vertical velocity is determined by the airflow rate through the mechanical ventilation system divided by the floor area of the building, which, for typical conditions is order 0.01 m s^{-1}, even lower than at the Norton Simon Museum.

It is also possible to employ the thermophoretic effect deliberately to reduce the particle-deposition rate. This control method can be viewed at two levels. First, situations where walls are chronically cooler than the room air (e.g., at the Getty Museum) can be avoided. This goal might be achieved by using better insulation in the building. Second, there may be cases where active use of thermophoresis to drive particles away from surfaces is possible by maintaining the surface of interest at a slightly higher temperature than the adjacent air. For example, this might be achieved in buildings located in warm climates by heat leakage through the exterior walls combined with cooling of the indoor air. An indication of the effectiveness of this measure is examined for a building the size of the Sepulveda House in Case 7 (Table 6.1, p. 101). In that case a temperature difference of 1 K is postulated between the surfaces and the air, with the air being cooler, and the natural convection flow regime is assumed to prevail at all times. Table 6.3 (p. 103) shows that these conditions—in combination with the previous controls of eliminating infiltration, using low

mechanical ventilation supply rates, and employing particle filters with high efficiency—eliminate particle deposition to the ceiling, and extend the characteristic soiling time from one century to more than two centuries due to elemental carbon particle deposition to the walls.

An alternative technique for reducing particle deposition velocities that may be easier to achieve, especially in an existing structure, is to obtain laminar forced flow conditions coupled with small surface-air temperature differences by employing a forced flow system similar to that at the Norton Simon Museum. In modeling Case 8 (Table 6.1, p. 101) applied to the Sepulveda House, the airflow regime for computing deposition velocities is assumed to be forced laminar flow with the free-stream air velocity and temperature difference as a function of time corresponding to conditions measured at the Norton Simon Museum on April 6–7, 1988 (see Chapter 4). Table 6.3 (p. 103) shows that these conditions also lead to a significant improvement in characteristic soiling times for walls and ceiling, but that the improvement is not as large as for Case 7.

For coarse particles, which migrate primarily due to gravitational settling, one should simply avoid, to the extent possible, any upward orientation of the surface. A benefit might be realized by mounting paintings with an orientation that is slightly downward from vertical, as this practice would reduce the rate at which coarse particles settle onto the rough elements of the surface.

Using Display Cases and Framing

An alternative means of effectively providing local pollution control in the vicinity of an art object is through the use of display cases and framing behind glass. When analyzed in this context, a display case may be considered as a room within a room. Thus, to predict the effectiveness of a display case, one may apply the aerosol dynamics model of Chapter 3, regarding the component concentration within the space of the room as if it were the outdoor particle concentration, and the component concentration inside the display case as if it were the indoor concentration. Then, as with the control problem for the museum as a whole, the control options within a display case include reducing the rate of air exchange between the display case and the room, improving particle filtration within the display case, reducing the particle deposition velocity to objects within the display case, controlling the concentration within the room outside of the display case, and eliminating emissions inside the display case.

To consider the potential effectiveness of the use of display cases, additional data from the Sepulveda House will be considered. In recognition of the soiling problem at this site, one of its rooms—a bedroom furnished with historical artifacts—has been retrofitted to be, in effect, a large display case. All identifiable air-leakage paths were sealed. In the room's one doorway, a glass-walled alcove from the hallway into the room was constructed, entirely sealing the doorway. By standing in this alcove, visitors may examine the entire room, but, except for maintenance activities, no one enters.

To determine the effectiveness of this approach in reducing soiling, measurements of the size distribution and concentration of fine particles were made at two locations: one inside the enclosed bedroom, the other on a stairway landing in a central location in the building. A pair of optical particle counters (OPCs, Particle Measuring Systems model ASASP-X) were used to take measurements continuously for a day and a half during the spring of 1988. These instruments are capable of detecting particles over a nominal size range of 0.09–3 μm optical diameter and classifying them, according to the amount of light scattered in the forward direction, into 32 size channels (Chapter 4). The air exchange rate between the bedroom and its surroundings (outdoors plus the rest of the building) was measured throughout this period by the tracer-gas decay technique (ASHRAE 1985), using sulfur hexafluoride as the tracer.

Figure 6.4 (p. 118) depicts results for a 24-hour segment of the monitoring period: the total volume concentration of fine particles detected by the OPCs as a function of time, and the 24-hour-average aerosol size distributions. By sealing the bedroom, the soiling hazard has been substantially reduced. For soot-sized particles of 0.1 μm diameter, the concentration in the bedroom is 32% of the concentration in the core of the building. For particles of 2 μm diameter, the corresponding ratio is 8%.

A substantial further reduction in the soiling rate could be achieved through the use of a local particle filtration unit in the room. The average rate of air leakage into this room is 4.3 $m^3 h^{-1}$. Employing an air filter having an effective filtration rate of 300 $m^3 h^{-1}$ ($\eta_{ii} f_{ii}$) would reduce the concentration of 0.1 μm particles by a factor in the range of 20–60. The power consumption rate of an unducted filtration unit is generally less than 100 W (Offermann et al. 1985); however, some attention must be given to heat dissipation if such a unit is to be used in a small, tightly enclosed space. If heat dissipation or aesthetic considerations dictate that an unducted unit may not be used in a small, enclosed space, it is possible to achieve the same benefit by using a ducted, local recirculation and filtration system. Using this approach, the heat and noise generated by the fan can be separated from the items in the exhibit.

Site Management to Achieve Low Outdoor Aerosol Concentrations

Some consideration may be given in the planning of a new facility to the outdoor concentrations of soiling particles. Within the central portion of the Los Angeles air basin, the annual average concentrations of fine elemental-carbon particles vary within a relatively narrow range (coefficient of variation among ten sites monitored in 1982 was 0.2; Gray et al. 1986). However, measurements taken outside of five museums during the summer of 1987 and the winter of 1987–88 show that the mean concentration of fine elemental carbon particles in Malibu, located along the coast northwest of Los Angeles, was 0.8 $\mu g\ m^{-3}$, only 27% of the corresponding mean for the four sites centrally located in the air basin (Table 6.2, p. 102). A significant benefit in reducing the soiling rate may therefore be realized through careful site selection.

In designing new museum facilities and in considering control measures to reduce the soiling hazard at existing sites, care should be taken to minimize aerosol-generating activities near the location of the air-intake register through which outdoor air is provided to the building. For example, in a new building, placing the intake register near a street should be avoided, because the soot and road-dust concentrations there are relatively high. Areas near parking lots should be avoided because of particle generation by idling vehicles. The use of landscape maintenance equipment, such as leaf blowers, may also generate high concentrations of airborne particles, as illustrated with data collected at the Sepulveda House in Figure 6.3 (p. 117). In that case, a prominent peak is observed in the number concentration of very large particles due to the suspension of soil dust by a leaf blower. A large fraction of the total number of very large particles to which the building inlet was exposed in the 24-hour period studied is due to this brief (10–15 minutes) episode of leaf-blower operation. A corresponding peak in the number of very fine particles also is observed at that time, probably due to the exhaust from the gasoline-powered leaf-blower engine. Preventing particles such as these from entering a museum can be largely achieved through careful planning.

Limiting Sources of Indoor Aerosol

Many activities may result in the direct emission of particles into the indoor air. Combustion processes that lead to the emission of elemental carbon indoors include the burning of candles (such as inside churches), the operation of motor vehicles in attached garages, combustion of wood in fireplaces, and the use of gas-fired cooking appliances in kitchens within the building.

Other activities that do not involve combustion may also generate particles that could contribute to the soiling hazard. Construction activities that involve abrasion or grinding will generate coarse airborne particles. Simply allowing people in a gallery will lead to some particle generation through the shedding of skin flakes, the tracking of soil dust into a building from clothes and shoes, and the abrasion of floors and clothing due to movement (Cooper 1986). Cleaning activities within the museum, such as vacuuming and floor polishing, may lead to resuspension or generation of airborne particles. With available information, it cannot be stated that these sources pose a significant soiling hazard in museums. However, since the control cost for reducing or eliminating indoor particle generation by many activities is small (if not zero), it is advisable to adopt measures to control indoor particle generation as part of the overall strategy for controlling the indoor soiling hazard.

Conclusions

In this report, techniques for quantifying and predicting soiling rates have been examined along with methods for protecting works of art from soiling due to the deposition of airborne particulate matter. Six control techniques were identified: reducing the rate of supply of outdoor air to the building, improving particle filtration, reducing particle deposition velocities, using display cases or framing, managing a site to achieve low outdoor aerosol concentrations, and eliminating indoor aerosol sources. Calculations based on the detailed model of indoor aerosol dynamics (Chapter 3) applied to the Sepulveda House show that, relative to the current uncontrolled conditions, characteristic soiling times could be increased by at least two orders of magnitude through a combination of adding a mechanical ventilation system, maintaining a low outdoor-air exchange rate, improving particle removal by filters, and designing the building and mechanical ventilation system to achieve lower particle deposition velocities. In the uncontrolled case at the Sepulveda House, the characteristic time to accumulate a perceptible deposit of soiling particles on walls and ceilings is measured in years; with the application of aggressive but achievable control measures, the characteristic times are measured in centuries (Table 6.3, p. 103). Furthermore, having a suite of control options from which to choose, more modest improvements may be obtained at a correspondingly lower cost. Through the use of display cases and localized air filtration, it is possible to protect a portion of a collection without the expense of modifying an entire building.

The control measures discussed in this chapter are not only technically feasible, they also either involve no additional equipment purchase or are based on commercially available products. Many of the measures are at least economically practical, if not economically attractive. For example, reducing the rate of supply of outdoor air to a building that does not contain important indoor sources can not only reduce soiling rates, but actually lower operating costs by reducing the amount of energy required to control the indoor air temperature and relative humidity. At the Sepulveda House, the cost of remodeling the bedroom to create a large display case has been offset by the reduction in the cost of cleaning the exhibit (John Coghlan, El Pueblo de Los Angeles State Historic Park, personal communication).

Thus, a variety of techniques are available to control the rate of particle deposition to surfaces. Many of these techniques have low associated costs; some may even yield savings. With sufficient information and careful planning, most museum collections can be protected from soiling due to the deposition of airborne particulate matter.

Figure 6.1. Schematic representation for a single-chamber mathematical model of the soiling rate.

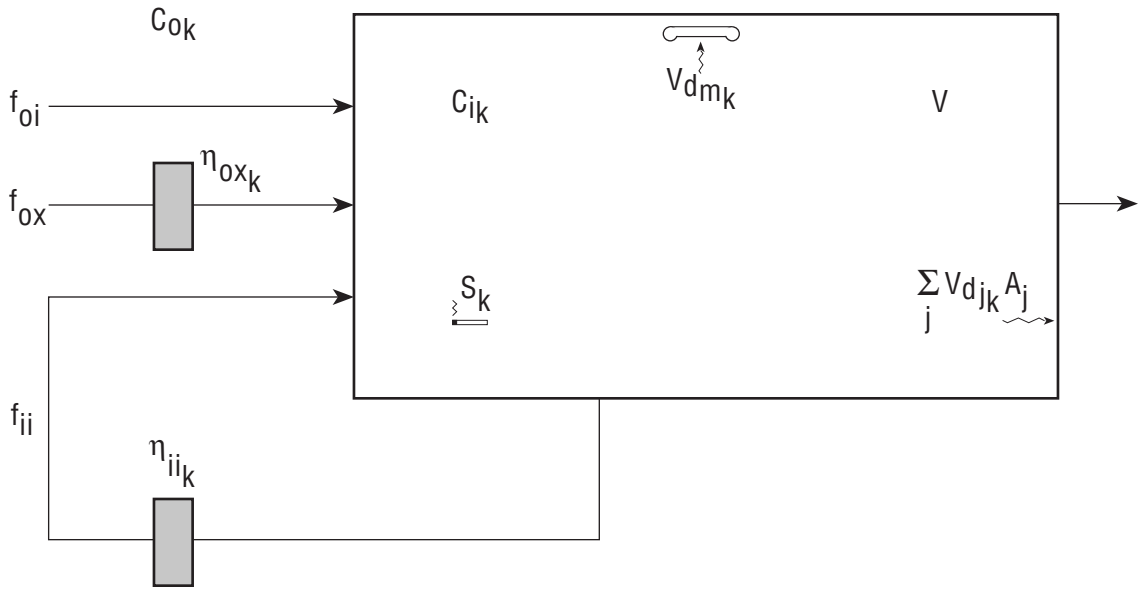

Figure 6.2. Average outdoor aerosol size distribution and chemical composition measured on the second-floor balcony of the Sepulveda House in downtown Los Angeles. Measurements were conducted over a 24-hour period beginning on March 30, 1988 at 2100 PST.

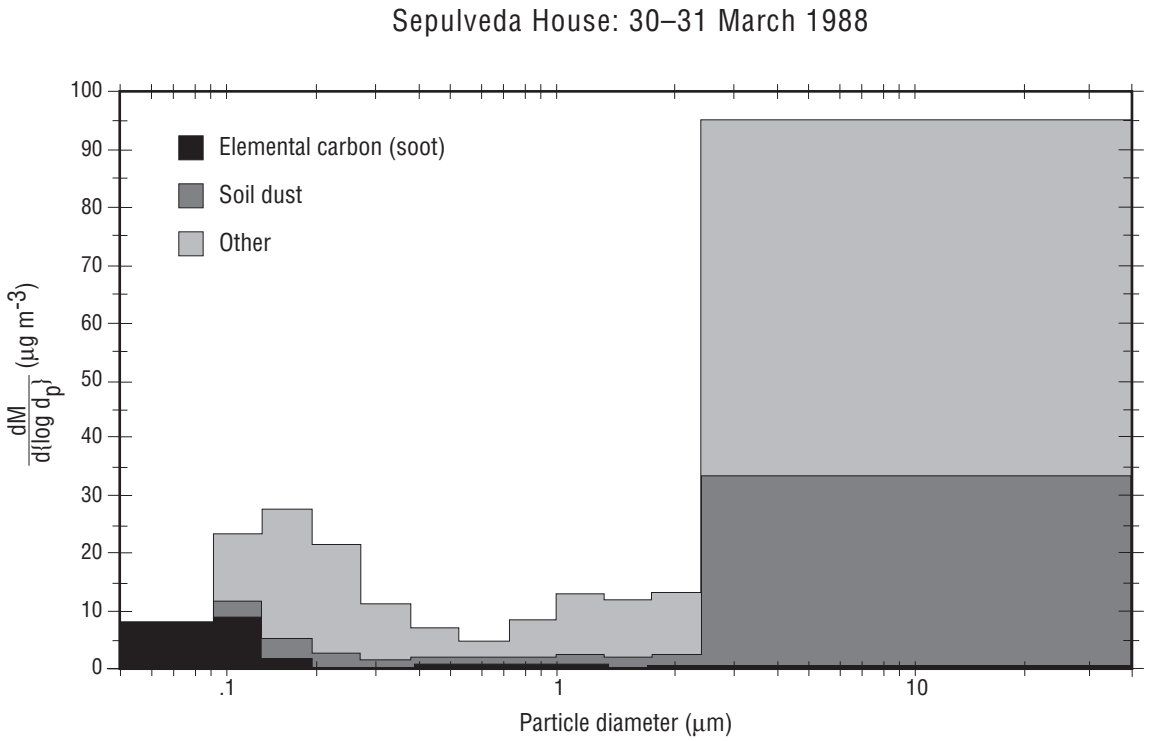

Figure 6.3. Outdoor aerosol mass concentration and particle number concentration versus time at the Sepulveda House in downtown Los Angeles. Measurements were made on the second-floor balcony.

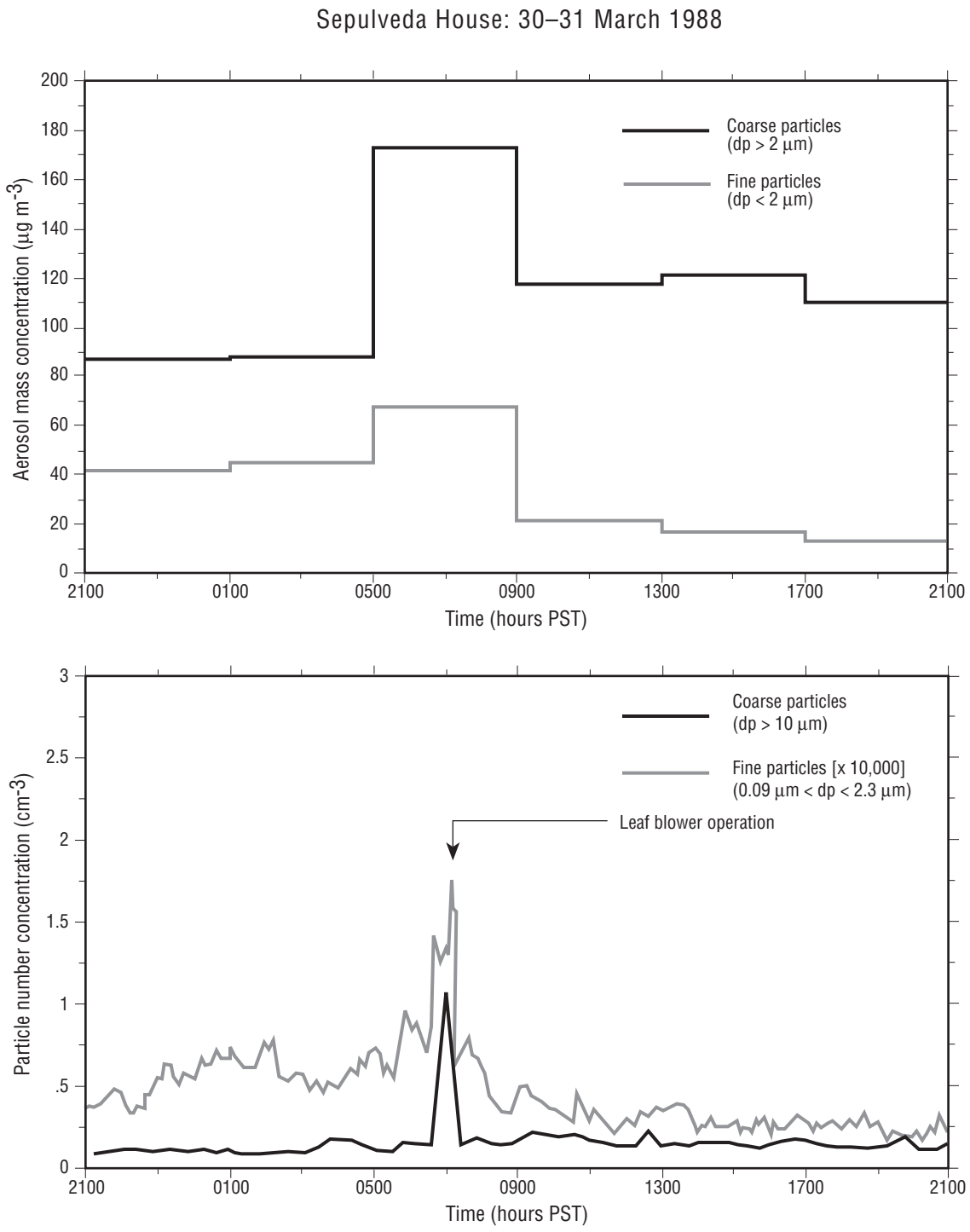

Figure 6.4. Volume concentration of fine particles (0.09–2.3 μm optical diameter) versus time and mean aerosol size distribution measured over a 24-hour sampling period, beginning at 2100 PDT on April 11, 1988, inside the Sepulveda House.

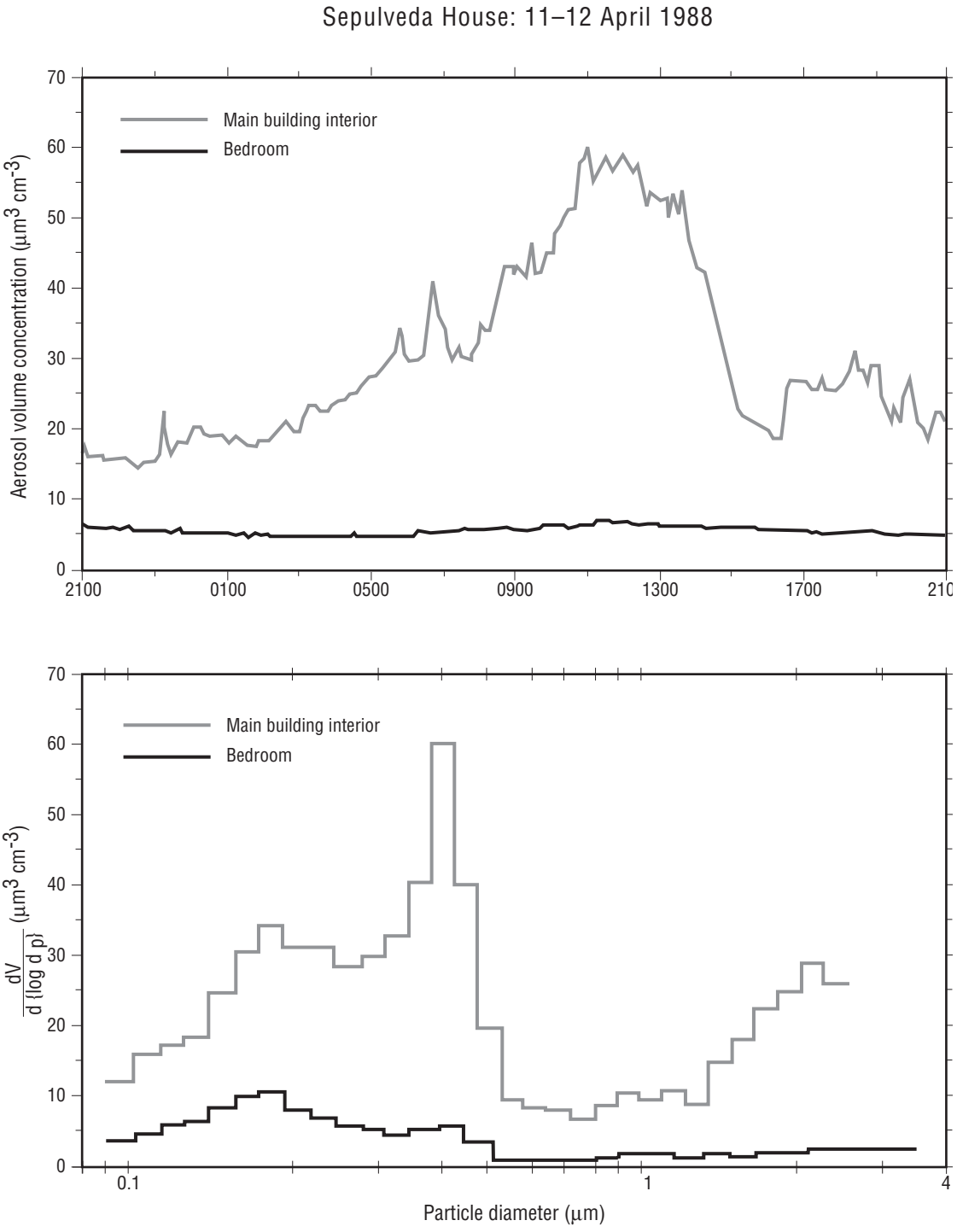

References

Allen, R. J., R. A. Wadden, and E. D. Ross

1978 Characterization of potential indoor sources of ozone. *American Industrial Hygiene Association Journal* 39: 466–71.

American National Standards Institute

1985 Practice for Storage of Paper-Based Library and Archival Documents, Draft. ANSI Standard Z39.xx–1985.

American Society of Heating, Refrigerating, and Air-Conditioning Engineers (ASHRAE)

1976 *Method of Testing Air-Cleaning Devices used in General Ventilation for Removing Particulate Matter*. ASHRAE Standard 52–76. Atlanta: American Society of Heating, Refrigerating, and Air-Conditioning Engineers.

1985 *ASHRAE Handbook: 1985 Fundamentals*. Atlanta: American Society of Heating, Refrigerating, and Air-Conditioning Engineers.

Baer, N. S. and P. N. Banks

1985 Indoor air pollution: Effects on cultural and historic materials. *International Journal of Museum Management and Curatorship* 4: 9–20.

Bejan, A.

1984 *Convection Heat Transfer*. New York: Wiley.

Billmeyer, F. W. and M. Saltzman

1981 *Principles of Color Technology*. New York: Wiley.

Biscotin, G., S. Diana, V. Fassina, and M. Marabelli

1980 The influence of atmospheric pollutants on the deterioration of mural paintings in the Scrovegni Chapel in Padua. In *Conservation within Historic Buildings*. N. S. Bromelle, G. Thomson, and P. Smith, eds. London: The International Institute for Conservation of Historic and Artistic Works.

Cammuffo, D.

1983 Indoor dynamic climatology: investigations on the interactions between walls and indoor environment. *Atmospheric Environment* 17: 1803–1809.

Cammuffo, D. and A. Bernardi

1988 Microclimate and interactions between the atmosphere and Orvieto Cathedral. *The Science of the Total Environment* 68: 1–10.

Carey, W. F.

1959 Atmospheric deposits in Britain: A study of dinginess. *International Journal of Air Pollution* 2: 1–26.

Cass, G. R., M. H. Conklin, J. J. Shah, J. J. Huntzicker, and E. S. Macias

1984 Elemental carbon concentrations: Estimation of a historical data base. *Atmospheric Environment* 18: 153–162.

Cass, G. R., J. R. Druzik, D. Grosjean, W. W. Nazaroff, P. M. Whitmore, and C. L. Wittman

1988 *Protection of Works of Art from Photochemical Smog*. Getty Conservation Institute Scientific Program Report prepared by the California Institute of Technology, Pasadena.

Committee on Preservation of Historical Records

1986 *Preservation of Historical Records*. Washington, D.C.: National Research Council, National Academy Press.

Cooper, D. W.

1986 Particulate contamination and microelectronics manufacturing: An introduction. *Aerosol Science and Technology* 5: 287–299.

Dockery, D. W. and J. D. Spengler

1981 Indoor-outdoor relationships of respirable sulfates and particles. *Atmospheric Environment* 15: 335–343.

Friedlander, S. K.

1977 *Smoke, Dust, and Haze*. New York: John Wiley and Sons.

Gelbard, F. and J. H. Seinfeld

1980 Simulation of multicomponent aerosol dynamics. *Journal of Colloid and Interface Science* 78: 485–501.

Goren, S. L.

1977 Thermophoresis of aerosol particles in the laminar boundary layer of a flat plate. *Journal of Colloid and Interface Science* 61: 77–85.

Gray, H. A., G. R. Cass, J. J. Huntzicker, E. K. Heyerdahl, and J. A. Rau

1986 Characteristics of atmospheric organic and elemental carbon particle concentrations in Los Angeles. *Environmental Science and Technology* 20: 580–589.

Hancock, R. P., N. A. Esmen, and C. P. Furber

1976 Visual response to dustiness. *Journal of the Air Pollution Control Association* 26: 54–57.

John, W. and G. Reischl

1980 A cyclone for size-selective sampling of ambient air. *Journal of the Air Pollution Control Association* 30: 872–76.

Nazaroff, W. W. and G. R. Cass

1986 Mathematical modeling of chemically reactive pollutants in indoor air. *Environmental Science and Technology* 20: 924–34.

1989 Mass-transport aspects of pollutant removal at indoor surfaces. *Environment International* 15: 567–84.

Nazaroff, W. W., M. P. Ligocki, L. G. Salmon, G. R. Cass, T. Fall, M. C. Jones, H. I. H. Liu, and T. Ma

1990 *Protection of Works of Art from Soiling Due To Airborne Particles*. Environmental Quality Laboratory Report no. 34. California Institute of Technology, Pasadena. Also printed as a Getty Conservation Institute Scientific Program Report, 1992.

Nielsen, R. A.

1940 Dirt patterns on walls. *Transactions, American Society of Heating and Ventilating Engineers* 46: 247–258.

Offermann, F. J., R. G. Sextro, W. J. Fisk, D. T. Grimsrud, W. W. Nazaroff, A. V. Nero, K. L. Revzan, and J. Yater

1985 Control of respirable particles in indoor air with portable air cleaners. *Atmospheric Environment* 19: 1761–71.

Ouimette, J.

1981 Aerosol Chemical Species Contributions to the Extinction Coefficient, Ph.D. diss., California Institute of Technology, Pasadena.

Report of the Study Committee on Scientific Support

1979 National Conservation Advisory Council. Washington, D.C.: Smithsonian Institution.

Rivers, R. D.

1988 Interpretation and use of air filter particle-size-efficiency data for general-ventilation applications. *ASHRAE Transactions* 94(2).

Sandberg, M.

1981 What is ventilation efficiency? *Building and Environment* 16: 123–35.

Schiller, G. E.

1984 A Theoretical Convective-Transport Model of Indoor Radon Decay Products, Ph.D. diss., University of California, Berkeley.

Shahani, C.

1986 Letter to the editor. *Abbey Newsletter* 10(2): 20.

Sinclair, J. D., L. A. Psota-Kelty, and C. J. Weschler

1985 Indoor-outdoor concentrations and indoor surface accumulations of ionic substances. *Atmospheric Environment* 19: 315–23.

Skåret, E. and H. M. Mathisen

1982 Ventilation efficiency. *Environment International* 8: 473–81.

Stolow, N.

1987 *Conservation and Exhibitions*. London: Butterworths.

Sutton, D. J., K. M. Nodolf, and K. K. Makino

1976 Predicting ozone concentrations in residential structures. *ASHRAE Journal* 18(9): 21–26.

Thomson, G.

1978 *The Museum Environment*. 2nd edition 1986. London: Butterworths.

Toishi, K. and T. Kenjo

1967 Alkaline material liberated into atmosphere from new concrete. *Journal of Paint Technology* 39: 152–55.

1968 A simple method of measuring alkalinity of air in new concrete buildings. *Studies in Conservation* 13: 213–14.

1975 Some aspects of the conservation of works of art in buildings of new concrete. *Studies in Conservation* 20: 118–22.

United States Department of Defense

1956 *Military Standard: Filter Units, Protective Clothing, Gas-Mask Components and Related Products: Performance-Test Methods*. *mil-std*-282. Washington, D.C.: U.S. Government Printing Office.

Volent, P. and N. S. Baer

1985 Volatile amines used as corrosion inhibitors in museum humidification systems. *The International Journal of Museum Management and Curatorship* 4: 359–364.

Wall, S. M., W. John, and J. L. Ondo

1988 Measurement of aerosol size distributions for nitrate and major ionic species. *Atmospheric Environment* 22: 1649–56.

Yocom, J. E., W. L. Clink, and W. A. Cote

1971 Indoor-outdoor air quality relationships. *Journal of the Air Pollutant Control Association* 21: 251–59.

Index

D

E

F

N

O

T